“Sapienza” University of Rome

PhD in

Biotechnology In Clinical Medicine

XXX Cycle

The transcription factor Foxm1 controls pro-stemness microRNAs in cerebellar neural stem cells (NSCs)

PhD Student: Luana Abballe

Matricola: 1243805

Tutor: Prof. Elisabetta Ferretti

Academic Year 2016-2017

Summary

Abstract

Background: Cerebellar neural stem cells (NSCs) maintenance is of great interest since NSCs can be used to treat impaired cells and tissues or improve regenerative power of degenerating cells in neurodegenerative diseases or spinal cord injuries. Under maintenance conditions, NSCs express a number of Hedgehog-Gli (Hh-Gli) linked and stemness genes (e.g. Nanog, Oct4, Sox2) whose mechanisms of regulation have been under investigation. However, the interplay between transcription factors and microRNAs in NSCs is still being charted.

Aim: Identification of new molecular players involved in NSCs' maintenance with particular interest in the major regulatory pathway Hedgehog-Gli.

***Materials and Methods*:** Cells used for the study were NSCs isolated from postnatal day 4 (P4) wild type (C57BL/6) mice cultured both as neurospheres in selective medium and as differentiated NSCs when cultured in medium with serum. NSCs and their differentiated counterparts were analysed by high-throughput technologies. Bioinformatics analysis was used for the identification of the Foxm1-regulated miRNAs; knock-down experiments and clonogenic assays were used for functional studies. Chromatin immunoprecipitation experiments (ChIP) were used to investigate the binding between Foxm1 and its targets and between Foxm1 and its regulators.

Results: NSCs and their differentiated counterparts were analysed using next-generation mRNA- and miRNA-sequencing. The transcriptional analysis allowed the identification of Foxm1 as one of the highest transcripts in NSCs and the miRNA-sequencing provided a number of highly expressed miRNAs. The use of bioinformatics analysis resulted in the Foxm1-regulated miRNAs, miR-15 ~ 16 cluster, miR-17 ~ 92 cluster, miR- 130b and miR-301a. Functional experiments, such as knock-down experiments and clonogenic assays enabled the identification of Foxm1 as a downstream mediator of the Hh-Gli signalling and with the ability to regulate the above mention miRNAs.

Conclusion: The study presented reveals a new Foxm1-microRNAs network with a major role in the maintenance of NSCs. These results add a previously unidentified important molecular aspect that could be used in future neurodegenerative disease studies, thus enriching the field of translational medicine.

Introduction

Neural stem cells

Stem cells have been a major focus of research because of their unique capacities of self-renewal and differentiation capacity. These capacities are defined by the expression of transcription factors and epigenetic modulations (Montalbán-Loro, R. et al. 2015).

They reside in specific environment or niches of the adult mammalian brain, the subgranular zone of the dentate gyrus of the hippocampus (SGZ), the subventricular zone (SVZ) lining the lateral ventricles, and the white matter of the cerebellum (Gage, F.H. 2000; Lee, A. et al., 2005), in which NSCs support neurogenesis and gliogenesis during adult life. A small number of NSCs may still be in other areas of the brain (**Fig. 1**).

In SGZ there are two types of NSCs, particularly type 1 that are quiescent characterized by the expression of specific molecular markers such as glial fibrillary acidic protein (GFAP), Nestin and Sox2. Type-1 NSCs (true stem cells) are the neurogenic entities that generate type-2 cells that proliferate actively and express Nestin, Sox2 but not GFAP.

In the SVZ area three types of NSCs can be distinguished (**Fig. 2**): A, B, C. Type-A is composed of migratory neuroblasts, type-B and -C correspond to type 1 and 2 in SGZ (Yao J. et al., 2012). The cell lineage differentiation goes from type-B, through type-C to type-A cells (Doetsch F. et al., 1999).

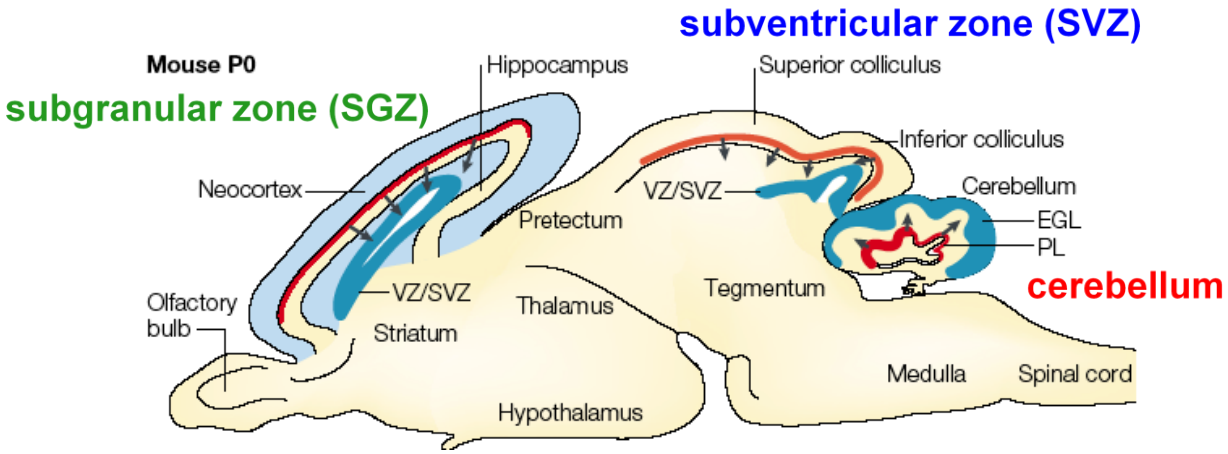

Figure 1. Postnatal mammalian neuronal stem cell "niches".

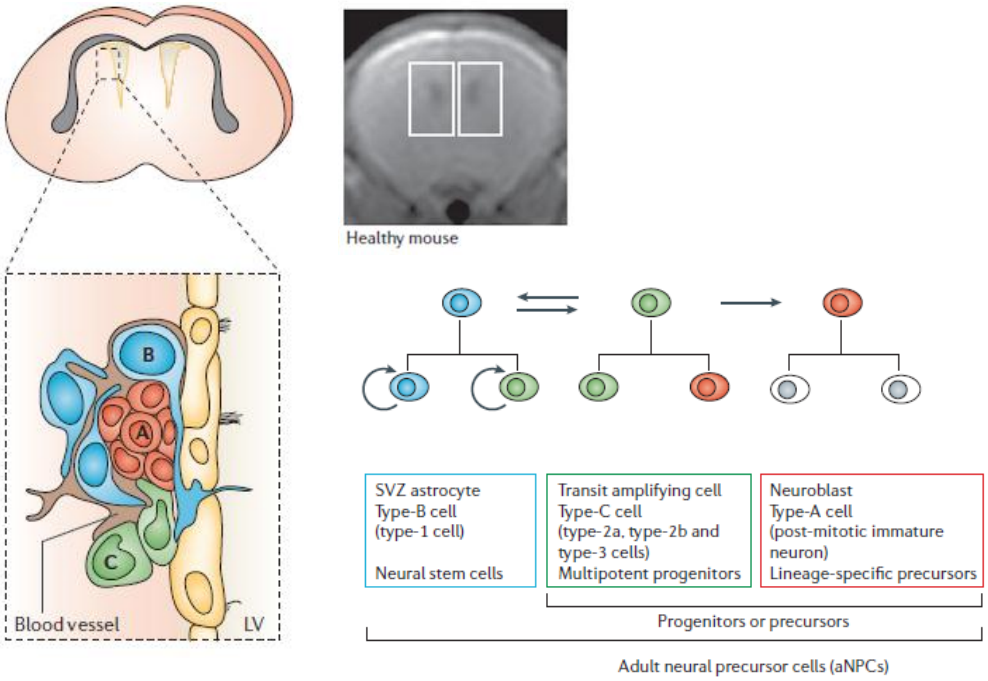

Figure 2. Cytoarchitecture of the subventricular zone of the healthy adult brain (Martino G. and Pluchino S. 2006).

Neural cerebellar Stem Cells (NSCs) have the ability to self-renewal and to give rise to neurons, astrocytes and oligodendrocytes (**Fig. 3**) (Davis, A. A. and Temple, S. 1994; Gage, F.H. 2000). They express stemness markers such as Sox2, Nestin, Nanog and Prom1 (Palm, T. et al., 2013; Po, A. et al., 2010).

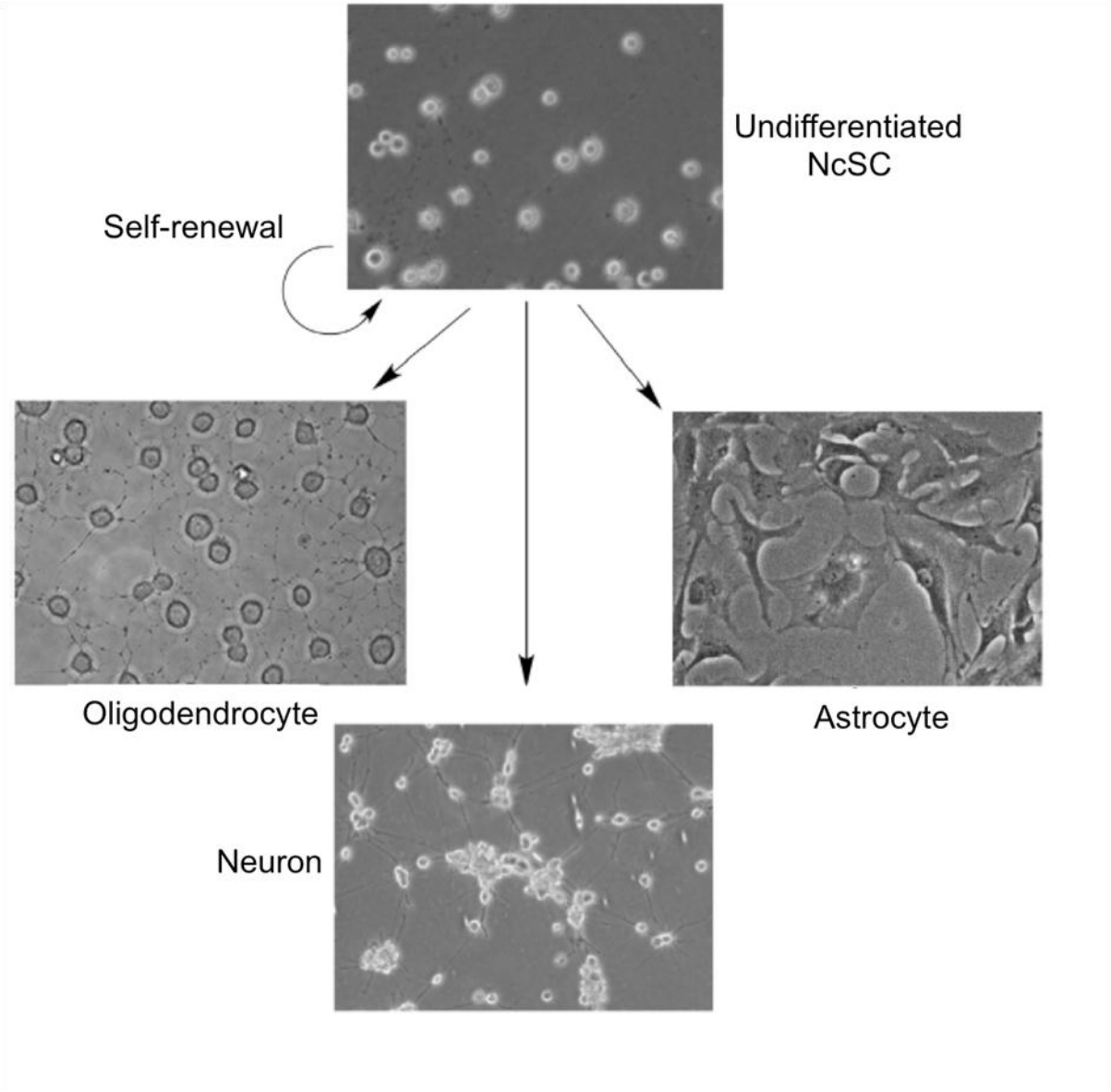

Figure 3. Self-renewal of Neural cerebellar Stem Cells and differentiation lineage (Wakabayashi, T. et al., 2014).

NSCs are in physical contact with the basal lamina, which regulates cytokines and growth factors derived from local cells (Campos, L. S. et al. 2006).

Moreover, the proliferation and differentiation are finely regulated by both intrinsic and extrinsic factors (Imayoshi, I. et al., 2010; Pierfelice, T. et al., 2011) consisting of morphogens, growth factors, tissue micro-environment (germinal niche), transcriptional factors and epigenetic mechanisms. Among the main determinants of differentiation, Notch is responsible for neuronal differentiation (Imayoshi, I. et al., 2010; Pierfelice, T. et al., 2011), fibroblast growth factor (FGF), WNT that

promotes differentiation in the subventricular zone (Lie, D.C. et al., 2002) and Sonic Hedgehog directs NSCs to the glial lineage (Ahn, S., and Joyner, A.L. 2005; Balordi, F., and Fishell, G., 2007; Han, Y.-G. et al. 2008).

NSCs are characterized by a low degree of epigenetic silencing, resulting in the activation of a multitude of genes that maintain self-renewal (Yao J. et al.,2012).

Up-regulated pathways consistent with NSCs self-renewal have been identified, such as G1-S cell cycle regulation, nucleic acid synthesis, DNA replication, packaging, and repair genes (Gage, F.H. 2000).

Advancing the understanding of the signalling molecules that are responsible for the transition of NSCs from proliferation to differentiation will further the potential use of NSCs as therapeutic agents (Gage, F.H. 2000; Harris, L. et al., 2016).

There are cues that NSCs can reach the target organ and differentiate into the appropriate cell lineage but the molecular mechanisms that sustain functional integration and repair capabilities are not clear (Martino G., Pluchino S., 2006).

The main goal is to use NSCs to treat impaired cells and tissues or improve regenerative power of degenerating cells in neurodegenerative diseases (for example Parkinson's disease, Huntington's disease, multiple sclerosis) or spinal cord injuries.

Hedgehog pathway in NSCs

A key signal sustaining NSCs is Hedgehog (Hh) signalling (Po, A. et al., 2010). Hh pathway has a central role in development and tumorigenesis in a wide variety of tissues, both processes being supported by stem cells (Ahn, S., and Joyner, A.L., 2005; Lai, K. et al., 2003; Palma, V. and i Altaba, A.R. 2004; Palma, V. et al., 2005).

The pivotal role of this signal pathway has already been described in embryonic stem cells and NSCs of SVZ, hippocampal regions (Ahn, S., and Joyner, A.L., 2005; Lai, K. et al., 2003; Palma, V. et al., 2005; Palma, V. and i Altaba, A.R. 2004) and cerebellum (Po, A. et al., 2010).

The canonical Hh pathway requires the presence of a transmembrane receptor, Smoothened (Smo), which can be inhibited by the Patched 1 (Ptc) receptor. Hh ligands (Desert Hedgehog (DHH), Indian Hedgehog (IHH), and Sonic Hedgehog (SHH) bind Ptc which is internalized, degraded, and thus not able to inhibit the activator receptor Smo. Smo, then, interacts and inhibits the Suppressor of fused (SUFU), this results in the activation and nuclear translocation of the only known transcriptional mediators of the Hh response, zinc-finger proteins of the glioma-associated oncogene (Gli) family. These are bifunctional transcription factors that can both activate or inhibit transcription. In detail,

Gli1 and Gli2 (GliA) are activated and transported in the nucleus where they activate the transcription of Gli1 itself, Gli2 and Ptc, thus amplifying the Hh signaling pathway. Gli3 (GliR) is a suppressor of the Hh pathway and is degraded after inhibition of Sufu by Smo (**Fig. 4**) (Ng, J.M., and Curran, T., 2011).

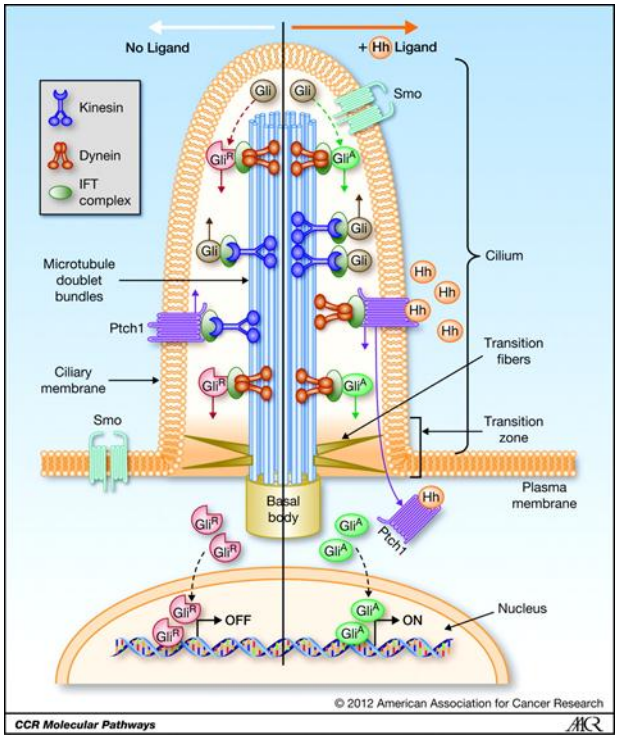

Figure 4. Hedgehog signaling pathway.

In NSCs Nanog and Hh/Gli are co-expressed and it has been demonstrated that both are essential in driving self-renewal. Nanog is a transcriptionl factor essential for maintaining the pluripotency of the inner cell mass during embryonic development and its expression is down regulated in differentiated cells. Nanog is a downstream factor of the Hh signal transduction, in fact Gli1 and Gli2 bind to specific consensus cis-regulatory responsive elements on Nanog promoter enhancing its transcription. This way, Gli1 and Gli2 mediate the Hh-dependent control of Nanog and downstream stemness genes, which promote self-renewal of NSCs (Po, A. et al., 2010).

Next Generation Sequencing

In 1977 F. Sanger and colleagues proposed a new innovative method for sequence DNA by chain termination and fragmentation techniques (first generation), that was used for the next 30 years, introducing the possibility to study genomes and for fast and low-cost DNA sequencing.

The Human Genome Project (HGP) (Consortium, I.H.G.S. 2004; Lander, E.S. et al., 2001), was an international, publicly funded consortium of scientists at universities and research institutes with the aim to provide a virtually complete sequence of human DNA, the genome.

The Sanger methods allowed the realization of the first human genome sequence in 2004. HGP was still very expensive and needed plenty of resources, so, in the same year the National Human Genome Research Institute (NHGRI) started a program to reduce the cost of the sequencing to US$1000 in ten years. This has led to the development of next-generation sequencing (NGS) technologies. These new technologies offered improvements respect to Sanger methods. First, in the preparation of libraries in a cell free system to fragment the DNA; second, they could generate gigabases of genomic data in a single run because the sequencing reactions are produced in parallel; and lastly, they didn't require the electrophoresis step (Van Dijk, E.L. et al., 2014). In this way, they largely reduced the cost and the complexity of the experiments.

NGS systems are based on shotgun sequencing approach which consists of random fragmentation from an entire genome, transcriptome, or smaller targeted regions and sequencing of DNA in a single run (Morozova, O. et al. 2009).

There are different commercial platforms, the widely utilized ones are Roche/454, Illumina, Applied Biosystems SOLiD, Oxford Nanopore, Ion Torrent, Pacific Biosciences and Helicos. They differ from each other on the type of chemistry used, in fact they can be based on either "sequencing by synthesis" or "sequencing by ligation" detection methods (Metzker, M.L. 2010).

The advantage of New-Generation Sequencing Methods can be applied to different areas of research and for different applications. These include a complete genome annotation, for example the knowledge of all regulatory sequences, splice variants and exon-intron structures (Morozova, O. et al., 2009). Omics technologies provided us data that allowed us to better understand the genotype–phenotype interaction. NGS has a wide application in the identification and quantifying of transcripts in cells, tissue and organisms (RNA-seq) (Morozova, O. et al., 2009; Voelkerding, K. V. et al., 2009).

In genomics they allow us to study whole genomes from microbes to humans and its products, and the communication between genes and environment. In the medical field NGS advances have improved the understanding of the relationship between genetic modification and phenotype,

moreover the re-sequencing of target genomic regions is useful to identify polymorphisms in genes to study rare variants in genetic diseases (Koboldt, D.C. et al., 2013; Voelkerding, K. V. et al., 2009).

RNA-Sequencing

The RNA sequencing, through NGS, allows for the quantification and characterization of transcripts, producing an adequate representation of transcriptome in both prokaryotes and eukaryotes. These technologies avoid several problems connected to the hybridization-based microarrays, previously used to gene expression, such as cross-hybridization artefacts, limited range of detection and a priori knowledge of gene sequences.

There are several applications of RNA-seq in transcriptomics that have an important impact on the study of diseases. For example, it is used for the characterization of splicing variants that could help us to understanding the contribution of alternative splicing in the development of human diseases. In the field of cancer research, it also can be used to find gene fusion events, such as a translocation or another genomic arrangements that produce aberrant RNAs, identifying potential targets for therapeutic approach (Ozsolak, F., and Milos, P. M., 2011).

It is largely used to map transcription start sites, to identify nucleotide variations and mutations and noncoding RNAs (ncRNAs) expression profiling in many species. RNA-seq is effective not only in the discovery of novel microRNAs and siNAs, but also in the detection of variants of microRNAs and editing events (Morozova, O. et al. 2009).

RNA-seq workflow (**Fig. 5**) starts with the conversion of total RNA in a library of cDNA containing sequencing adaptors. Then, each molecule is sequenced to obtain short sequences (reads) from one end (single-end sequencing) or both ends (pair-end sequencing). The size of the resulting reads obtained are very short, between 35 and 500 bp (Wang, Z. et al., 2009), so it is necessary to reassembly the full-length RNAs, except in the case of small classes of RNA (miRNAs, piRNAs snoRNAs and siRNAs). Following sequencing, there are three different strategies to perform the assembly of the transcriptome: a reference-based strategy, a de novo strategy or a combined strategy that merges the two. The “reference-based” is easier to perform, it aligns the reads to a

reference genome and the advantage is that can assemble transcripts of low abundance (Martin, J.A. and Wang, Z., 2011).

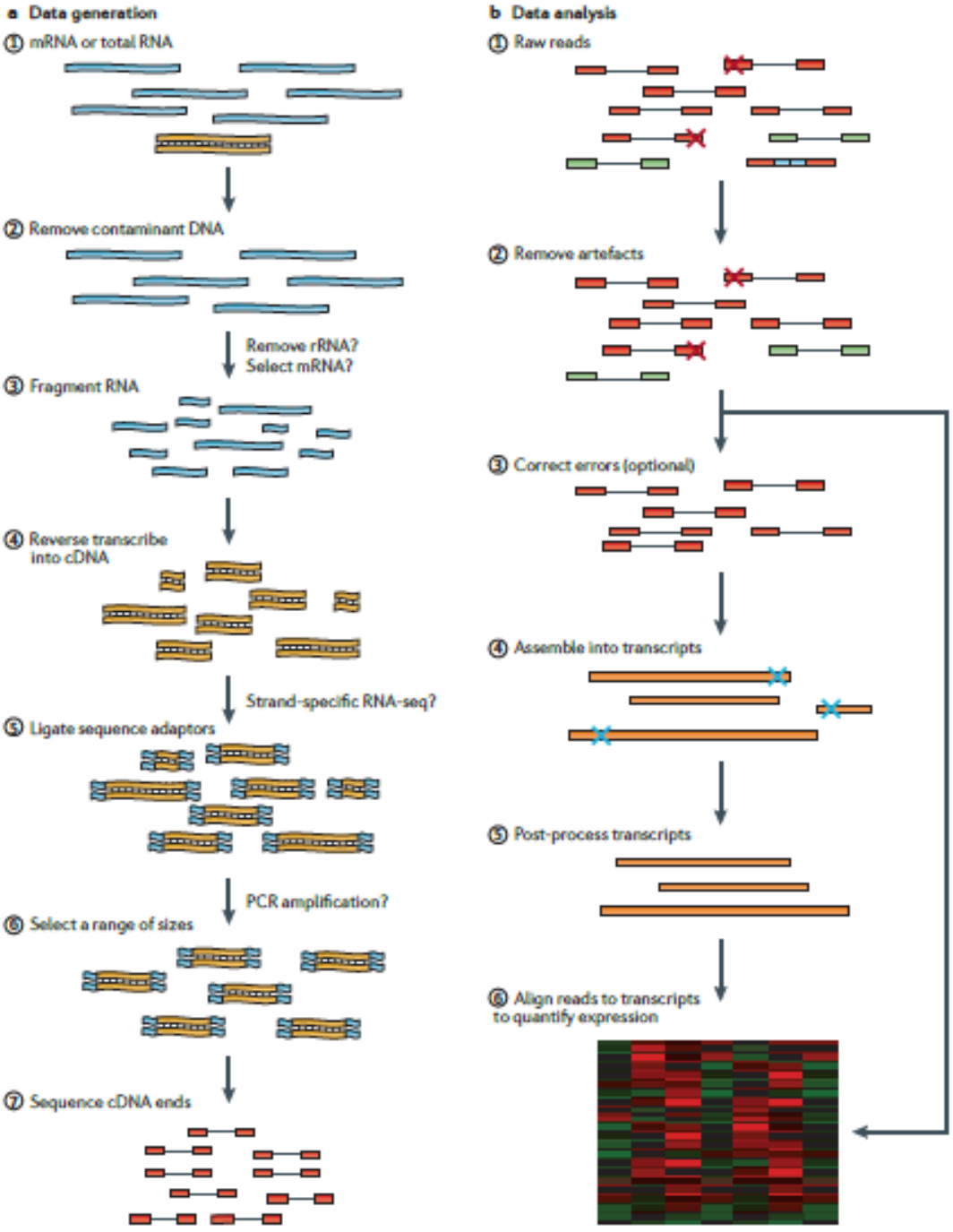

Figure 5. Example of a typical RNA-sequencing experiment (Martin, J.A. and Wang, Z., 2011).

MicroRNAs

The discovery of microRNAs twelve years ago (Ambros, V., 2004) brought to the forefront of epigenetic research the post-transcriptional gene regulation.

MicroRNAs are known to be involved in the maintenance of stem cell self-renewal and promotion of differentiation (Blakaj A, Lin H. 2008; Tay, Y. et al. 2008).

MicroRNAs are a class of small (~22 nt) non-coding RNAs that bind through a 5´ "seed region" to the 3´untranslated region (3´ UTR) of target mRNAs driving them to translation repression and/or mRNA degradation (**Fig. 6**) (Bartel, D.P. 2009).

It has been estimated that since microRNAs only need as few as 7 nucleotides of complementarity to bind to their target, computational and experimental approaches indicate that more than 60% of human protein coding genes are predicted to contain microRNA-binding sites. This fact highlights the necessity for microRNA profiling in order to acquire a more complete understanding of their identity and role in different biological contests. The small size of mature microRNAs renders them suitable for characterization using RNA-seq technologies by implementing the appropriate modifications in sequencing and bioinformatics analysis.

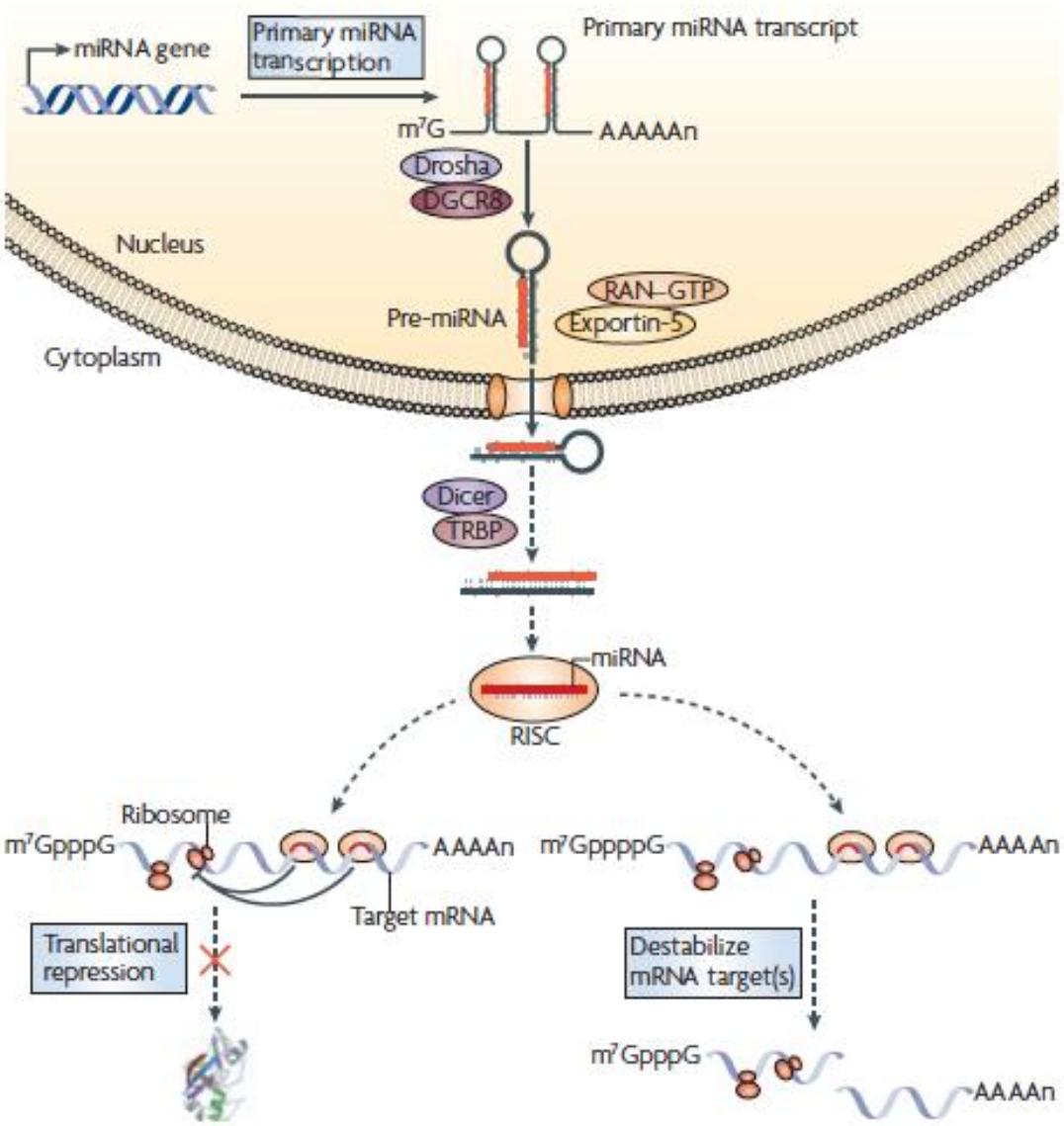

Figure 6. Biogenesis and function of microRNAs in mammals.

Scope of the study

Since the discovery of NSCs, researchers have focused on maintenance mechanisms of these cells. The main goal is to use them to treat impaired tissues or to improve regenerative power of degenerating cells in neurodegenerative diseases or spinal cord injuries. Under maintenance conditions, NSCs express several stemness genes (e.g. Nanog, Oct4, Sox2) whose mechanisms of regulation have been investigated (Garg, N. et al., 2013; Po, A. et., 2010; Kim, J. B., 2009; Zhang S, Cui W., 2014). However, the interplay between other transcription factors and NSCs maintenance is still being charted.

Therefore, the aim of the study was to understand stemness molecular mechanisms, investigating the role of transcription factors and microRNAs, in NSCs compared to their differentiated counterparts. With this aim next-generation RNA sequencing was used that allowed the identification of transcripts and microRNAs characterizing NSCs. The highest expressed transcript in NSCs implicated in the Hh signaling was Forkhead Box m1 (Foxm1), part of the FOX superfamily of transcriptional regulators that play a pivotal role in cell cycle progression. Therefore, the study focused on identifying a Foxm1-microRNA network involved in maintaining NSCs.

Results

High-throughput transcriptome profiling of cerebellar NSCs

Cerebellar NSCs from postnatal day 4 (P4) mice were grown in stem-cell-selective medium, as described elsewhere (Po, A. et al., 2010). As expected, under these conditions, the cells displayed high-level expression of stemness genes (Nanog, Nestin) and of Gli1 (**Fig. 7A**). Transfer of these NSCs to differentiation medium (Po, A. et al., 2010) was followed by significant increases in the expression of genes encoding astrocytic, neuronal, Purkinje, and oligodendrocytic cell markers (**Fig. 7B**).

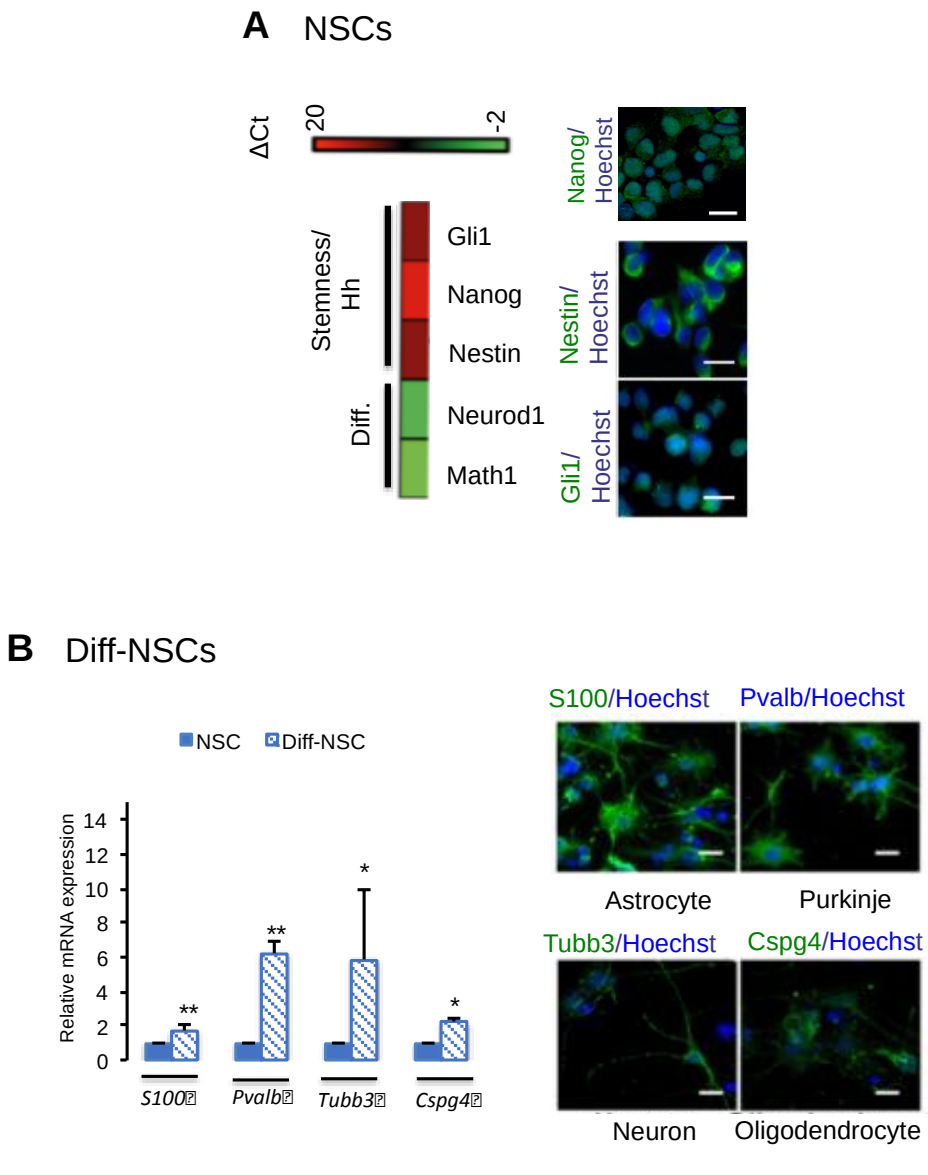

Figure 7. Characterization of P4 murine cerebellar NSC cultures before and after differentiation.

A *Heatmap*: Levels of mRNA for markers of stemness (Nanog, Nestin), Hh-Gli signaling (Gli1), and neuronal differentiation (Neurod1, Math1) in NSCs grown in stem-cell-selective medium. Transcript levels are represented on a green-red color scale based on ΔCt values. Immunofluorescence images: Representative results of NSC staining for markers of stemness and Hh-Gli signalling (green); nuclei are counterstained with Hoechst (blue).

B *Left*: Levels of mRNA for genes encoding neuronal differentiation markers in NSCs grown for 48 h in differentiation medium (Diff-NSCs), as measured by RT-qPCR single assays. P values vs. pre-differentiation NSC controls: **P<0.01: 0.0019 (S100 P), 0.0083 (Pvalb); *P<0.05: 0.0298 (Tubb3), 0.0316 (Cspg4) (unpaired T-test). *Right*: Representative results of immunofluorescence staining of Diff-NSCs for neuronal differentiation markers (green); nuclei are counterstained with Hoechst (blue). Scale bar: 5 µm for all panels.

Paired-end polyA+ RNA-sequencing was used to profile the transcriptomes of NSCs grown in stem cell and differentiation media (NSCs and Diff-NSCs, respectively; three replicates of each). A total of 988 genes were differentially transcribed by the cells under these two conditions. NSCs and Diff-NSCs were clearly segregated, as observed in the hierarchical clustering of the 988 differentially expressed transcripts (DETs) (**Fig. 8 and Supplementary Table 5).**

Transcripts displaying significant differential expression (DETs) in NSCs and Diff-NSCs

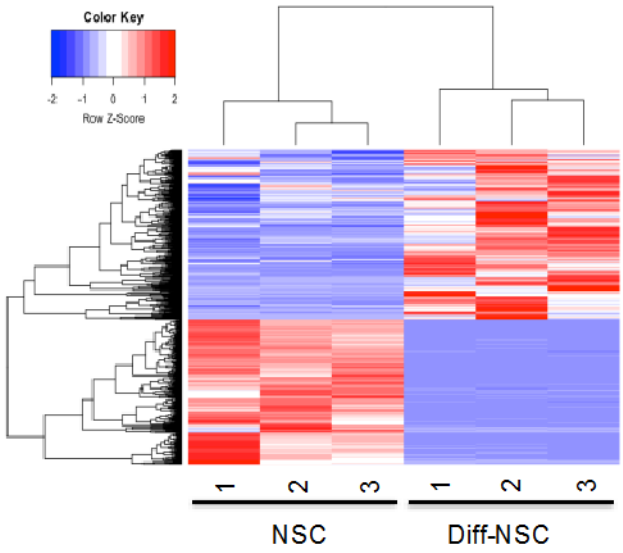

Figure 8. Clustering of differentially expressed transcripts (DETs) in NSCs and Diff-NSCs.

Hierarchical clustering of the 988 transcripts differentially expressed (adj. $P < 0.05$) (Bray-Curtis method with average linkage).

Functional analysis of the DETs using the DAVID platform (Database for Annotation, Visualization and Integrated Discovery) revealed significant enrichment (Bonferroni-corrected $P<0.05$) for the four Gene Ontology categories reported in **Table 1** and detailed in **Figure 9**. The most interesting clue that emerged from this analysis was the over-representation of genes involved in p53 signalling. This pathway is a well-known negative regulator of NSCs self-renewal (Garg, N. et al., 2013; Solozobova, V. & Blattner, C., 2011), whose activity is modulated by signalling through the Hh-Gli-Nanog axis (Lin, T. et al., 2005; Po, A. et al., 2010).

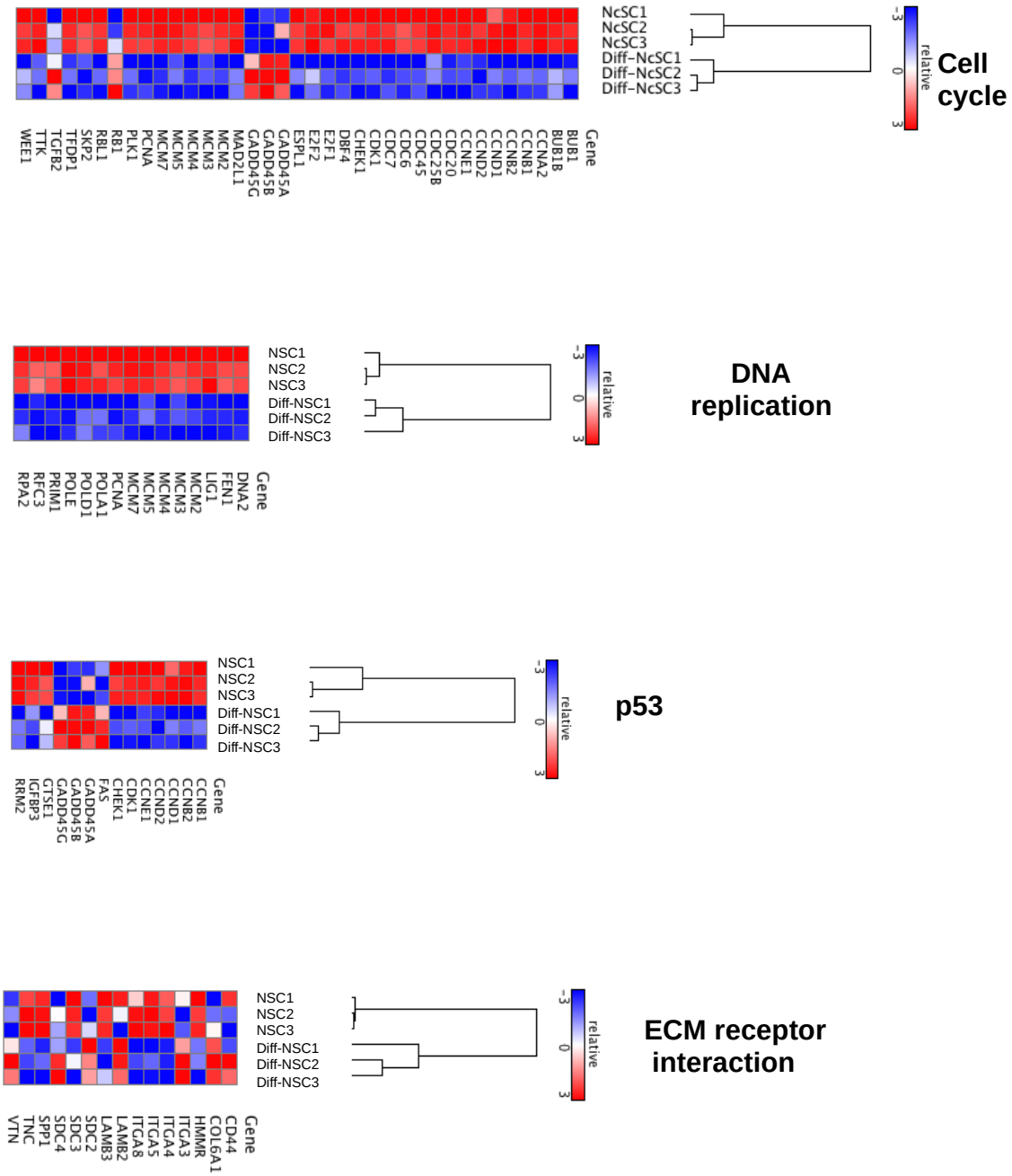

Figure 9. Functional analysis of DETs in NSCs and Diff-NSCs.

Functional analysis with DAVID (see **Table 1**). Clusters are shown with heat maps indicating transcript abundance (based on normalized FPKM values) for genes belonging to each Gene Ontology (GO) category.

Hedgehog–Gli pathway components enriched in NSCs

In order to identify other molecular players with potential roles in Hh-Gli-driven self-renewal of cerebellar NSCs, a compiled list of 53 genes known to be regulated by Hh-Gli signalling in settings (physiologic or pathologic) other than NSCs (**Supplementary Table 1**) was used. Nine of these genes were differentially transcribed in NSCs before and after differentiation (**Supplementary Table 2**, **Figure 10**). Six of the nine genes encode cyclins (Ccnb2, Ccnb1, Ccna2, Ccnd2, Ccne1, Ccnd1) known to be involved in the regulation of cell cycle and cell division in NSCs. The seventh, Sema6a, is involved in nervous system development, in particular, in axon guidance (Rivron, N. C. et al., 2012), and the eighth gene, Insm1, has been reported to be involved in mouse cerebellar development (De Smaele, E. et al., 2008).

Analysis of this list revealed that Foxm1 was the Hh-Gli-regulated transcription factor most markedly expressed in NSCs prior to differentiation. Foxm1 is a transcriptional activator (Wierstra, I., 2013) whose role as a downstream mediator of Hh-Gli signalling has been documented exclusively in human cancer cells (Teh, M.T. et al., 2002; Katoh, Y. and Katoh, M. 2006; Shi, C. et al., 2016). The relation between Foxm1 and Hh-Gli signalling was evident in our NSC model. Consistent with their high-level expression of Gli1 (**Fig. 7A**), the NSCs displayed strikingly higher levels of Foxm1—at both the transcriptional (**Fig. 11A**) and protein levels (**Fig. 10B**)—prior to their differentiation. Review of our mRNA-seq data confirmed this NSC-associated upregulation for two of the four known protein-coding Foxm1 transcript isoforms (ENSMUST00000073316 [Foxm1-201] and ENSMUST00000112148 [Foxm1-202]). As shown in **Figure 11B**, this finding was validated by PCR performed with isoform-specific primers and by immunoblot analysis, which revealed clear predominance in the NSCs of the 757-amino-acid Foxm1-201 protein isoform.

A

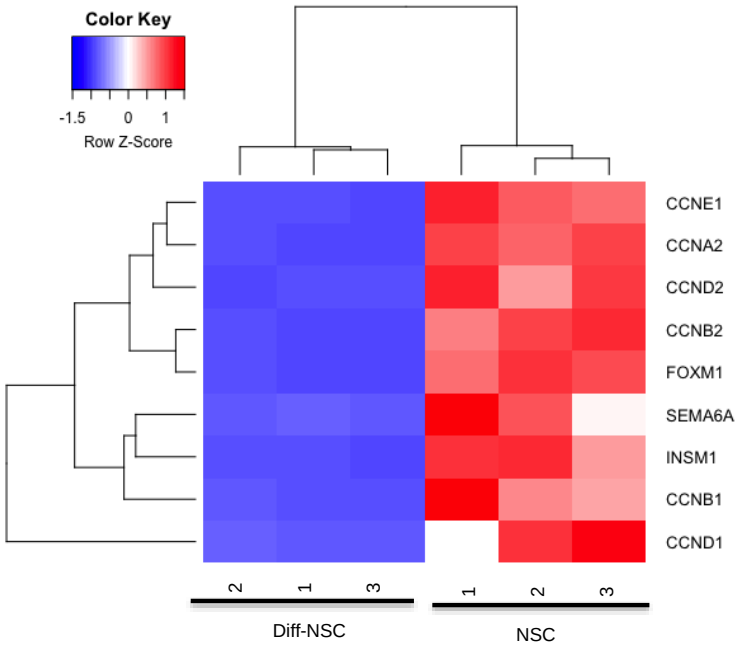

B

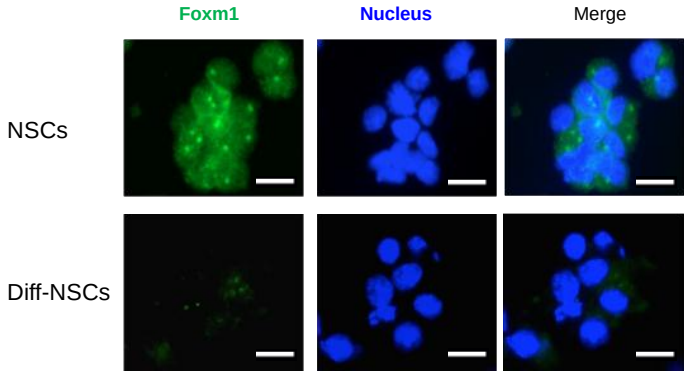

Figure 10. The Hh-signalling mediator Foxm1 is differentially expressed in NSCs and Diff-NSCs.

A Heatmap and dendrogram of the nine DETs whose genes are regulated by Hh signalling.

B Immunofluorescence staining of endogenous Foxm1 (green) in NSCs and in Diff-NSCs. Nuclei were counterstained with Hoechst (blue). Scale bar: 5 μm.

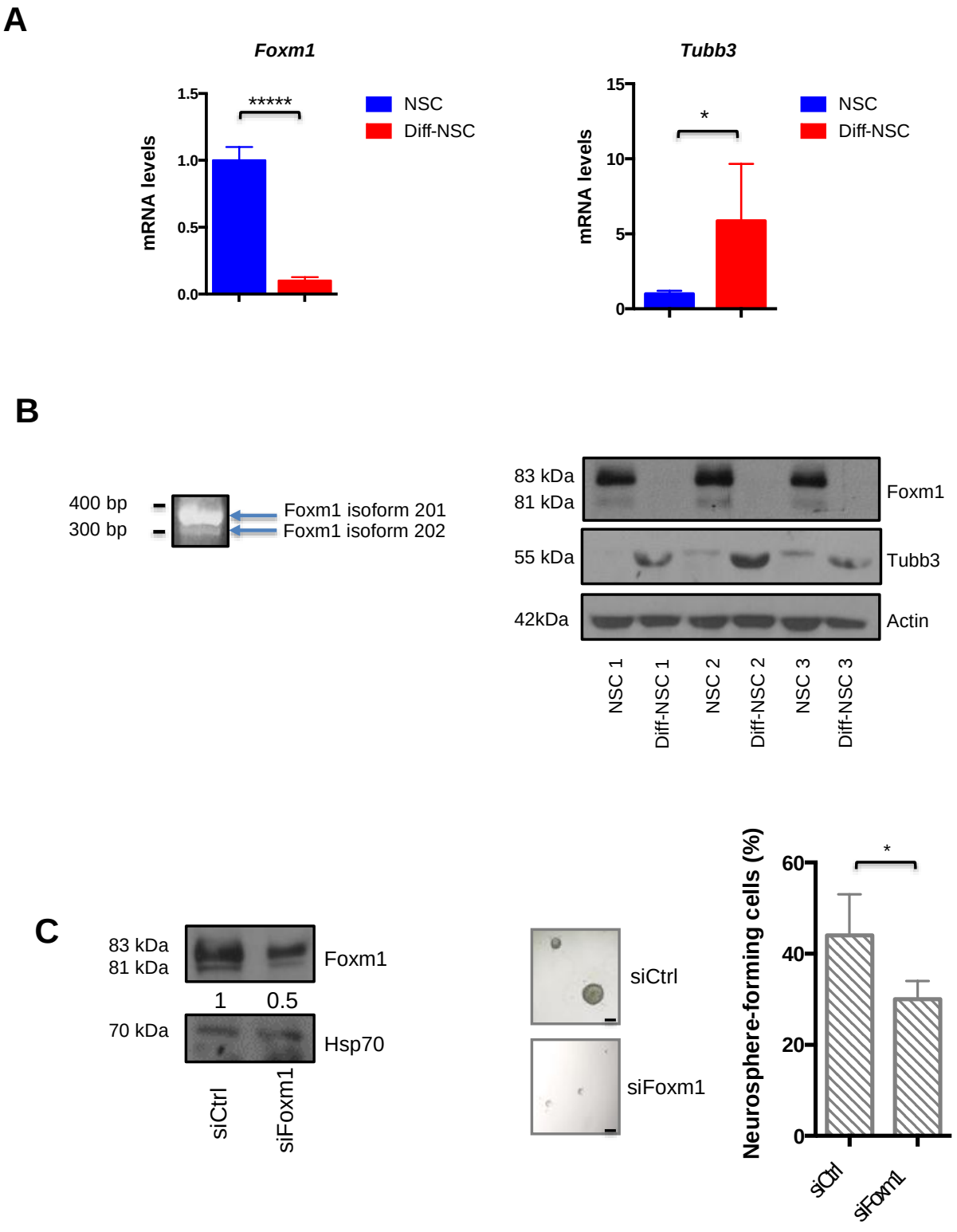

Figure 11. Upregulated expression of Foxm1 in P4 cerebellar NSCs and its effect on self-renewal.

A RT-qPCR data showing differential expression in pre- and post-differentiation NSCs of mRNA for Foxm1 (*****P<0.0001: 0.0000089) and the neuronal differentiation gene Tubb3 (*P<0.05: 0.029) (Mann–Whitney U test).

B *Left*: PCR assay of Foxm1 expression using isoform-specific primers. Agarose (2%) gel separation of the amplified product yielded two bands corresponding to Foxm1 isoforms 201 (400 bp) and 202 (300 bp). *Right*: Immunoblots showing endogenous levels of Foxm1, Tubb3, and Actin (loading control) in three NSC cultures before and after induced differentiation.

C *Left*: Immunoblots showing endogenous levels of Foxm1 and Hsp70 (loading control) in NSCs transfected with siRNA against Foxm1 or non-targeting siRNA controls (siCtrl). Densitometric values appear below blots.

Right: Representative bright-field images of neurospheres formed by NSCs transfected with siCtrl and siFoxm1. Scale bar: 100μm. Graphs show percentages of seeded cells that formed neurospheres (*P<0.05: 0.036) (Two-tailed paired t-test).

Bars in panels A and C represent the mean (SD) of three independent experiments.

Foxm1 mediates Hh–Gli-driven self-renewal of the NSCs

To explore the functional relevance of this upregulation, NSCs were transfected with siRNA directed against Foxm1 (siFoxm1) and evaluated for their self-renewal capacity, as reflected by their ability to form neurospheres. As shown in **Figure 11C**, Foxm1 knock-down was associated with significantly impaired neurosphere formation.

Comparison of the human FOXM1 and murine Foxm1 promoter regions revealed a high percentage of identical base pairs (36%-45%), which indicated substantial similarity. Consistent with recent findings on its human ortholog (Shi, C. et al., 2016; Wang, D. et al., 2017), the murine Foxm1 promoter was found to harbour eight putative Gli-binding sites (s1–s8) (**Figure 12A** and **Supplementary Information-Section 1**). Quantitative PCR-ChIP assays were performed in order to determine whether both transcriptional activators of the Hh-Gli pathway could occupy the Foxm1 promoter in these putative binding sites. Experiments were performed in NSCs both before and after differentiation to quantitatively assess Gli recruitment and histone H3 acetylation (AcH3, a marker of transcriptional activation). Transcriptional activation was reported in all putative Gli binding sites (s1-5) and (s6-8) as evidenced by the higher percentage of promoter occupancy in NSCs when compared to Diff-NSCs. In particular, Gli2 reported a significantly higher percentage of occupancy in the Gli (s1-5) binding sites of the Foxm1 promoter in NSCs in respect to Diff-NSCs (**Fig. 12B**). Similarly, Gli1 promoter occupancy in the Gli (s6-8) binding sites of the Foxm1 promoter was

significantly higher in NSCs when compared to Diff-NSCs (**Fig. 12C**). These data concluded that Gli-binding sites were bound by both transcriptional activators of the Hh-Gli pathway in NSCs.

Luciferase reporter assays showed significant activation of Foxm1 by Gli2 binding and to a somewhat lesser extent by the binding of Gli1 (**Fig. 12D**). Collectively, these findings strongly support the importance of Foxm1 as a major mediator of Hh–Gli-driven self-renewal of the NSCs phenotype in the post-natal murine cerebellum.

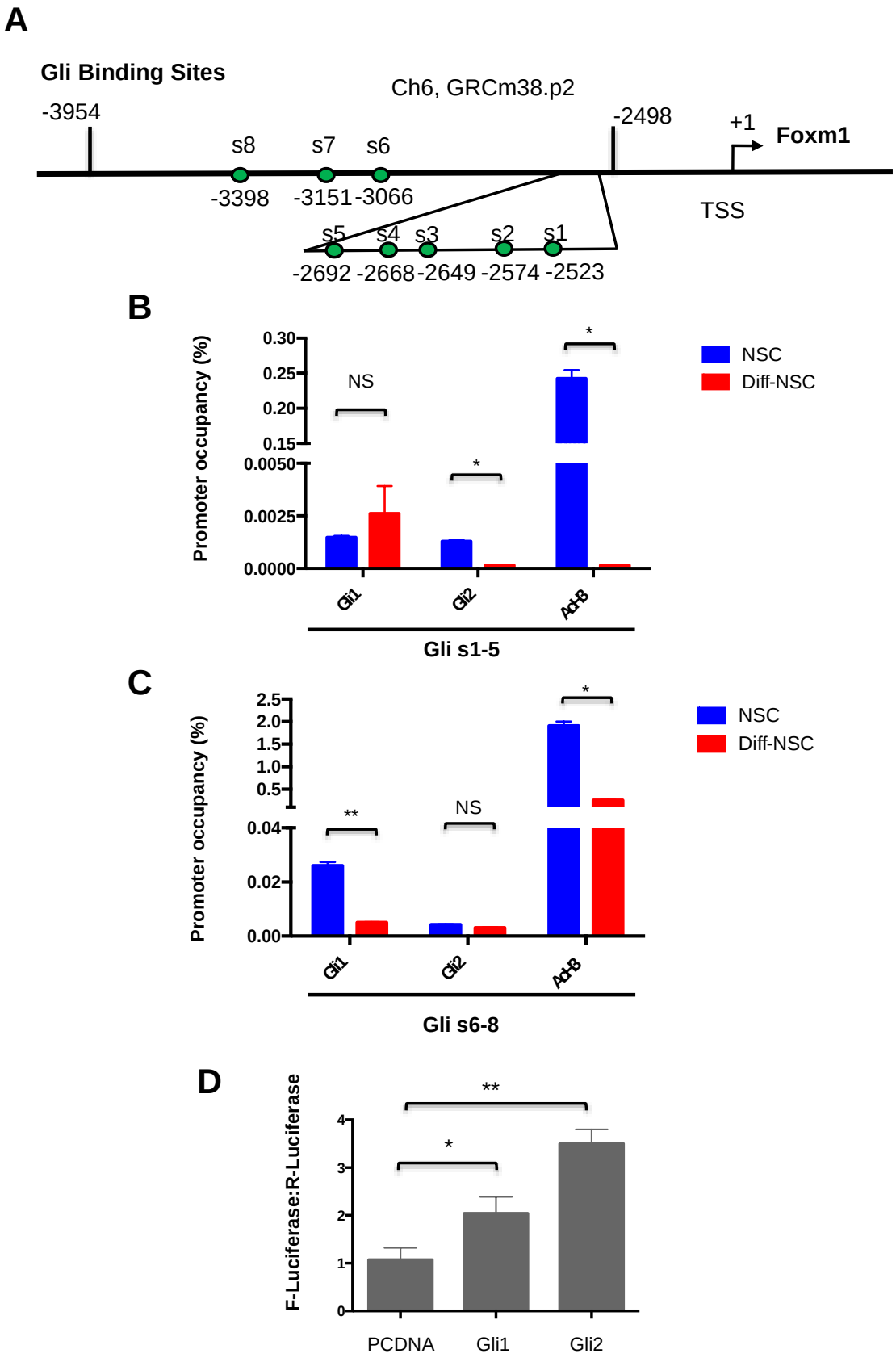

Figure 12. Foxm1 promoter occupancy by Gli1 and Gli2.

A Schematic of the Foxm1 promoter showing locations of the 8 putative Gli-responsive elements (s1–s8).

B-C qPCR-ChIP assay of endogenous Gli1 and Gli2 occupancy of the Foxm1 promoter region in NSCs and Diff-NSCs. Immunoprecipitation with anti-acetyl-H3 antibodies was used to detect Foxm1 transcriptional activation. Eluted DNA was qPCR-amplified using primers for putative Gli binding sites [s1–s5 (B) and s6–s8 (C)]. Results are expressed as fold induction values relative to ChIP input controls. Bars represent means (SD) of three independent experiments. P values vs. Diff-NSCs (Mann-Whitney U test): (B) *P<0.05: 0.04797 (s1-5, Gli2), 0.03271 (s1-5, AcH3); NS (not significant): 0.2514 (s1-5, Gli1). (C) *P<0.05: 0.0490 (s6-8, AcH3); **P<0.01: 0.001374 (s6-8, Gli1); NS: 0.296763205 (s6-8, Gli2).

D Luciferase activity induced in the Foxm1 promoter region in 293T cells by Gli1, Gli2, and PCDNA (negative control). Results are normalized to pRL-CMV-Renilla luciferase (R-Luciferase). Bars represent means (SD) of at least three independent experiments, each performed in triplicate. P values vs. control cells (One-way ANOVA test): *P<0.05: 0.02 (Gli1); **P<0.01: 0.005 (Gli2).

Foxm1 modulates stemness through the activation of specific microRNAs in NSCs

As previously noted, the Hh-Gli-regulated stemness marker, Nanog, modulates the proliferation and self-renewal of murine cerebellar NSCs via miRNA-mediated suppression of genes promoting cell-cycle arrest and differentiation (Garg, N. et al., 2013; Po, A. et al., 2010). This observation lead to the question whether miRNAs might also play a role in Foxm1's effects on NSC self-renewal. As shown in **Figure 13A**, miRNA-sequencing studies identified 80 microRNAs that were differentially expressed in NSCs and Diff-NSCs.

To identify miRNAs likely to be direct targets of Foxm1, the promoter regions of the 40 miRNAs that were upregulated in NSCs (**Supplementary Table 3)** were examined and putative Foxm1 binding sites were found in 20. To increase the chances of identifying targets with biological relevance to NSC self-renewal, subsequent analyses were restricted to the 15 miRNAs on this list with the most statistically significant upregulated expression in the NSCs (**Table 2**, **Fig. 14**). (See **Supplementary Information-Section 2** for the promoter regions of the miRNAs).

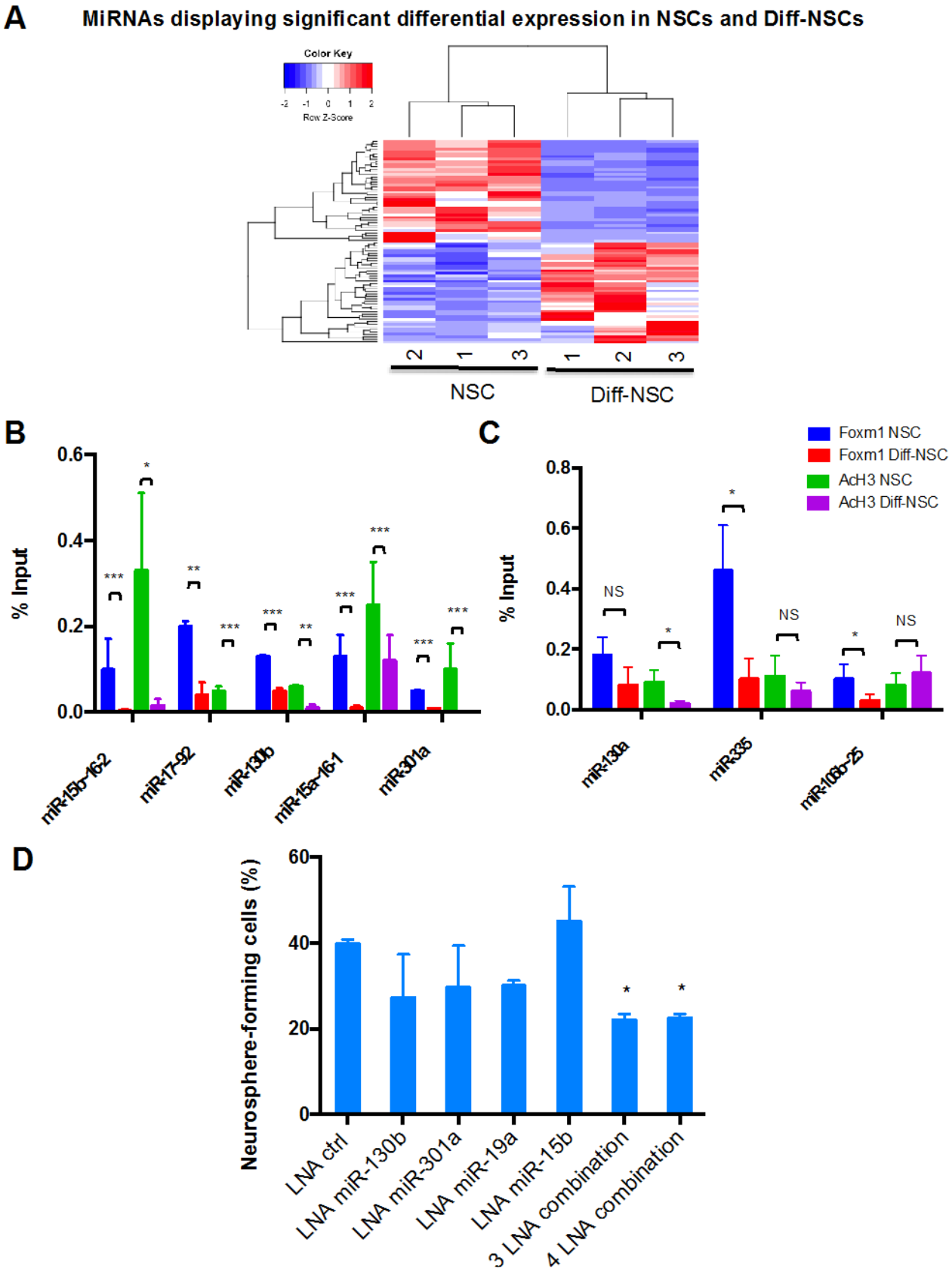
A
MiRNAs displaying significant differential expression in NSCs and Diff-NSCs
Color Key
-2 -1 0 1 2
Row Z-Score
2 1 3 1 2 3
NSC
Diff-NSC
B
% Input
0.6
0.4
0.2
0.0
miR-15b~16-2
miR-17-92
miR-130b
miR-15a~16-1
miR-301a
C
Foxm1 NSC
Foxm1 Diff-NSC
AcH3 NSC
AcH3 Diff-NSC
% Input
0.8
0.6
0.4
0.2
0.0
NS
miR-130a
miR-335
miR-106b~25
D
Neurosphere-forming cells (%)
60
40
20
0
LNA ctrl
LNA miR-130b
LNA miR-301a
LNA miR-19a
LNA miR-15b
3 LNA combination
4 LNA combination

Figure 13. Foxm1 controls the transcription in P4 murine cerebellar NSCs of multiple miRNAs and miRNA clusters that affect NSC neurosphere formation.

A Heat map and dendrogram depiction of the 80 miRNAs displaying significant differential expression in NSCs before and after induction of differentiation.

B-C qPCR-ChIP assays of NSCs and Diff-NSCs using anti-Foxm1 antibody and anti-acetyl-H3 antibody. Eluted DNA was PCR-amplified with primers annealing to promoter regions of the microRNA genes of interest. Findings for miRNA candidates belonging to a cluster are based on assays of one representative cluster member. Results are expressed as fold induction versus input controls. Bars represent the mean (SD) of three independent experiments. P values NSCs vs. Diff-NSCs (Mann–Whitney U test):

Statistically significant (B) Foxm1: **P<0.01: 0.002204 (miR-17~92); ***P<0.001: 0.000 (miR-15b~16-2), 0.0003471 (miR-130b), 0.00004 (miR-15a~16-1), 0.0003906 (miR-301a).

AcH3: *P<0.05: 0.049416827 (miR-15b~16-2); **P<0.01: 0.008868 (miR-130b); ***P<0.001: 0.0008656 (miR-17~92), 0.00000069 (miR-15a~16-1), 0.00000920 (miR-301a). Not Significant

(C) Foxm1: *P<0.05: 0.01467 (miR-335), 0.01021 (miR-106b~25); NS: not significant: 0.07214 (miR-130a). AcH3: *P<0.05: 0.02903 (miR-130a); NS: 0.5259 (miR-335), 0.4417 (miR-106b~25).

D LNA anti-miR-130b, -miR-301a, miR-19a (to inhibit miR-17-92 cluster members) and miR-15b (to inhibit miR-15-16 cluster members) were used separately and combined. [3 LNA combination: anti-miR-130b, -miR-301a, and miR-19a; 4 LNA combination: anti-miR-130b, -miR-301a, miR-19a, and miR-15b]. Bars represent means (SD) of at least three independent experiments performed in triplicate. P values vs. scrambled LNA control (One-way ANOVA test): *P<0.05: 3 LNA combination: 0.0424 ; 4 LNA combination: 0.0500).

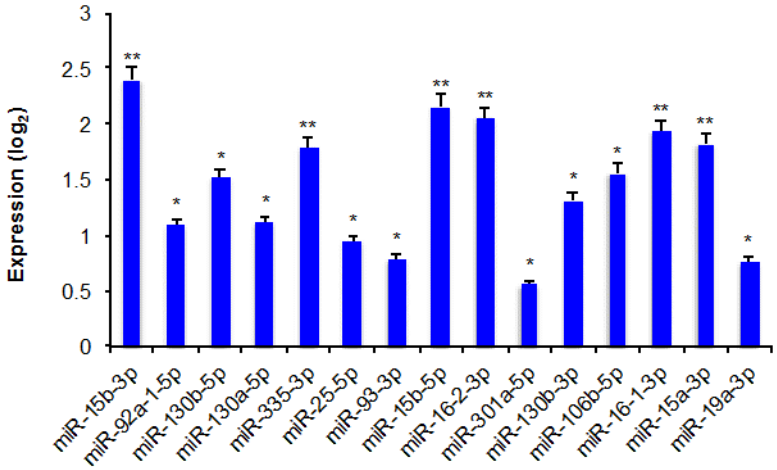

Figure 14. Validation of miRNAs displaying significant differential expression in NSCs vs. Diff-NSCs.

Q-PCR single assay validation of NSC expression of the top 15 DE miRNAs listed in Table 2. Results for each miRNA are expressed as the log2 fold change relative to NSC expression of the endogenous control gene U6. Bars represent the mean (SD) of three independent experiments. P values vs. U6 control (Mann–Whitney U test): **P<0.01: 0.0058 (miR-15b-3p), 0.0092 (miR-335-3p), 0.0069 (miR-15b-5p), 0.0074 (miR-16-2-3p), 0.0078 (miR-16-1-3p), 0.0099 (miR-15a-3p); *P<0.05: 0.029 (miR-92a-1-5p), 0.0204 (miR-130b-5p), 0.022 (miR-130a-5p), 0.031 (miR-25-5p), 0.037 (miR-93-3p), 0.042 (miR-301a-5p), 0.021 (miR-130b-3p), 0.019 (miR-106b-5p), 0.032 (miR-19a-3p).

Quantitative PCR-ChIP assays were then performed on NSCs before and after differentiation to quantitatively assess Foxm1 recruitment and histone H3 acetylation (AcH3) at the promoter region of each miRNA gene putatively targeted by Foxm1. The 15 microRNAs were either transcribed singularly or as part of a cluster (**Table 2**), in case of a cluster for further experiments expression levels of one representative miRNA are reported. For all miRNAs tested Foxm1 recruitment was higher in the NSCs when compared to Diff-NSC. Attention was focused on the cases where transcriptional activation of these promoters, as evidenced by AcH3, was significantly more intense in NSCs than in Diff-NSCs (**Fig. 13B-C**). Foxm1 recruitment indeed was statistically significant for miR-130b, miR-301a, and miRNAs belonging to the miR-15~16 and miR-17~92 clusters (**Fig. 13B**).

The results of the previous experiments pointed to miR-130b, miR-301a, and miRNAs of miR-15~16 (n=4) and miR-17~92 clusters (n=2) as particularly important mediators of Foxm1's effects in NSCs. This conclusion was supported by the effects observed in the cells after locked nucleic acid (LNA)-mediated depletion of these miRNAs. As shown in **Figure 13D**, the NSCs' capacity for neurosphere formation was not significantly reduced by anti-miR knockdown of any single miRNA or miRNA cluster. However, it was significantly impaired by combined depletion of miR-130b, miR-301a, and miR-19a (3 LNA combination). The additional depletion of miR-15b (4 LNA combination) resulted in an equally significant impairment of neurosphere formation.

To investigate mechanisms underlying the stemness-promoting effects of this miRNA network, genes targeted by the ChIP-confirmed miRNAs listed in **Table 2** were explored. A miRTarBase (http://mirtarbase.mbc.nctu.edu.tw/) search returned validated murine targets for only three of these miRNAs: miR-15b-5p, miR-130b-3p, and miR-92a-3p (**Supplementary Table 4**). Thus requiring, the extension of the search to the literature on each miRNA, focusing specifically on validated or putative target genes (in any species) whose downregulation could explain the combined effect of these miRNAs in NSC self-renewal.

The results that emerged reiterated the importance of p53 signalling, whose loss/suppression is essential for the maintenance of embryonic stem-cell pluripotency (Hong, H. et al. 2009; Kawamura, T. et al. 2009). Of particular interest was a report showing that miR-130b-3p regulates CD133+ tumour-initiating cells in human hepatocellular carcinoma by targeting TP53INP1 (Ma, S. et al. 2010), which encodes a downstream component of the p53 signalling pathway. Previous work of the laboratory showed that Trp53inp1 expression in murine cerebellar NSCs is also suppressed by microRNAs of the miR-17~92 cluster, and the upregulated expression of these miRNAs was attributed to signalling through the Hh-Gli-Nanog axis (Garg, N. et al., 2013). In light of the current findings, p53 signalling in these cells also appears to be under the control of a second miRNA network, this one regulated by Foxm1. In support of this hypothesis, mirSVR prediction scores provided by microRNA.org (http://www.microrna.org/microrna/home.do) indicate that murine Tp53inp1 is a very likely target of miR-130b (mirSVR score: -0.0029). The same applies to miR-301a, another Foxm1-regulated microRNA belonging to the miR-130b family (mirSVR score: -0.0030). The Foxm1-regulated miRNA network that modulates p53 signalling might also comprise miR-92a-3p, whose validated targets include Trp63, another member of the p53 family of transcription factors. Because of the high-level sequence homology that characterizes these transcription factors, p63 and p73 are capable of transactivating p53-responsive genes, thereby causing cell cycle arrest and apoptosis (NCBI).

A role for Nanog in Foxm1 regulation

Interestingly, members of the miR-17~92 cluster are components of both the Nanog-regulated (Garg, N. et al., 2013) and Foxm1-regulated miRNA networks, but this was the only commonality observed. This evidence indicates that Nanog and Foxm1 activate largely non-overlapping cohorts of miRNAs to ensure suppression of p53 signaling in cerebellar NSCs. How these two networks interact to achieve this goal is unclear. Interestingly, Nanog has been identified as a target of Foxm1 (Wang, Z. et al. 2011; Xie, Z. 2010). To determine whether this relation might be reciprocal, the Foxm1 promoter region was re-examined for evidence of Nanog binding sites. As shown in **Figure 15A**, four putative binding sites for Nanog were found -3790 to -3277 bp upstream from the Foxm1 TSS. (For details, see **Supplementary Information-Section 1**).

ChIP experiments (**Fig. 15B**) demonstrated endogenous Nanog at these four sites in both NSCs and Diff-NSCs. However, pre- and post-differentiation occupancy rates were significantly different only at s2–s3, where the higher Nanog occupancy in NSCs was associated with greater activation of Foxm1. To further elucidate the relation between these two transcription factors, dual luciferase reporter assays was performed in 293T cells transfected with Foxm1 wild-type promoter or an s2- or s3-defective mutant promoter (**Fig. 15C**). Ectopic expression of Nanog in these cells resulted in

substantial activation of the wildtype promoter, whereas luciferase activity was appreciably reduced in the absence of s2 in the promoter and even more so by the deletion of s3, suggesting that this site is required for Nanog binding onto the Foxm1 promoter.

Taken together, these results indicate that the Hh-Gli-driven miRNA networks regulated by Nanog and Foxm1 are characterized by bidirectional crosstalk, which might conceivably allow more finely tuned, combinatorial regulation of cerebellar NSC self-renewal.

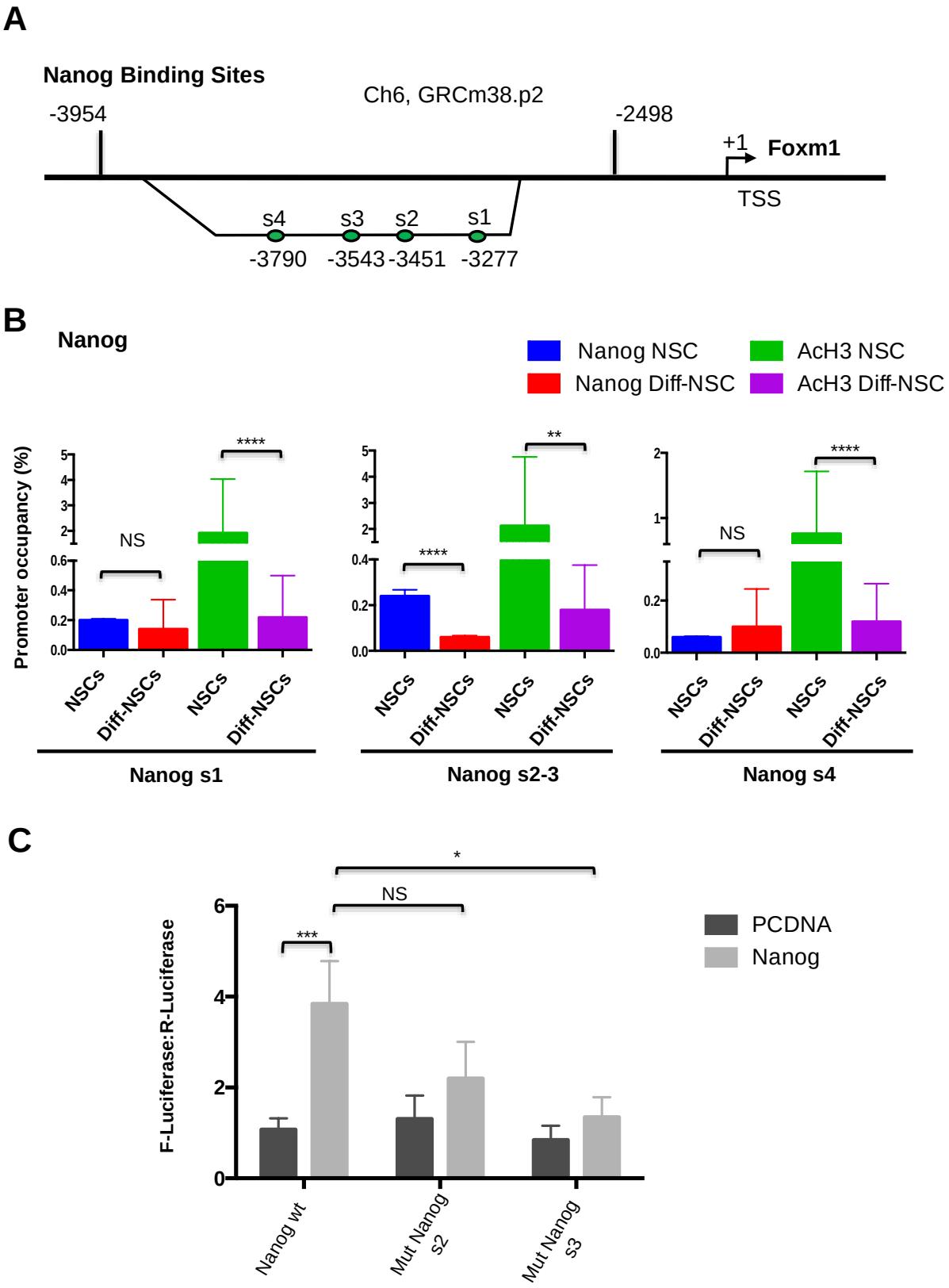

Figure 15. Foxm1 promoter occupancy by Nanog.

A Schematic of the Foxm1 promoter showing putative Nanog-responsive elements (s1; s2 and s3 which are fairly close to one another and s4).

B qPCR-ChIP assay of endogenous Nanog occupancy of the Foxm1 promoter region in NSCs and Diff-NSCs. Immunoprecipitation with anti-acetyl-H3 antibodies was used to identify Foxm1 transcriptional activation. Eluted DNA was PCR-amplified with primers for Nanog binding sites s1, s2-s3, s4. Results are expressed as fold induction values relative to input controls. Bars represent means (SD) of three independent experiments. P values vs. Diff-NSCs (Mann-Whitney U test): **P<0.01: 0.002572 (s2-3, AcH3); ****P<0.0001: 0.00000718 (s2-3, Nanog), 0.0001051 (s1, AcH3), 0.00004356 (s4, AcH3); NS: 0.4531 (s1, Nanog), 0.7118 (s4, Nanog).

C Luciferase activity induced by ectopic expression of Nanog and PCDNA (negative control) in 293T cells transfected with luciferase vector carrying the wild-type Foxm1 promoter (wt) and its mutant lacking the Nanog binding sites s2 and s3 (mutants s2, s3). Results are normalized to pRL-CMV-Renilla luciferase (R-Luciferase). Bars represent means (SD) of at least three independent experiments, each performed in triplicate. P values vs. indicated controls (Mann–Whitney U test): *P<0.05: 0.01849; ***P<0.001: 0.0002265; NS: 0.08604.

Discussion

The main goal of this study was to characterize new molecular Hh-related mechanisms responsible for maintaining stemness features in cerebellar NSCs. These results permit the proposal of a model where Hh-Gli signalling controls the self-renewal of murine NSCs through the transcription of a series of microRNAs. As shown in **Figure 16**, two stemness miRNAs networks are described, via Nanog and via Foxm1, that partially overlap in our system and shed light to the role of Foxm1 in NSCs self-renewal. Hereby identifying the transcription factor Foxm1 as transcriptionally regulated by Hh through Gli 1 and 2 and Nanog. These results expand the list of known downstream effectors in the canonical Hh-Gli signalling pathway, as well as the list of molecules capable of activating Foxm1.

Foxm1 is an activating transcription factor that plays a role in several different cellular contexts. In human epidermal stem cells, Foxm1 sustains the balance between self-renewal and terminal differentiation (Gemenetzidis, E. et al., 2010). Foxm1 is known to regulate neuronal precursor induced mitosis (Gemenetzidis, E. et al. 2010), as well as several stem cell-like properties. It is required for proper execution of mitosis and this is highlighted by the fact that Foxm1 knockout is embryonically lethal (Wierstra, I. 2013). It has been reported that Foxm1 upregulates the expression of the neural stemness marker Nestin1 in NSCs from the embryonic cerebral cortices of mouse and is critical for their self-renewal (Wierstra, I. 2013). Mutants conducted with loss-of-function Foxm1 suggest that in the murine cerebellum its main function is the adjustment of the transition in G2 / M phase (Schuller U. et al, 2007; Gage, F.H. 2000). All previous studies did not however provide information regarding Foxm1's regulation or other functions in cerebellar NSCs.

Previous works of the laboratory reported Hh-related miRNAs involved in the maintenance of cerebellar NSCs (Ferretti, E. et al, 2008, Garg, N. et al, 2013). The present study has allowed to identify, through mRNA- and miRNA-sequencing, a series of Foxm1-controlled miRNAs highly expressed in NSCs. As a result, miR-130b, miR-301a and the clusters miR-17~92 and miR-15~16 were identified as direct transcriptional targets of Foxm1. Combined knock-down of these microRNAs leads to a significant decrease in terms of NSC abilities to form neurospheres. Such results show how microRNAs are fundamental for the self-renewal of these cells, through mediating the effects of Hh signal.

Subsequently, Foxm1-miRNAs were analysed. In support of this hypothesis, one of these miRNAs, miR-130b, has already been correlated with pro-proliferative effects in NSCs (Gong, X. et al., 2013) and that one of its target is Trp53inp1, a molecule involved in p53 pathway.

Also, the miR-17~92 cluster is part of the miRNA network, whose expression is required for the expansion of cortical NSCs in vivo (Bian, S. et al., 2013). Previous investigations of the group identified miR-17~92 cluster members as direct targets of signaling through the Hh-Gli-Nanog axis

and important regulators of NSC self-renewal (Garg, N. et al, 2013). This study demonstrated that these miRNAs are also components of the Foxm1-miRNA network.

In previous works it has been reported that Foxm1 regulates Nanog expression (Wang and Park et al., 2011; Xie, Z. 2010, Wierstra, I. 2013), and the presented data of this thesis have shown that Foxm1 itself is transcriptionally activated by Nanog, leading to a positive feedback regulation. It is evident from the proposed model that a crosstalk between Gli, Nanog and Foxm1 exists.

Moreover, Garg et al reported the maintenance of NSC self-renewal via the Gli-Nanog-miR-17~92 axis by counteraction of p53 inhibition of Gli and Nanog, through Trp53inp1 regulation. The dual suppression of Trp53inp1 via miR-17~92 cluster (Hh-Nanog- and Hh-Foxm1-microRNAs) and miR-130b (Hh-Foxm1-microRNAs alone) suggests a convergence, also partially overlapping on p53 pathway control. This convergence could suggest the possibility of some functional redundancy that could be part of a cellular protection mechanism in case of a gene mutation affecting key components of the regulatory network.

In the present work, it is demonstrated that miR-15~16 is part of the miRNAs regulated by Foxm1 and it cooperates to maintain the undifferentiated status of NSCs. In support to this hypothesis, a role for miR-15a has been described in neuronal context. It has been shown that the high expression of miR-15 appears to be involved in neuronal maturation in MeCP2-deficient adult-born new neurons (Gao, Y. et al., 2015). So, in cerebellar NSCs context it could act as a regulated of the balance between pro- and anti-stemness cues, mediating the effect of Hh-Gli-Foxm1 axis.

In conclusion, this project presents an in depth investigation of the Hh pathway in the context of the cerebellar NSCs. In addition, a new molecular mechanism Gli-Nanog-Hh-related that participates in the maintenance of the stemness features of these cells was described. The identified network is composed of a downstream effector of the Hh-Gli signalling, Foxm1, and a series of microRNAs transcribed by itself. It has been demonstrated how the Hh-Foxm1-microRNAs axis is involved in the fine-tuning of pro-proliferative and pro-apoptotic cues in these cells.

Based on the results of this study that identified Foxm1 as a downstream effector of the Hh-Gli signalling, and due to the high similarity of the human and mouse promoter regions of Foxm1, Foxm1 could be a major player and should be taken into consideration in future investigations regarding not only mouse but also human cells.

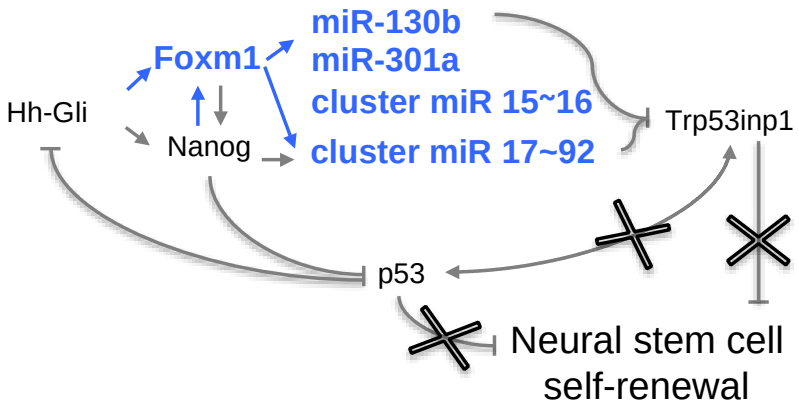

In blue the results of our study; in grey and black data from literature

Figure 16. Regulation of cerebellar NSCs self-renewal by the Hh-Foxm1-miRNA axis.

The tumour-suppressor p53 checks NSC self-renewal directly, by activating Trp53inp1, and by inhibiting Gli and Nanog. Increased Hh-Gli signalling promotes NSC self-renewal by inhibiting p53 and upregulating Nanog expression. Our data show (bold-face type) that it also upregulates the expression of Foxm1 (directly and indirectly via Nanog). These two transcription factors activate the expression of several miRNAs that target Trp53inp1. Silencing of Trp53inp1 allows expansion of the NSC pool by promoting proliferation and diminishing apoptosis. Its loss also disrupts a feedback loop that maintains high p53 levels, thereby diminishing the tumour suppressor's ability to repress Gli and Nanog expression.

Methods

Murine cerebellar NSC cultures

Cerebellar NSCs were isolated from P4 wild type black 6 /C56 (C57BL/6) mice (n=8 per group) and cultured, as previously described 3. In brief, freshly dissected cerebella were placed in HBSS supplemented with 0.5% glucose and penicillin-streptomycin and dissociated, mechanically and enzymatically. The cells were maintained as mycoplasma-free neurosphere cultures in selective stem-cell medium consisting of serum-free DMEM-F12 supplemented with 0.6% glucose, insulin 25 mg/ml, N-acetyl-L-cysteine 60 mg/ml, heparin 2 mg/ml, B27 supplement without vitamin A, EGF 20 ng/ml, and bFGF 20 ng/ml. To induce differentiation, the cells were transferred for 48 h to differentiation medium consisting of the medium described above, prepared without the EGF/bFGF and supplemented with platelet-derived growth factor (PDGF; 10 ng/ml) (Sigma, P3076). Mycoplasma contamination was excluded by routine screening with the PCR Mycoplasma Detection Kit (ABM, Cat. No. G238). The neurosphere-forming cells from these cultures were selected and re-plated in the same medium, where they gave rise to new neurospheres, thereby confirming the capacity for self-renewal. Animal experiments were performed according to the European Community Council Directive 2010/63/EU and were approved by the local Ethical Committee for Animal Experiments of the Sapienza University of Rome.

Experimental and analysis design

Overview of study design

NSCs (n=3) and Diff-NSCs (n=3) were subjected to RNA (mRNA-seq) and small-RNA (microRNA-seq) sequencing. A consensus-based approach was used to analyse the mRNA-seq dataset, in order to overcome any methodological bias inherent in specific alignment and differential expression tools. Two different tools were used for mapping and alignment, and three different approaches were used for the differential expression analysis. The intersection of all three methods resulted in common genes with similar expression changes (**Supplementary Table 5**). The expression values reported by the DESeq algorithm were used for the remaining analysis as representative of all methods. The common genes were used as input for the pathway enrichment analysis using DAVID (david.ncifcrf.gov). Potential downstream targets of the Hedgehog (Hh) pathway were taken under further consideration (**Fig S1**).

In parallel, the microRNA-Seq dataset was analysed using the DESeq2 algorithm to detect differential expression of microRNAs between NSCs and Diff-NSCs (**Fig S1**). Subsequently, from the list of up regulated microRNAs in NSCs, the binding sites of the highest expressed gene

implicated in the Hh pathway were searched in the promoter region of the microRNAs. Then, the candidate Transcription Factors (TFs) were validated and the network connecting the TFs and microRNAs was created (**Fig S1**).

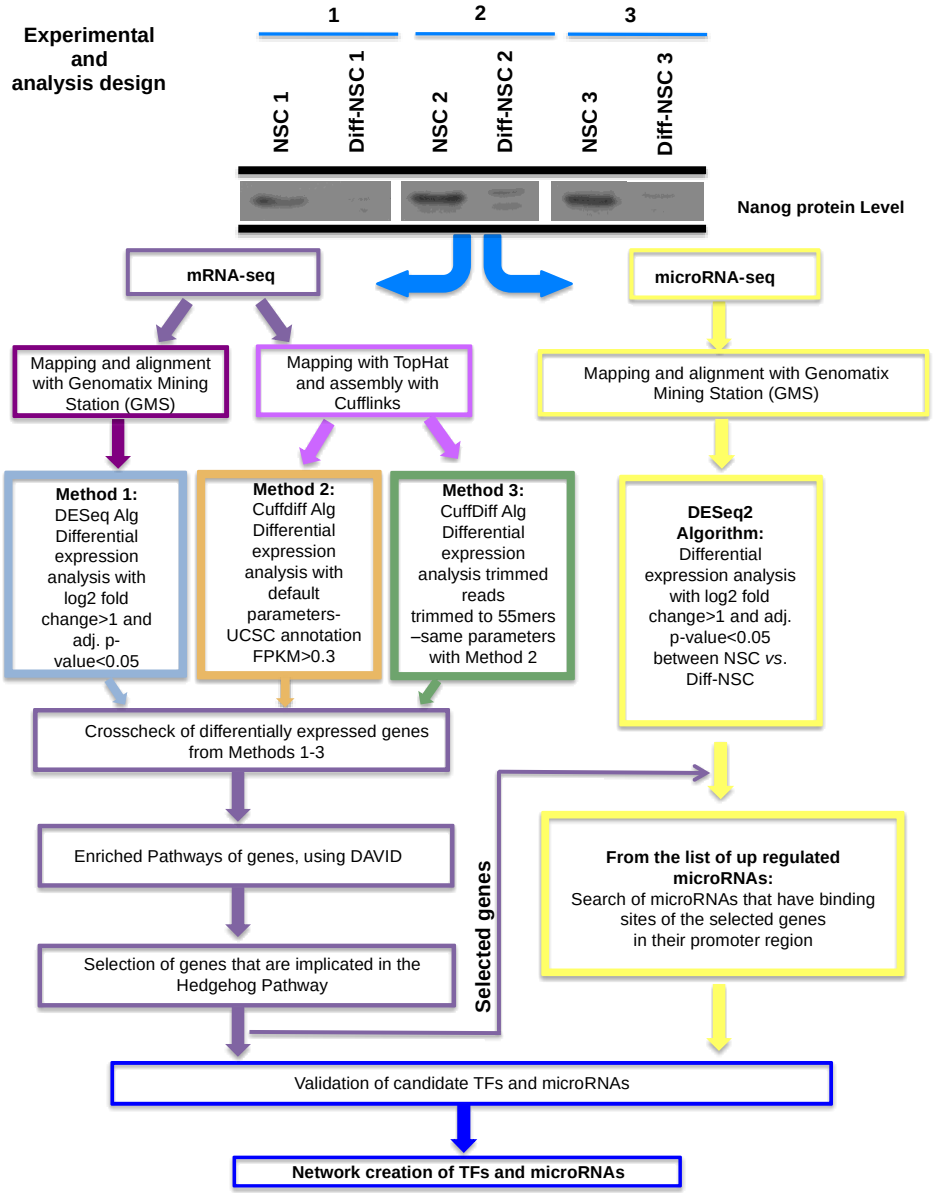

Fig S1.

Figure S1. Experimental and analysis design.

mRNA- sequencing

Library preparation and RNA sequencing

RNA extraction. Total RNA was extracted from NSCs and Diff-NSCs using Trizol reagent (Life Technologies, USA). Quality-control assays were performed on an Agilent BioAnalyzer using the RNA Nano Kit (Agilent # 5067-1511). Only RNAs with RIN values > 9 were used for library preparation. The standard Illumina protocol and TruSeq RNA Sample Prep Kit were used to construct the mRNA-seq libraries. The mRNA in 400 ng of total RNA was converted into a library of template molecules suitable for deep sequencing analysis. All samples were sequenced using the Illumina Genome Analyzer IIx.

Mapping and differential expression analysis of RNA-seq reads

Transcriptome mapping with Genomatix Mining Station and differential expression analysis with Genomatix Genome Analyzer (Method 1)

All 70mer paired-end sequenced reads were aligned to the latest version of the Mus musculus genome available at the time, (NCBI38/mm10), using the Genomatix Mining Station (GMS, Sesame 2.4, https://www.genomatix.de/). All samples were quality-controlled with the FastQC tool (http://www.bioinformatics.babraham.ac.uk/projects/fastqc/) before mapping, and an average of 75% of reads with a quality score >30 was obtained. In terms of annotation, the read distributions for NSCs and Diff-NSCs were similar (**Fig. S2B**), confirming the absence of biases in sequencing and normalization.

Differential expression analysis with Genomatix Genome Analyzer

The RNA-Seq sequenced samples were subjected to differential expression analysis using the DESeq method in the Genomatix Genome Analyzer platform (GGA, v3.30126, https://www.genomatix.de/). Differentially expressed transcripts were selected as those exhibiting a minimum log2 fold change of 1 and adj. P-value < 0.05 (P-value adjusted with multiple testing correction using the Benjamini and Hochberg method).

Transcriptome mapping with TopHat and differential expression analysis with Cuffdiff (Methods 2 and 3)

Mapping of RNA-Seq reads

All sequenced 70mer paired-end reads were aligned to the Mus musculus genome (NCBI37/mm9) using the spliced read aligner TopHat version v1.3.1 3. Two iterations of TopHat alignments have been made to maximize the use of splice site information derived from all samples.

RNA-Seq transcriptome assembly

The transcriptome of each sample was assembled separately from the mapped reads using Cufflinks V1.2.1 5 with default parameters and the UCSC reference annotation. Transcript abundance was estimated as fragments per kilobase of exon per million fragments mapped (FPKM).

Analyses of the transcript distributions after TopHat mapping and Cufflinks assembly among different samples, biological replicates and cell types exclude the presence of biases in sequencing and normalization (**Fig S3B, S3C and S3D**). The samples displayed similar proportions of alternatively spliced genes. Transcribed isoforms not annotated in the reference version of the UCSC were found in all samples (1100-1500 per sample). Clustering analysis of the expression data confirmed clear separation of NSCs from their respective Diff-NSCs and the similarity of biological replicates within each group (**Fig S3F**).

The RNA-Seq reads were processed using two variations of the same protocol: the standard whole-read protocol (Cuffdiff-WR, Method 2), as well as the variation of this protocol based on the analysis of trimmed reads (Cuffdiff-TR, Method 3). The motivation for the trimmed reads approach is based on the observation that some NSC samples had comparatively lower average base quality towards the end of the reads. By trimming all datasets to 55bp reads, mappability has been enhanced by eliminating low-quality bases, and avoiding mapping artifacts across samples, by ensuring a consistent read length. Additionally, the follow-on impact on differential expression analysis was tested by using these trimmed reads.

Comparison of the differential expression results from all different methods

After analysing our samples with three different methods, the intersection of the results was selected, which yielded 988 DETs (**Supplementary Table 5**). Comparing the expression among the three different algorithms, the Pearson correlation was confirmed between the DESeq method and Cuffdiff, and it was extremely high. Additionally, the ANOVA test was performed to verify that the values obtained using the DESeq method are representative of the other two methods (p-value=0.9567, no statistically significant differences among means and standard deviations). The Pearson correlation and ANOVA test were performed using GraphPad Prism version 6 (La Jolla, CA, USA, http://www.graphpad.com/). In conclusion, the three approaches show a high degree of synergy and that results are not affected by methodological bias, alignment artefacts, or sequence quality. For downstream analyses, the expression values obtained from the DESeq algorithm were selected as representative of all methods.

Functional Analysis

The Database for Annotation, Visualization and Integrated Discovery (DAVID, david.ncifcrf.gov) was used for functional annotation, Gene Ontology categories with a Bonferroni correction adjusted p-value < 0.05 were reported10.

Clustering analysis

Clustering and heat maps were generated in Gene-E (version 3.0.238, http://www.broadinstitute.org/cancer/software/GENE-E/) (**Supplementary Figure 2** for better visualization) and in R (http://www.r-project.org/) (the rest of the figures) using differentially expressed transcript levels as input. In Gene-E, the one minus Pearson correlation method was used for clustering and the complete linkage as a linkage method whereas in R the Bray-Curtis method and the average linkage were used in hclust to cluster the samples and heatmap.2 to generate the heat maps.

miRNA-sequencing

microRNA library preparation and sequencing

Small RNA-seq libraries were prepared in accordance with Illumina's TruSeq Small RNA Sample Prep Kit protocol.

Mapping of microRNA-seq reads and differential expression analysis with DESeq

Mapping of microRNA-seq reads

All sequenced single-end reads (31 bases) of the three biological replicates for each cell type (NSC and Diff-NSC) were controlled with FastQC (http://www.bioinformatics.babraham.ac.uk/projects/fastqc/) before mapping and they showed an average of 89% of reads with a quality score >30. All samples were aligned to the Mus musculus small RNA library (12-2013), (miRBase V20) using the Genomatix Mining Station (GMS, Sesame 2.4, https://www.genomatix.de/). The microRNA-seq read distributions for the NSCs and Diff-NSCs are shown in **Figure S5B**.

microRNA-seq reads and differential expression analysis

The microRNA-seq reads were analysed for differential expression in NSCs vs. Diff-NSCs in the Genomatix Genome Analyzer (GGA, v3.30126, https://www.genomatix.de/) using the DESeq2 method. Differences characterized by a minimum log2 fold change of 1 and an adjusted p-value of < 0.05 (Benjamini–Hochberg correction for multiple testing) were selected for further analysis.

Identification and characterization of binding sites in promoter regions

The MatInspector tool in the Genomatix Genome Analyzer was used to identify putative binding sites in the Foxm1 promoter for Gli and Nanog (**Supplementary Information – Section 1**. The Foxm1 promoter region) and putative Foxm1 binding sites in the promoters of miR-130b, miR-301a and representative members of miR-17~92 and miR-15~16 clusters (**Supplementary Information – Section 2.** The miRNA promoter regions). Occupancy of the Foxm1 promoter by endogenous Gli1, Gli2, and Nanog in NSCs and Diff-NSCs was assessed by real-time qPCR-ChIP assay. Anti-acetyl-H3 antibodies were used to identify transcriptional activation of Foxm1.

mRNA-Seq mapping statistics

mRNA-seq data were analysed with the Genomatix Mining Station (GMS) (Genomatix GmbH, Münich, Germany) and TopHat/Cufflinks. Mapping statistics for the two methods are summarized in **Figures S2A** and **S3A**, respectively. The number of reads per biological replicate that could be aligned to the mouse genome and the transcript distributions were similar with the two methods, thereby excluding the presence of biases in sequencing and normalization (**Fig S2-3**).

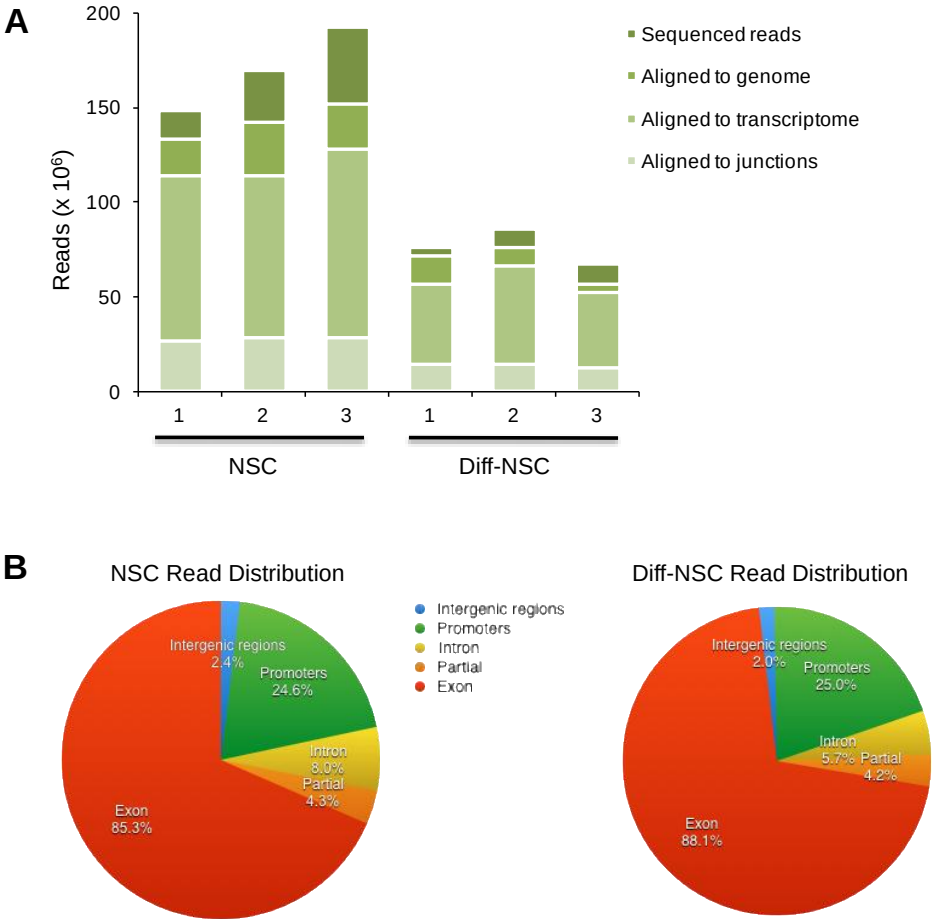

Fig S2.

Figure S2. mRNA-seq mapping statistics with Genomatix Mining Station.

A. Mean (SD) number of reads successfully aligned to the mouse genome, transcriptome, and exon junctions for each NSC and Diff-NSC sample.

B. Average distribution of reads mapped to the genome for NSC and Diff-NSC samples.

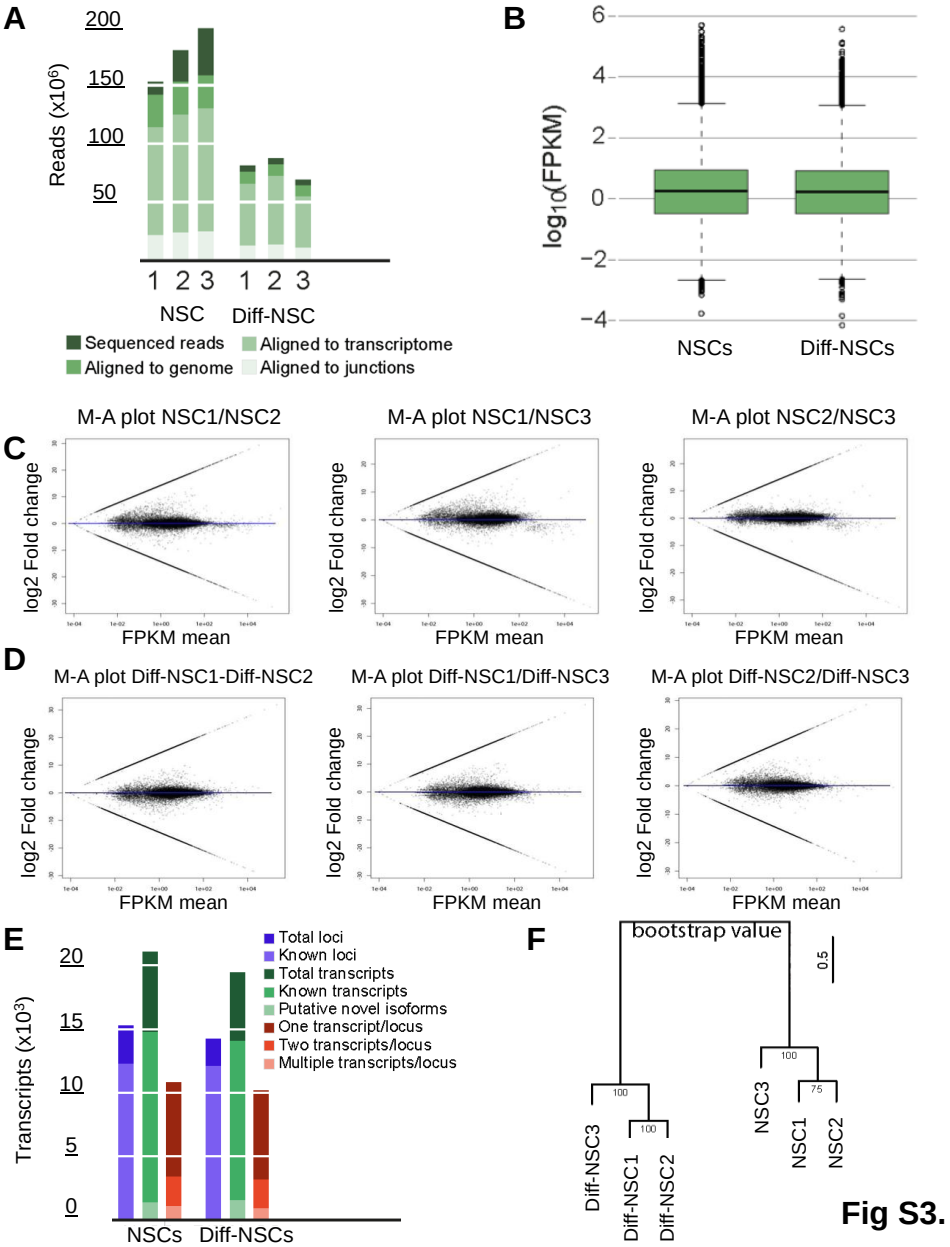

Fig S3.

Figure S3. mRNA-seq mapping statistics with TopHat and Cufflinks assembly.

A. Mean (SD) number of reads successfully aligned to the mouse genome, transcriptome, and exon junctions for each NSC and Diff-NSC sample.

B. Box plots showing FPKM values (median [IQR]) for NSCs and Diff-NSCs.

C-D. M-A plots for the (C) NSC and (D) Diff-NSC replicates showing the expression ratio (M) of each transcript as a function of its average abundance.

E. Compositions of the NSC and Diff-NSC transcriptomes.

F. Unsupervised hierarchical clustering of all samples using all expressed transcripts. Nodal numbers indicate bootstrap values obtained by resampling the data 10,000 times.

Differentially expressed transcripts

A total of 988 DETs were identified with all three methods (**Fig. S4**). Pearson correlation analysis disclosed strong correlation between the DET expression values obtained with DESeq and those generated with the other two methods (DESeq vs. Cuffdiff-WR: r=0.985, P value=0.00; DESeq vs. Cuffdiff-TR: r=0.997, P value=0.00). ANOVA confirmed that the DESeq expression values were reliably representative of the others (P value=0.9567), and they were therefore used for subsequent analyses of the 988 DETs.

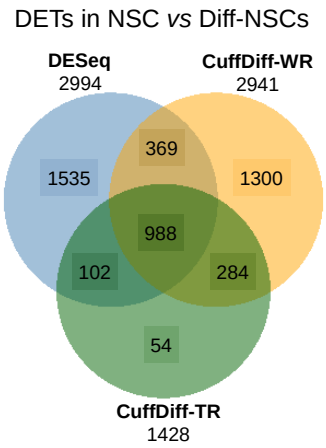

Fig S4.

Figure S4. Transcripts displaying differential expression (DETs) in NSCs and Diff-NSCs.

Venn diagram of DETs identified with DESeq, Cuffdiff-WR, and Cuffdiff-TR.

microRNA-seq mapping statistics

The mapping and read distribution results allowed us to proceed with the differential expression analysis without fear of bias from the sequencing and mapping (**Fig S5**).

Differentially expressed microRNAs

Using the DESeq2 algorithm, 1893 differentially expressed (DE) miRNAs were identified, of which 80 were statistically significant. In detail, 40 miRNAs were up-regulated and 40 were down-regulated in NSC in respect to Diff-NSC (**Supplementary Table 3**). Hierarchical cluster of these 80 miRNAs is reported in **Figure 13A**.

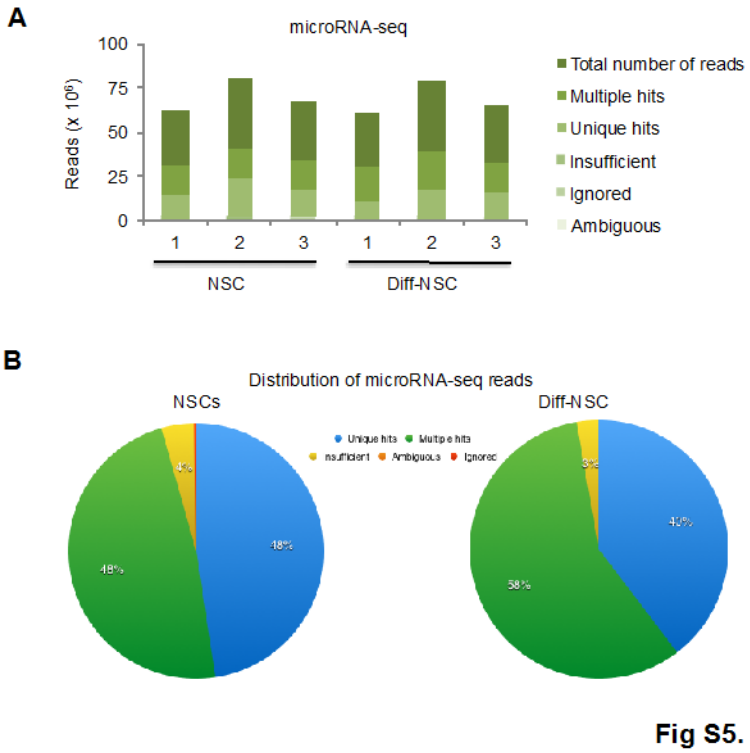

Fig S5.

Figure S5. MiRNA-seq mapping and DE analysis statistics.

A. Alignment of microRNA-seq mapping reports the Total number of reads and hits are classified as Ignored, Ambiguous, Insufficient, Multiple and Unique (Millions).

B. Percentages of unique, multiple and insufficient hits among microRNA-seq reads for NSCs and Diff-NSCs.

Neurosphere-forming assay

Neurospheres grown in the stem-cell-selective medium were dissociated to single cell through dissociation solution non-enzymatic buffer (Cod: C5789, Sigma-Aldrich). Viable cells were counted after Trypan-blue exclusion and re-plated at clonal density (1-2 cells/mm²) in 96-well plates containing stem-cell selective medium. Results were expressed as the percentage of cells plated that formed neurospheres (neurosphere-forming cells NFCs).

Immunofluorescence

Neurospheres were placed in Cell Dissociation Solution Non-enzymatic 1x (Sigma-Aldrich,) to obtain aggregates of around 5-10 cells. The latter were plated on poly-lysine-coated Lab-Tek chamber slides (cover slips) and allowed to adhere for 3 h or differentiated for 48 h, as described above, to detect differentiation markers. Cells were fixed with 4% paraformaldehyde for 20 min at room temperature and incubated in blocking solution (5% normal goat serum (NGS), 1% BSA, 0.1% Triton X-100). Cells were incubated overnight with primary antibodies diluted in blocking solution and for 2 h with secondary antibodies. Primary antibodies were rabbit anti-Nanog polyclonal (Abcam ab80892); mouse anti-Nestin (Abcamab 11306); mouse anti-Gli1, #2643 (Cell Signaling Technology Inc); mouse anti-parvalbumin P3088 (Sigma); rabbit anti-S100 S2644 (Sigma); mouse anti-b-III tubulin MAB1637 (Millipore); rabbit anti-Foxm1 (Santa Cruz Biotechnology, sc-502). Secondary antibodies (488-conjugated anti-mouse and anti-rabbit) were purchased from Molecular Probes (Invitrogen). Nuclei were Hoechst-counterstained and cover slips were mounted with fluorescence mounting medium (S3023) (Dako). Images were acquired with a Carl Zeiss microscope (Axio Observer Z1) using Apotome technology and AxioVision Digital Image Processing Software.

Immunoblotting assay

Cells were lysed in Tris–HCl pH 7.6, 50 mM, deoxycholic acid sodium salt 0.5%, NaCl 140 mM, NP40 1%, EDTA 5 mM, NaF 100 mM, Na pyrophosphate 2 mM, and protease inhibitors. Lysates were separated on an 8% acrylamide gel and immunoblotted using standard procedures. Membranes were blocked for 1 h at room temperature in 5% nonfat dry milk and incubated overnight at 4 °C with the following antibodies: rabbit anti-Foxm1 (Santa Cruz Biotechnology, sc-502), rabbit anti-Hsp70, (Santa Cruz Biotechnology, sc-33575), mouse anti-βIII Tubulin (MAB 1637 Millipore), goat anti-actin I-19 (sc-1616; Santa Cruz Biotechnology), anti-Nanog Antibody (PA1-41577, Thermo Fisher). HRP-conjugated secondary antisera (Santa Cruz Biotechnology) were applied and binding visualized by enhanced chemiluminescence (ECL Amersham).

RNA isolation and quantitative RT-PCR

RNA was isolated from cells, as previously described (Ferretti, E. et al., 2006). The High Capacity cDNA reverse transcription kit (Applied Biosystems Life Technologies, ThermoFisher) was used to synthesize cDNA, as previously described (Ferretti, E. et al., 2009).

Quantitative reverse transcription (RT–PCR) analysis was performed using a High Capacity cDNA Reverse Transcription kit. mRNA expression was analysed on cDNAs using the ViiA™ 7 Real-Time

PCR System, SensiFAST™ Probe Lo-ROX (Bioline), TaqMan gene expression assay according to the manufacturer's instructions (Applied Biosystems). Each amplification reaction was performed in triplicate, and the average of the three threshold cycles was used to calculate the amount of transcripts in the sample (SDS software, AB). mRNA quantification was expressed, in arbitrary units, as the ratio of the sample quantity to the calibrator or to the mean values of control samples. All values were normalized to 2 endogenous controls: ß-2-MICROGLOBULIN and HPRT.

MiRNA expression was assessed with Taqman probes, as previously described, 25 using the following miRNAs: miR-15b-3p (Code: 002173), miR-92a-1-5p (Code: 464504_mat), miR-130b-5p (Code: 002460), miR-130a-5p (Code: 462691_mat), miR-335-3p (Code: Mm03307393_pri), miR-25-5p (Code: PM12401), miR-93-3p (Code: PM12787), miR-15b-5p (Code: 000390), miR-16-2-3p (Code: 462713_mat), miR-301a-5p (Code: 006346_mat), miR-130b-3p (Code: 000456), miR-106b-5p (000442), miR-16-1-3p (Code: 002489), miR-15a-3p (Code: 002488), miR-19a-3p (Code: 000395).

PCR for Foxm1 isoforms

cDNA from NSCs was used to discriminate Foxm1 isoforms. PCR was performed according to the manufacturer's protocol (GoTaq® DNA Polymerase, Promega), using the following isoform-specific primers:

Forward primer 5'-CAAGCCAGGCTGGAAGAACTC-3'

Reverse primer 5'-GTTCACTGGGAACTGGATGGG-3'

PCR products were separated on 2% agarose gel.

Statistical analysis of in vitro experiments

Unless otherwise indicated, statistical analyses were performed with StatView 4.1 software (Abacus Concepts). The Mann–Whitney U test for unpaired data was used to analyse differences in gene expression between NSCs and Diff-NSCs and the unpaired T-test, paired T-test and one-way ANOVA were used where appropriate. Results are expressed as means (S.D.) from at least three experiments.

Luciferase-reporter assays

293T cells purchased from ATCC (Milan, Italy) were seeded into 24-well plates and transfected 24 h later with mouse Foxm1 promoter luciferase vector (1457 bp) (Genecoepia, Catalogue No. : MPRM26630-PG02, Gene Accession: NM_008021). Transfection was done with Lipofectamine® 2000 Reagent (Invitrogen) and included 80 ng of the Foxm1 promoter luciferase vector, 400 ng of inductor (Nanog, Gli1, Gli2, or (as a negative control) PCDNA), and 2 ng of CMV-Renilla Luciferase control vector. Cells were harvested 24 h post-transfection and tested with the dual-luciferase assay (Promega). Results were expressed as firefly / Renilla luciferase activity ratios (F-luc/R-luc) and represent means (SD) of at least three experiments, each performed in triplicate. Foxm1 promoter luciferase vector was used to generate, by site-directed mutagenesis, the mutant derivatives lacking Nanog-binding sites.

Site-directed mutagenesis

The QuickChange Multi Site-Directed Mutagenesis Kit (Agilent Technologies) was used to mutagenize Foxm1 promoter construct by deleting critical nucleotides in Nanog-binding sites s2 and s3. The reaction was carried out with the following primers:

NBS2 Fw: CGGCTTTACTGTCCTAAGTCAAGAAAATAAACAAAGTTATCACAGGAG

NBS3 Fw: GGTTTCCCTCTCTTCTGTTAACAGATCTTACACCGC.

Chromatin immunoprecipitation (qPCR-ChIP assay)

ChIP was performed using the MAGnify™ Chromatin Immunoprecipitation System (Invitrogen). Briefly, for each ChIP reactions 300000 cells were used, the cells were cross-linked 10 min with 1% formaldehyde and the reaction was stopped with 0.125 M glycine for 10 min at room temperature. Cells were washed and harvested, and membranes were lysed with Lysis Buffer and Protease Inhibitors (200X) for 5 min on ice. Chromatin was fragmented to obtain chromatin fragments of about 400–600 nucleotides. After sonication, the samples were spun at 10000 rpm at 4°C for 10 minutes to pellet the cell debris. The primary antibody was coupled for 1 h to the protein A/G Dynabead, at the same time the lysate samples were diluted in Dilution Buffer/Protease Inhibitor (200X). After 1h the lysates were added to their respective antibody/beads for 2 h. After which the lysates were washed three times with IP Buffer 1 and twice with IP Buffer 2. After the final washing, the cross-linking was reversed with Reverse Crosslinking Buffer and proteinase K at 55°C for 15 minutes and then the DNA was purified and precipitated. Eluted DNA was PCR amplified with primers encompassing the Gli- and Nanog- responsive sites of murine Foxm1 promoter. The following

antibodies were used: rabbit polyclonal anti-Foxm1 C-20 (Santa Cruz Biotechnology, code: sc-502), rabbit polyclonal anti-Gli1 2553 (Cell Signaling), rabbit monoclonal anti-Nanog (Cell Signaling, code: 8600), rabbit polyclonal anti-Gli2 (Santa Cruz Biotechnology, code: sc-271786x), rabbit polyclonal anti-acetyl-histone 3 (Millipore, code: 06599). Eluted DNA has been analysed with Q-PCR. Primers were designed with Primer-Blast designing tool (http://www.ncbi.nlm.nih.gov/tools/primer-blast/) (Ye, J. et al. 2012) and Primers tool (Genomatix Genome Analyzer, GGA, v3.30126, https://www.genomatix.de/).

Foxm1 promoter Fw: 5'-GCCACGTAACCGCAAGTCTA-3'

Foxm1 promoter Rev: 5'-CTACCCACTCGGTTACCCCT-3'

Primers for miR-301a upstream region (RT–qPCR)

Site miR 301a Fw: CAGACGCTTTGGAAAAGGAG

Site miR 301a Rev: GCTAACATGGGCATCATAAAAA

Primers for miR-130b upstream region (RT–qPCR)

Site miR 130b Fw: TGTAATGCTTCCGAGTAGGTAGGA

Site miR 130b Rev: CCCCCAAAGGGCTTTAGCT

Primers for miR-335 upstream region (RT–qPCR)

Site miR 335 Fw: GCGTTCAGAAGCTCTGTCCT

Site miR 335 Rev: GCCACAACTACCAGCTTCGT

Primers for miR-16-2 upstream region (RT–qPCR)

Site miR 16-2 Fw: GGAGCCATCGCTGAGTATAAAAA

Site miR 16-2 Rev: CCGTTTAGGCTCAGCAAAATTT

Primers for miR-15a upstream region (RT–qPCR)

Site miR 15a Fw: CCATTGGGAGGTGAAGGAAGGA

Site miR 15a Rev: GAACAAGAGCACGGGCTCCTTA

Primers for miR-130a upstream region (RT–qPCR)

Site miR 130a Fw: GGGTCATGGAAATGAGTGTGAA

Site miR 130a Rev: GCCACCGGTTCCTGTCTATC

Primers for miR-17 Bs2-3upstream region (RT–qPCR)

Site miR 17 Fw: GACTGCTGGGTCTGGAGAAG

Site miR 17 Rev: TGTGCTGCCCAAATGTAGAA

Primers for miR-106 Bs4 upstream region (RT–qPCR)

Site miR 106 Fw: CCCCTTGGAAGACAGAATGA

Site miR 106 Rev: GGGTTCAACTTTCACCGTGT

Primers for Gli s1-5 upstream region (RT–qPCR)

Site Gli s1-5 Fw: GACGCTCCGTCACGTGACCG

Site Gli s1-5Rev: CAGCGCCGCTTTCAGTTGTTCC

Primers for Gli s6-8 upstream region (RT–qPCR)

Site Gli s6-8 Fw: GAGCCGCGTGGACTGAG

Site Gli s6-8 Rev: CAGTGGTCGACTTCCTTCCG

Primers for Nanog s1 new upstream region (RT–qPCR)

Site Nanog s1 Fw: CACCGGCCTCTAACTTGTTC

Site Nanog s1 Rev: AGGGAGCACAGAATGAGATGA

Primers for Nanog s2-3 upstream region (RT–qPCR)

Site Nanog s2-3 Fw: AGAAAGAACGGCTTTACTGTCCT

Site Nanog s2-3 Rev: CGCAGCCTCCTGTGATAACT

Primers for Nanog s4 upstream region (RT–qPCR)

Site Nanog s4 Fw: GAGGCCCTTTTGTCTCACAC

Site Nanog s4 Rev: TTTGAAGGAACCCGGTTAGA

Knockdown studies

Small-interfering-RNA knockdown of Foxm1 was performed in NSCs with ON-TARGETplus SMARTpool (L-057933-01-0005) and control ON-TARGETplus Non-targeting siRNA knockdown (D-001810-02-05) (Dharmacon). Hiperfect reagent (Qiagen) was used for transfections. Cells were harvested for assay 72 h post-transfection.

Knock-down of miRNA expression was done with miRCURY LNA™ miRNA inhibitor (Exiqon, miR-130b-5p: code 4101000-011; miR-301a-5p: code 4101560-011, miR-15b-3p: code 4101249-011, miR-19a-3p: code 4101300-101), individually or in combination, and a scrambled control, referred to as LNA ctrl (Exiqon mirCURY knockdown probe control A: code 199002-08) (Exiqon). Hiperfect reagent (Qiagen, Hilden, Germany) was used to transfect the siRNA constructs into NSCs. The final concentrations were 10 nM (for single transfection) and 50 nM (for combination transfections).

Validated targets of miRNAs

The validated miRNA targets reported in were identified with miRTarBase (http://mirtarbase.mbc.nctu.edu.tw/) (Chou, C.-H. et al. 2015), where each Foxm1-regulated miRNA was used as input.

Putative miRNA target genes

MicroRNA.org (http://www.microrna.org/microrna/home.do) database was queried for putative miRNA target genes, where miRNA-target interactions were predicted with miRanda 3.3a and scores were calculated with mirSVR (good mirSVR score less than or equal to -0.1).

Supplementary Information:

Foxm1 promoter (mouse)

ttgtacaaaaaagcaggcttcgaaggagatagaaccagatcttggaattcTGGCTAGCCTGGGGCTGGCAATGTAGA
CCTGGCTGGCCTGGAATTCAGAGATCTGCCTGCCTCTGCCTCCTGGGTGCTGGAATTAAAGG
TGTGCACCACCACACTCTGCTCACTCTTCAAACACAGTCTTATTATGTAGCCCAGACTAGACT
AATGTGAGGCCCTTTGTCTCACACCAGGATTATTGGTACGTGCCACATACCTAGCTGCTTAC
AACTTCTAACCGGGTTCCTTCAAATATTAAATAAGAACAAAATTCAGAAAGGCGAAGACCCTGC
CTCCTGTCTCATAGCATACCACACTCACTACATCTTAGGCCTTTGTATTCAGCAGGCCTCCTC
CCGGTCAAAGCAGCTCTCCCTTCTCTATTTACTTCAGGGTTTCCCTCTCTTCTGTGTAATGGG
TAACAGATCTTACACCGCGTTCTCAGCTCCTTTAAAAAAAAAAAAAGGAAAGAAAGAAAGAAC
GGCTTTACTGTCCTAAGTCAAGATCTCATTAAAATAAACAAAGTTATCACAGGAGGCTGCGGG
AGGGCGAGCCAGTGACCCCGGCTACTCCGAAGGCGGAAACACGAGGATCCAGAATTCTACA
CAACCTTGTGTCAGACAAAACCCACCGGCCTCTAACTTGTTCCTCTGTAGCTAGAATTCTACC
GATCTGTTCATCTCATTCTGTGCTCCCTCGCCATCAGACGCTGAGGCCAGGGGGAGGACGCC
CGGGTCCGCCGCTGTATCCTCCGCTCTTATCGTAAAGTACTTCGAGGGAATAAACGATCGTC
CGGACACCTCGGGGGCTGGGGCCCCGGGAGGAGGCGGCCACAGACCGGAGCGGGGCGGAG
CCACGTAACCGCAAGTCTAGGGCCAGAAACCCAAGCCGGACCCCACGGAGCCGCGTGGACT
GAGCGGGGCGGGGGACCCAGGGGTAACCGAGTGGGTAGCCAGCCCGGGGAAGTGGCGTA
CGCTGTCCCGGAACTGCTGGCCGCCGTCCGCGCGTCCCCGCGTCCCTCCCGCCGCCCCTC
GAGCCCCGCCGGGGCCGCCTTACCCGCCCTCCCGGCCGCGGCCGCCGCTCCTCAGGACAC
CGAGCGTTCGGGGCCGGAACCCGGAGACAAGCCGGTGCCGATTGGCGACGCTCCGTCACG
TGACCGCAACGCTCCGCCGGCGCCAATTTCAAACAGCGGAACAACTGAAAGCGGCGCTGCG
GGACCCACCCCCGGCCCGGGCTCCCCCGTCACCCCGCCCCGGGCTCCCACCCCGGCCGTC
CCGCCGGGACCCGCCGCCCGGGCCCGGCTCGGCCCCGCGTGGAGCAGACGCGGCCTGTG
AGGTGAGTGGGGGTGCGGCCGGGTCCAGGGAGGGCTCGGAGTCGGCACTGCCGGGGCTGTG
GGGCGCGAGGGGGTGTTGGGCACCGCCGGGAAGAAGGTCTGAGCCTCCGGCCTCGGCCTT
GCCGCCGCCGTGTTCTCCGAGCATCCCCGGACCCTGGGAACAGGCCTGCCCTCGGAGTCTG
CATTTGCAGTCAACCCTGCCTCCGCCTCCACCGCTGCAGGGCGGGATCCTGGCTGAGTGTTG
GTTGCAAGGTTCCCTGTTGAGTGTGGAGAATAATGGGGTCGTGGGGTGG

Provided below is the sequence (50 nt) upstream of the promoter for mouse Foxm1.

5'-ttgtacaaaaaagcaggcttcgaaggagatagaaccagatcttggaattc-3'

Putative binding sites for GLI:

5'-cggaCCCCacggagc -3’

Putative binding sites for NANOG:

5'-ggtggtAATGagacaccta-3’

3’-taggtgtcTCATTaccacc-5'

Supplementary Information-Section 1. The Foxm1 promoter region.

Foxm1 weight matrix for putative binding sites using the Genomatix Genome Analyzer:

5'-AACA-3'

3'-TGTT-5'

Cluster miR-15b~16-2

miR-16-2 promoter region

chr=3, start=69032759, end=69033359

CAGTTCTAAGCCAGGAGGAGCTTGAGGCAATCAAGAATCCAGAGTCTATAACAAATGAAATTG
CACTTTTGGAAGCTCAGTGTCGTGAAATGAAACCAAACCTTGGAGCCATCGCTGAGTATAAAA
AAAAGGTGTGAGTGAATTGTTTCTAGTAGAAATTTTGCTGAGCCTAAACGGGGTATTTAATTGT
GCATAATGACCAGTGCTAATTCTCAGATTTGTATGTGTGTGAAAGGGTTTTGTTTTTTTGTTTTA
CAATCTTCACAGGAAGATTTATATTTGCAAAGAGTAGCCGAACTGGACAAAATTACTTCTGAAA
GAGATAATTTTAGACAAGCATATGAAGATCTTCGAAAACAAGGCTGAATGAATTTATGGCTGG
TTTTTACGTAATAACAAATAAACTAAAAGAAAACTACCAGATGCTCACATTGGGAGGAGATGCT
GAACTGGAGCTTGTGGACAGTTTAGATCCTTTTTCTGAAGGAATCATGTTCAGGTTGGTGAGA
TTTTAATCCTGCATCTTTTCCAAACTACTATTTCTTTAGTGTGTGAAGGTTGGAACTACATTTAT
TTGGTAATAACTATCTTGCTCTTACA

miR-130a-3p promoter region

chr=2, start=84741545, end=84742145

GGTGGGAGGAGGCTGGAGGGGGAAGCACAGAGGAAGAGCTCCCAAATGAAATTCAGGCCTC
CATTTTTCCTGCTTGTTGCAATGGGGGTGGGGGGGTGGTCTCCCTGAGGCTACTCCATGGTCT
GAATGGATCTCCACAGGGAGGAGCCTTGCAGTCTCTGTCCCTTAGGTTAGAGCTGTAACTGG
CTTCTGACCAGTATGCTTAGCTGCTGTGTGACTCTAGAGGCCTGCATGGCTCTGAGCCTTGG
GTTTCAAGTGCACCTGGCTTTGGAATTTTATCAGTCTCTATTGTCCTCAATGAAATTAAGGGGG
ATGGCCTGGGGTCATGGAAATGAGTGTGAAGACTCCACTACTAAACCCTTGGGATAGACAGG
AACCGGTGGCTTCTAAGCCCAGTGTCAATGAGAGCTTATCCTTAACTCAAGAGCCAAATCACT
GGCCATTTCGCTTAATACCATATCCATAGAGTACTTTGAAGACATCAGAAAGGAAACAGTGGG
GTTTCAGTTGCTTGCACCTCCAGATCTGGGAGCTTCTTTCTCCTGCCTAAGCACCTGTAGTTA
GGTTCCATTATTCTAGACCTGGAGGTCACCTGAGATCAT

Cluster miR-17~92

chr=14, start=115045026, end=115045626

AAAGATGGCAAACTGATGGTCAGTAGAGTGACAGGTACACATGACACTCGAGTGCTGGGTCT
GGAGAAGCTGCAGTTAGTATTTAGGATAACAGTATATATAATATATAGTTCTACATTTGGGCAG
CACAGTTGGTTTCAGGCTATGAATAAAAATCATTGGAGTGAAACCTAAAGAAAAGTAAAATTAA
TAAGGAAGAGCTGCTAAAATCAGGTTTAAGCTGACACTATCTACAGAGCTAAAGTTTTCCATAA
TATGTTGCTTTTTTTAAAAGAAATGCAAGAAGCTGACTGATGGATCCCTGAGCTGCCAGGTAA
GGATTCCACAGGCCTGGGTTTGATTGTGAGTGACCAGAATTGTACAATTATTACTAAAACAGA
AACATAGTCACTTCTGACTCCATTCTTAACATTTTTGGATTAAAACTTGTTTCAGATGACTAATG
AAAACTTCCTTTAAAACGTGATAAAGCTCTAATGTCAGCACGATCCACATGATCCATGTGCCTC
CTATAAAGGGAGGGGTCTGTCACCAGTGTTACGGATTGAATGCTACGTTTATCTTCCAACATA
GGAAGCCTGCCAGGTACTTTCTTCAATAT

miR-335-3p promoter region

chr=6, start=116405759, end=116406359

AAATCAAGCAGGGTCAGGTAACAGGTGAGTATATGGGCCGTGAGGTGAGTGCTGTACACAGG
TCCTGGGGACTGAGGTTCTGGGGTTTAGAGCTCTGTTTCCTGAGAGAGCAGAGTAAACTACA
TTGAGAACACTTCCTGCTCCTTTTGGGGAGGGAGGACTTGATGAGTCAGAAATGTACAGAGT
GGTTGTGGGCGTTCAGAAGCTCTGTCCTGCTTCCTTCTGACATGAGACCTCCTGATGAGCTAA
CTGAGTCTCCCCTGCAGGAATCCTAGAGTGGCCTTTCTGGACGAAGCTGGTAGTTGTGGCCA
TCGGCTTCACTGGAGGACTTCTCTTTATGTATGTTCAGTGCAAGGTGTACCTACAGTTATGGA
AAAGACTCAAGGCTTACAATAGAGTGATCTATGTTCAGAACTGTCCAGAAACAAGTAAAAAGA
ATATTTTTGAAAAGTCTGCACTTACAGAGCCCACCCTTGAAAATAAAGAAGGACATGGAATGT
GTCATTCCACCACAAATTCTTCTTGCACAGAGCCTGAAGACACTGGAGCAGAAATTATTAACG
TCTGACCATGTGAGGGTGTCATTTCCTTGATGTCCACC

Cluster miR-106b~25

chr=5, start=138171718, end=138172922

TCTTAAGTGCCTGTCCCAACTCTACTCACCGGGAAAGCAGCTCCAGAAGGCTGAAAGGAGAG
ACGTTTTCTAAGGTTGTGGCCACCAAATAGAGCCCACTGTGTCTGATGTGAATAAAATGACGA
TCACCGTGATACTGAGGCAGAGTTGAGGACAGAGGCCATTAAGAAAAGACCAGAATTGTAGT
AAGGAAACCTGCAAGATGGCACCCTGAGGTCTACTAGTGATGGGCGATGCCCCAGATCTAAG
ACCTGGCCGCCTAACGTGGAAAGGTAGTATCTACCTCTCAAAGTTGTTGATAGTCAAAAAATA
GGGTGCATGGCTCTGTAACTGGCTTCTTGTTAGTACTCAAAACATTTATAAACAAATCCTCCCC
ACACACACACCCCCGCCCCCAAGCTTCCTACCAAGCTGCCCTTGACAGGGAGGAGGCACTCA
CCCACCTCCACAGTTCTAAGGCCCTGCACACCAACCACAGTAGTTACCATGACAACCGGGGA
CTCGCCTCCAGGCAGTCCCGTCAGCTTCCGGTAGAAGAGCTCTGCCACATCACGACCACCAC
TGTCCCCGCGGACTAGCCAGGTGGAAAGATAGTTAAGGAACAGGCGACACAGACTGATCTGG
ATTCGATTTCTACCCAGCTACCCTACCCCGTCTCCCGGGTCAAAGGATACAGTCTTTATAGAT
GAGCGGATCCCCCTTGGAAGACAGAATGAAGAACTGGGAAATCATGGCGGTTCTGGAGGATA
GACGAGAACACGGTGAAAGTTGAACCCACCCCGCCTTGTGGACGCGGAACAAAGGCCGCA
CGGAGGCTGGCGCTTTAAGAAACACTCCTCCCACACACACACTCGCGAGCATTAATTTCGAA
CCGCGGGAAACAGGGTGTCCAACCCGCCAGGATCTGGCAATCTTTCAACGGCCCGCCCTCA
AGCCCCTTGTCATTCAATCTAGACTCGTCCATTGATTGGTTAAAGTTAGGGGCTGGCAGCAGT
TGGGAACCCCCTATCTGATTGGCGGGTTCTCAGCCGCACGGGTCACATGGGTGACGACGTTT

CGCGCCAATTTCGGTTGGCCGGCTACGTCCCGCCGCGCGTTCGTTTTCTGCTTCCCCAGAGA
GAGATTTTTGAGCCCTTCAAGTCCTGCCACACCGTCCCCGGCAGCGATGGCGCTTAAGGACT
ACGCGATCGAAAAAGGTGAAGAT

miR-130b promoter region

chr=16, start=17121616, end=17122216

AATATAGCTAGAATTACATAGGAGACCTTGTCTCAAAAAACAAGCAAAAGAAGTGGTCAGGAC
ATGATCTGGAGAGGGATGTGTGTAATGCTTCCGAGTAGGTAGGAAACTCAGAGGGTGCAAAA
GCCAGAGCTAAAGCCCTTTGGGGGGCAGAAGGAAGTCCTTTTGGATATTATCTTAGTGAACTG
GAAAGTAGATTCAATTACCAGGGCGGTCTGGTAGGGCAGAGTATGGAGGGAACTGCAAACTG
GGAGAGGGCTGGGTGCTTTGAAACGGAAAGGACCACGGCTCAGAAGGAGGTCAAAATCCAG
GAGCTCAAAATCCAGAAGGTACCTGGGTGCCTTTGGCGGTCACAGTGAGGGGTGGAGCAGT
GGGGGCGGGGTGGGGTGGGGAGCACACCAATGCGCATGCCTAGAGAAGTGAGCATTGTTAC
GCGTACTGGTGCTGGACCCGCCCCCTGTCTCTGTGGGCATTCATTCCCTGGGGTAGACCGG
GAGGGGGGTGGGTAGTCTGGGGATCTGGAGTCTGCACTGCGGCTGTAGGGAGAGAGTGGG
TACGCCCTGCAGTCCTCATCCCGATGGTTTCCCATCACCTTTCTCAG

miR-301a promoter region

chr=11, start=86926083, end=86926683

TTTTCATTTGTTTTTTGAAGTAATTACTCAAAGGACTTGTTTTCTATGGTAGGTAACCCAGACGC
TTTGGAAAAGGAGTTAACCAACATTACATTTAGGCAAAAAACATAGTTTTTCACATATTTGCCTT
AGTAGTAATTACAGCTGATTTTGTTAATATCAATTATAAAGTTTTTATGATGCCCATGTTAGCTA
CTAAAGGCTCAGGACATATTACAAAATTCCTTTACATCTGTGCATGTTTTATGTCTGAATGCTGC
TAATTTCAGGTTAGTCAACAAAAACCAATTATCACTTTGGTCCTTTGCCCTTCCAAAAATATACT
GGTATAAATGTTTTTTAGGTTTTGGATGTCTTCTGACTAAAATGGCAACTCAACTTTAAGGTCTTT
GCACACTGAGCCTTGCATTCCTTTCCTGCTCACTCCTGCTAACGGCTGCTCTGACTTTATTGC
ACTACTGTACTTTACAGCGAGCAGTGCAATAGTATTGTCAAAGCATCCGCGAGCAGGTTGCAC
ACCTTTCCTGGTTCTTGTCTTACATCTTCAGTATTTGTGAAAAGGTTTCTATAACTTTCAGTGTG
GAAAACTGTATAATTTTGTTA

cluster miR-15a~16-1 promoter region

miR-15a promoter region

chr= 14, start= 61619651, end= 61620251

CCTATAGTTTTGGCATTTGAATGGTAGAGTTGGCAGAATGAGAAGTTCAATTTGTCTTCAGCTA
TATAAGGTTGACATTAAGCTAGCCTATAGAGAACCCCATACCCCCAAAAGAAAAAGTCTTTGTT
TTATAAGTTGTGGCCTACCAACTTTCAAAGTATAGGACACGATGCATTCTCAGATATCCTGGTT
TATAGTAGTTTTGTTTTTTTGTTTGTTTGCTCCTTGAGGCAGGGTCTTTGTAGTACTGCCTGGCC
TGGGACTCACTATGCTGAAAAAGCTGTCCTGGAATTCATGAAGTCTTCTAGCAAGGAAGTTGG
ACGTGATTATTTTTGTCTCCTAAGAGTAAAGAATATCTAAATCAAATAGCAATAAGAATGGAACT
GATCCTGAAGCAAAGTGATACCTGCGTGTATCCTAGCCATTGGGAGGTGAAGGAAGGAAGTG

GGAAACAGCATATCAAGGTAAAAAACTTGGAACATTATTAAGATAGAAAGGAGGTATAAGGAG
CCCGTGCTCTTGTTCTGGAAGGTGACGGTGATGTTACTGAAGGATGAGAAACCACCTGAAAC
ACTGAGCCTTCTCACAATATTACATTTGAA

Supplementary Information – Section 2. The miRNAs promoter regions**.**

Tables:

Table 1. Gene Ontology categories over-represented in the set of 988 DETs. *				
Gene Ontology Category	**Fold Enrichment**	**Count**	**%**	**Bonferroni-corrected *P*-value**
Cell cycle	5.4	37	4	2.50E-15
DNA replication	8.1	15	1.6	1.50E-07
p53 signaling pathway	3.8	14	1.5	9.00E-03
ECM-receptor interaction	3.4	15	1.6	1.70E-02
* Findings are ranked according to Bonferroni-corrected *P* values				

Table 1. Gene Ontology categories over-represented in the set of 988 DETs.

Table 2. MiRNAs with putative Foxm1 binding sites that are most markedly upregulated in NSCs.

No.	MicroRNA	log_2 fc *	adj. P-value	Member of microRNA Cluster	Part of microRNA Family	ChIP-confirmed
1	mmu-miR-15b-3p	2.75	2.33E-07	15b~16-2	15a, 15b, 16-1,16-2, 195a	Yes
2	mmu-miR-92a-1-5p	2.56	3.66E-04	17~92	25, 92a-1, 92a-2, 92b	Yes
3	mmu-miR-130b-5p	1.97	6.72E-04	-	130a, 130b, 301a, 301b	Yes
4	mmu-miR-130a-5p	1.98	1.54E-03	-	130a, 130b, 301a, 301b	No
5	mmu-miR-335-3p	2.66	2.27E-03	-	-	No
6	mmu-miR-25-5p	1.58	2.77E-03	106b~25	25, 92a-1, 92a-2, 92b	No
7	mmu-miR-93-3p	1.49	2.77E-03	106b~25	17, 18a,18b, 20a, 20b, 93, 106a, 106b	No
8	mmu-miR-15b-5p	1.6	3.88E-03	15b~16-2	15a, 15b, 16-1,16-2, 195a	Yes
9	mmu-miR-16-2-3p	1.71	7.46E-03	15b~16-2	15a, 15b, 16-1,16-2, 195a	Yes
10	mmu-miR-301a-5p	1.95	1.08E-02	-	130a, 130b, 301a, 301b	Yes
11	mmu-miR-130b-3p	1.69	1.14E-02	-	130a, 130b, 301a, 301b	Yes
12	mmu-miR-106b-5p	1.82	1.19E-02	106b~25	17, 18a,18b, 20a, 20b, 93, 106a, 106b	No
13	mmu-miR-16-1-3p	1.96	1.76E-02	15a~16-1	15a, 15b, 16-1,16-2, 195a	Yes
14	mmu-miR-15a-3p	1.48	1.89E-02	15a~16-1	15a, 15b, 16-1,16-2, 195a	Yes

15	mmu-miR-19a-3p	1.82	3.91E-02	17~92	17, 18a,18b, 20a, 20b, 93, 106a, 106b	Yes
* NSC vs. Diff-NSC						

Table 2. The miRNAs with putative Foxm1 binding sites that are most markedly upregulated in NSCs.

Supplementary Table 1. Putative and validated downstream mediators of Hh-Gli signaling.			
Gene	**Title**	**Reference**	**Context**
Ang-1	Sonic hedgehog (Shh) regulates the expression of angiogenic growth factors in oxygen-glucose-deprived astrocytes by mediating the nuclear receptor NR2F2	Li, Y. et al, 2013	Astrocytes oxygen-glucose deprivation (OGD) could induce the expressions of Ang-1 with the expression of Shh signaling components increased.
Ang-2	Sonic hedgehog (Shh) regulates the expression of angiogenic growth factors in oxygen-glucose-deprived astrocytes by mediating the nuclear receptor NR2F2	Li, Y. et al, 2013	Astrocytes oxygen-glucose deprivation (OGD) could induce the expressions of Ang-2 with the expression of Shh signaling components increased.
BCL2	Activation of the BCL2 Promoter in Response to Hedgehog/GLI Signal Transduction Is Predominantly Mediated by GLI2	Regl, G. et al, 2004.	GLI2 activating the prosurvival factor BCL2, may represent an important mechanism in the development or maintenance of cancers associated with inappropriate HH signaling.
BMI1	Sonic hedgehog regulates Bmi1 in human medulloblastoma brain tumor-initiating cells	Wang, X .et al 2012.	In human medulloblastoma brain tumor-initiating cells, Gli1 preferentially binds to the Bmi1 promoter, and Bmi1 transcript levels are increased and decreased by Gli1

			overexpression and downregulation, respectively.
BMP4	Hedgehog signaling restrains bladder cancer progression by eliciting stromal production of urothelial differentiation factors	Shin, K. et al, 2014.	In bladder cancer decreased Bmp4 expression resulting from loss of Hh signaling may account for the accelerated rate of tumor progression observed in mice with ablated Smo function.
BMP5	Hedgehog signaling restrains bladder cancer progression by eliciting stromal production of urothelial differentiation factors	Shin, K. et al, 2014.	In bladder cancer decreased Bmp5 expression resulting from loss of Hh signaling may account for the accelerated rate of tumor progression observed in mice with ablated Smo function.
bmp6	Expression of indian hedgehog, bone morphogenetic protein 6 and gli during skeletal morphogenesis	Iwasaki, M. et al., 1997.	During skeletal morphogenesis Gli surrounded the ihh domains and bmp6 was expressed immediately adjacent to ihh.
Ccna1	Sonic hedgehog controls growth of external genitalia by regulating cell cycle kinetics	Seifert, A.W. et al, 2010.	In external genitalia loss of Shh causes a transient downregulation of G2 / M promoting genes and a sustained decrease in the expression of genes that govern the G1 / S transition.
Ccna2	Purmorphamine Induces Osteogenesis by Activation of the Hedgehog Signaling Pathway	Wu, X. et al, 2004.	In osteogenesis, at early time points (24 hr), purmorphamine treatment led to the upregulation of cell

			cycle control genes, including Cyclin A2 (3.5-fold).
Ccnb1	Hedgehogs tryst with the cell cycle	Roy, S. and Ingham, P.W., 2002.	Barnes and colleagues unexpectedly identified PTC1 amongst prey that associate with a bait mimicking phosphorylated cyclin B1.
CCNB2	Hedgehog signaling pathway and gastric cancer	Katoh, Y. and Katoh, M., 2005.	In gastric cancer FOXM1 is reported to be upregulated by the Hedgehog signaling and induces transcriptional activation of CCNB2 gene encoding Cyclin B2.
Ccnd1	Hedgehogs tryst with the cell cycle	Roy, S. and Ingham, P.W., 2002.	Examination of the status of D-type cyclins, central regulators of G1 phase progression, revealed that, upon incubation with SHH, the CGNPs preferentially upregulate cyclin D1 RNA and cyclin D1 protein.
Ccnd2	Hedgehogs tryst with the cell cycle	Roy, S. and Ingham, P.W., 2002.	Examination of the status of D-type cyclins, central regulators of G1 phase progression, revealed that, upon incubation with SHH, the CGNPs preferentially upregulate cyclin D2 RNA.
Ccne1	Hedgehogs tryst with the cell cycle	Roy, S. and Ingham, P.W., 2002.	These effects of modulated HH signalling on the proliferation patterns of eye cells are mirrored by corresponding alterations in

			the levels of cyclin E transcript and protein.
Ccne2	Hedgehogs tryst with the cell cycle	Roy, S. and Ingham, P.W., 2002.	The effects of modulated HH signalling on the proliferation patterns of eye cells are mirrored by corresponding alterations in the levels of cyclin E transcript and protein.
Cdc2a	Hedgehog modulates cell cycle regulators in stem cells to control hematopoietic regeneration	Trowbridge, J.J. et al, 2006.	In ptc WT, Cdc2a is up-regulated but down-regulated in ptc-1/ cells during hematopoietic regeneration, suggesting that ptc-1/ cells are unable to up-regulate expression of these genes as necessary for hematopoietic regeneration.
CUL7	The cullin protein family	Sarikas, A. et al, 2011.	Cyclin D1 and insulin receptor substrate 1 (IRS-1) are potential proteolytic targets of the CUL7 E3 ligase.
cyyr1	Characterization of human gene locus CYYR1: a complex multi-transcript system	Casadei, R. et al, 2014.	Xu et al. indicated CYYR1 as a putative target gene regulated by Hedgehog (Hh) signalling during vertebrate development.
ERBB	Alternative splicing of the ErbB-4 cytoplasmic domain and its regulation by hedgehog signaling identify distinct medulloblastoma subsets	Ferretti, E. et al, 2006.	Low-level Hh signalling in human MB is associated with the selective maintenance of high ErbB-4 CYT-1 expression, an alteration that exerts tumor-promoting effects.

FGF-(1,7,8,10)	The Sonic Hedgehog Signaling Network in Development and Neoplasia	Chari, N.S. and McDonnell, T.J., 2007.	Known Transcriptional Targets of Hh Signaling
MAPK/ERK1/2 signaling	Regulation of the hedgehog signaling by the mitogen-activated protein kinase cascade in gastric cancer	Seto, M. et al, 2009.	PTCH expression was significantly correlated with extracellular signal-regulated kinase (ERK) 1/2 phosphorylation as well as SHH expression in the gastric cancers assessed by immunohistochemistry. KRAS-MEK-ERK cascade has a positive regulatory role in GLI transcriptional activity in gastric cancer.
FOXE1	Hedgehog signaling pathway and gastric cancer	Katoh, Y. and Katoh, M., 2005.	Forkhead-box transcription factor FOXE1 is reported to be upregulated by the Hedgehog signaling.
FOXM1	Hedgehog signaling pathway and gastric cancer	Katoh, Y. and Katoh, M., 2005.	Forkhead-box transcription factor FOXM1 is reported to be upregulated by the Hedgehog signaling. FOXM1 gene is a direct transcriptional target of Hedgehog signaling pathway, and FOXM1 induces transcriptional activation of CCNB2 gene encoding Cyclin B2.
FST	Clinical and Therapeutic Implications of Follistatin in Solid Tumours.	Shi, L. et al, 2016.	Strong FST expression was found in basal cell carcinoma and seemed to be mainly activated by transcription

			factor GLI2, which as a Hedgehog signalling mediator, has been shown to be up-regulated by the expression of FST.
Gli1	SnapShot: Hedgehog Signaling Pathway	Chen, M.H. et al, 2007.	HH responding cell: Flies and vertebrates may use different strategies downstream of Smo to modulate activity of the Ci/Gli transcription factors.
Gli2	SnapShot: Hedgehog Signaling Pathway	Chen, M.H. et al, 2007.	HH responding cell: Flies and vertebrates may use different strategies downstream of Smo to modulate activity of the Ci/Gli transcription factors.
Gli3	SnapShot: Hedgehog Signaling Pathway	Chen, M.H. et al, 2007.	HH responding cell: Flies and vertebrates may use different strategies downstream of Smo to modulate activity of the Ci/Gli transcription factors.
PRKG1 (cGMP)	cGMP Enhances the Sonic Hedgehog Response in Neural Plate Cells	Robertson, C.P. et al, 2001.	Cells in chick neural plate explants respond to Shh by differentiating into ventral neural-cell types. Exposure of intermediate-zone explants to cGMP analogs enhanced their response to Shh in a dose-dependent manner.

Hhip	SnapShot: Hedgehog Signaling Pathway	Chen, M.H. et al, 2007.	HH responding cell: Two general mechanisms exist to downregulate Hh signaling after the initial response. Ci/Gli transcription factors are ubiquitinated by Cullin (Cul3) and HIB/SPOP complexes; the expression of Hh-binding proteins, such as Ptc and Hhip1, is upregulated to serve as a sink for extracellular ligand.
IGF1	Hedgehog Promotes Neovascularization in Pancreatic Cancers by Regulating Ang-1 and IGF-1 Expression in Bone-Marrow Derived Pro-Angiogenic Cells	Nakamura, K. et al, 2010.	In vitro co-culture and matrigel plug assays demonstrated that PDAC cell-derived Shh induced IGF-1 production in BMPCs, resulting in their enhanced migration and capillary morphogenesis activity.
IGF2	The Sonic Hedgehog Signaling Network in Development and Neoplasia	Chari, N.S. and McDonnell, T.J., 2007.	Known Transcriptional Targets of Hh Signaling
Insm1	An Integrated Approach Identifies Nhlh1 and Insm1 as Sonic Hedgehog-regulated Genes in Developing Cerebellum and Medulloblastoma	De Smaele, E. et al, 2008.	Insm1 and Nhlh1/NSCL1 as novel HH targets induced by Shh treatment in cultured cerebellar granule cell progenitors.
Mycn	Nmyc upregulation by sonic hedgehog signaling promotes proliferation in developing cerebellar granule neuron precursors	Kenney, A.M. et al, 2003.	Nmyc upregulation occurred in proliferating neural precursor cells exposed to ectopic Shh in transgenic mice and in

			medulloblastomas of Ptch heterozygotes.
Nhlh1	An Integrated Approach Identifies Nhlh1 and Insm1 as Sonic Hedgehog-regulated Genes in Developing Cerebellum and Medulloblastoma	De Smaele, E. et al, 2008.	Insm1 and Nhlh1/NSCL1 as novel HH targets induced by Shh treatment in cultured cerebellar granule cell progenitors.
Ntrk3	Sonic Hedgehog-responsive Genes in the Fetal Prostate	Yu, M. et al, 2009.	In primary urogential sinus (USG) mesenchymal cells and in the cultured UGS Ntrk3 exhibited Shh-regulated expression.
PDGFRA	Hedgehog Target Genes: Mechanisms of Carcinogenesis Induced by Aberrant Hedgehog Signaling Activation	Katoh, Y. and Katoh, M., 2009.	Hedgehog signals upregulate PDGFRA gene, encoding PDGF receptor, to upregulate ERK signaling cascade in basal cell carcinoma.
PDPN	Significance of podoplanin expression in cancer-associated fibroblasts: A comprehensive review	Pula, B. et al, 2013.	In cancer associated fibroblasts podoplanin (PDPN)-positive A431 cells exhibited high expression of CD44 and sonic hedgehog (SHH), which are both markers of tumor initiating cells.
POU3F2	Integrative genomic analyses of ZEB2: Transcriptional regulation of ZEB2 based on SMADs, ETS1, HIF1·, POU/OCT, and NF-κB.	Katoh, M. and Katoh, M., 2009.	Hedgehog signals are predicted to indirectly upregulate ZEB2 via TGFß. POU3F2 (BRN2) was coexpressed with ZEB2 in brain corpus callosum, spinal cord, and fetal brain.

Rac1/Rhoa	Sonic Hedgehog Activates the GTPases Rac1 and RhoA in a Gli-Independent Manner Through Coupling of Smoothened to Gi Proteins	Polizio, A.H. et al, 2011.	Hh ligands induce important changes in the actin cytoskeleton that modulate cell motility and morphology through stimulation of the small guanosine triphosphatases (GTPases) Rac1 and RhoA in a manner that is dependent upon the heterotrimeric G protein Gi.
satb2	Bmp and Shh signaling mediate the expression of satb2 in the pharyngeal arches.	Sheehan-Rooney K. et al, 2013	We propose that Bmp signaling establishes competence for the neural crest to respond to Hh signaling, thus inducing satb2 expression.
SEMA6A	Sonic Hedgehog-activated engineered blood vessels enhance bone tissue formation	Rivron, N.C. et al, 2012.	Cyclopamine treatment regulated axon guidance molecules such as semaphorin 6A (SEMA6A), demonstrating a role for endogenous Hh activity in regulating the formation of vascular structures and lumens.
SFRP1	WNT antagonist, SFRP1, is Hedgehog signaling target.	Katoh, Y., and Katoh, Y. (2006).	These facts indicate that SFRP1 is the Hedgehog target to confine canonical WNT signaling within stem or progenitor cells.
Tiam-1	Sonic hedgehog signaling regulates actin cytoskeleton via Tiam1-Rac1 cascade during spine formation.	Sasaki, N. et al, 2010.	These findings demonstrate a novel Shh pathway that regulates the actin cytoskeleton via Tiam1-Rac1 activation.

Vegf	Sonic hedgehog (Shh) regulates the expression of angiogenic growth factors in oxygen-glucose-deprived astrocytes by mediating the nuclear receptor NR2F2	Li, Y. et al, 2013.	Astrocytes oxygen-glucose deprivation (OGD) could induce the expression of VEGF with the expression of Shh signaling components increased.
VEGFA	Hedgehog inhibition reduces angiogenesis by downregulation of tumoral VEGF-A expression in hepatocellular carcinoma.	Pinter M et al, 2013.	Hh inhibition with GDC-0449 downregulates tumoral VEGF production in vitro and reduces tumoral VEGF expression in an orthotopic HCC model.
Wnt10a	Hedgehog Target Genes: Mechanisms of Carcinogenesis Induced by Aberrant Hedgehog Signaling Activation	Katoh, Y. and Katoh, M., 2009.	In E1A-immortalized RK3E rat kidney cells Wnt10a is upregulated in volar skin M2SMO transgenic mice with Hedgehog signaling activation.
Wnt10b	Hedgehog Target Genes: Mechanisms of Carcinogenesis Induced by Aberrant Hedgehog Signaling Activation	Katoh, Y. and Katoh, M., 2009.	In E1A-immortalized RK3E rat kidney cells Wnt10b is upregulated in volar skin M2SMO transgenic mice with Hedgehog signaling activation.
Wnt2	Hedgehog Target Genes: Mechanisms of Carcinogenesis Induced by Aberrant Hedgehog Signaling Activation	Katoh, Y. and Katoh, M., 2009.	In E1A-immortalized RK3E rat kidney cells Wnt2 is upregulated in volar skin M2SMO transgenic mice with Hedgehog signaling activation.
WNT2B	Transcriptional regulation of WNT2B based on the balance of Hedgehog, Notch, BMP and WNT signals	Katoh, M., and Katoh, M., 2009.	Hedgehog signals should induce WNT2B upregulation through GLI family members

			as well as FOX family members.
Wnt4	Gli1 acts through Snail and E-cadherin to promote nuclear signaling by b -catenin	Li, X. et al, 2007.	In RTOG10 cells, a clone of RK3E that contains a tetracycline (tet)-inducible Gli1 allele, microarray analysis of these cells identified Wnt4 as early response to Gli1.
Wnt5a	Characterization of *Wnt* gene expression in developing and postnatal hair follicles and identification of *Wnt5a* as a target of Sonic hedgehog in hair follicle morphogenesis	Seshamma, R. et al, 2001.	Wnt5a is expressed in the developing dermal condensate of wild type but not Sonic hedgehog(Shh)-null embryos, indicating that Wnt5a is a target of SHH in hair follicle morphogenesis.
Wnt5b	Wnt5a and Wnt5b exhibit distinct activities in coordinating chondrocyte proliferation and differentiation.	Yang, Y. et al, 2003.	Wnt5b appears to coordinate chondrocyte proliferation and differentiation by differentially regulating cyclin D1 and p130 expression, as well as chondrocyte-specific Col2a1 expression.
Wnt7b	Gli1 acts through Snail and E-cadherin to promote nuclear signaling by b -catenin	Li, X. et al, 2007.	In RTOG10 cells, a clone of RK3E that contains a tetracycline (tet)-inducible Gli1 allele, microarray analysis of these cells identified Wnt7b as early response to Gli1.
WNT8B	Mutation and expression of WNT8b gene and SHH gene in Hirschsprung disease	Gao, H. et al, 2010.	WNT8b and SHH mutations and abnormal expressions are present in the peripheral blood of children with

			sporadic HSCR. These two genes may be related to the development of sporadic HSCR in children in the northeastern China.

Supplementary Table 1. Putative and validated downstream mediators of Hh-Gli signalling.

Supplementary Table 2. Downstream mediators of Hh signaling that are differentially transcribed in P4 murine cerebellar NSCs before and after differentiation.			
Gene	**log2 fold change (NSC vs. Diff-NSC)**	**adj. p-value**	**Function and Process (NCBI- Gene Dataset)**
Foxm1	**4.81**	**4.21E-18**	**G2/M transition of mitotic cell cycle**
			cell cycle
			negative regulation of cell aging
			negative regulation of transcription, DNA-templated
			positive regulation of cell proliferation
			positive regulation of transcription, DNA-templated
			regulation of cell cycle arrest
			regulation of cell proliferation
Insm1	**2.98**	**0.0000053**	cell cycle
			cell differentiation
			negative regulation of cell proliferation
			negative regulation of protein phosphorylation

			nervous system development
			noradrenergic neuron development
			positive regulation of cell cycle arrest
			positive regulation of cell differentiation
			positive regulation of cell migration
			positive regulation of cell proliferation
			positive regulation of neural precursor cell proliferation
Sema6a	**1.51**	**0.0204**	transmembrane signaling receptor activity
			apoptotic process
			axon guidance
			cell differentiation
			nervous system development
			neuron migration
			positive regulation of neuron migration
Ccnb2	**6.6**	**2.7E-27**	cell cycle
			cell division
			growth
			in utero embryonic development
Ccnb1	**7.39**	**6.63E-24**	patched binding
			cell cycle
			cell division
			in utero embryonic development
			negative regulation of gene expression
			negative regulation of protein phosphorylation

			positive regulation of cell cycle
			positive regulation of cyclin-dependent protein serine/threonine kinase activity involved in G2/M transition of mitotic cell cycle
			positive regulation of fibroblast proliferation
			positive regulation of mitotic cell cycle
			regulation of mitotic cell cycle spindle assembly checkpoint
Ccna2	**4.91**	**1.02E-18**	cell cycle
			cell cycle G1/S phase transition
			cell division
			positive regulation of fibroblast proliferation
			regulation of G2/M transition of mitotic cell cycle
Ccnd2	**3.93**	**0.00000000000081 4**	G1/S transition of mitotic cell cycle
			cell division
			long-term memory
			negative regulation of apoptotic process
			positive regulation of G1/S transition of mitotic cell cycle
			positive regulation of cell proliferation
			regulation of cell cycle
Ccne1	**3.2**	**0.0000000178**	cell division
			negative regulation of transcription from RNA polymerase II promoter
			positive regulation of cell differentiation
			regulation of cell cycle

			synapsis
Ccnd1	**4.94**	**0.00002**	cell division
			negative regulation of cell cycle arrest
			negative regulation of transcription from RNA polymerase II promoter
			positive regulation of G2/M transition of mitotic cell cycle
			positive regulation of cell proliferation
			re-entry into mitotic cell cycle
			regulation of G1/S transition of mitotic cell cycle
			regulation of cell cycle
			regulation of transcription, DNA-templated

Supplementary Table 2. Downstream mediators of Hh signaling that are differentially transcribed in P4 murine cerebellar NSCs before and after differentiation.

Supplementary Table 3. The 80 miRNAs displaying differential expression in NSCs *vs*. Diff-NSCs.		
Up-regulated miRNAs in NSCs *vs.* Diff-NSCs		
miRNA	**log2 (fold change)**	**adj. P-value**
mmu-miR-6399	3.85	1.37E-05
mmu-miR-210-5p	2.87	5.18E-03
mmu-miR-15b-3p	2.75	2.33E-07
mmu-miR-7221-3p	2.75	1.38E-03
mmu-miR-335-3p	2.66	2.27E-03
mmu-miR-92a-1-5p	2.56	3.66E-04
mmu-miR-181b-2-3p	2.42	1.24E-02

mmu-miR-193a-3p	2.34	1.38E-03
mmu-miR-301b-5p	2.23	1.18E-02
mmu-miR-29b-3p	2.10	3.95E-02
mmu-miR-5103	2.10	1.98E-02
mmu-miR-32-5p	2.07	2.26E-02
mmu-miR-33-5p	2.02	4.85E-02
mmu-miR-130a-5p	1.98	1.54E-03
mmu-miR-503-5p	1.97	4.33E-02
mmu-miR-130b-5p	1.97	6.72E-04
mmu-miR-16-1-3p	1.96	1.76E-02
mmu-miR-421-5p	1.96	6.10E-03
mmu-miR-301a-5p	1.95	1.08E-02
mmu-miR-7685-3p	1.91	1.97E-03
mmu-miR-450b-5p	1.86	3.87E-02
mmu-miR-879-5p	1.83	4.45E-02
mmu-miR-19a-3p	1.82	3.91E-02
mmu-miR-106b-5p	1.82	1.19E-02
mmu-miR-16-2-3p	1.71	7.46E-03
mmu-miR-7a-5p	1.70	1.98E-02
mmu-miR-130b-3p	1.69	1.14E-02
mmu-miR-6417	1.68	3.02E-02
mmu-miR-5122	1.64	4.16E-02
mmu-miR-126a-5p	1.62	3.96E-02
mmu-miR-126b-3p	1.60	4.14E-02
mmu-miR-15b-5p	1.60	3.88E-03

mmu-miR-25-5p	1.58	2.77E-03
mmu-miR-345-5p	1.54	1.87E-03
mmu-miR-3963	1.51	1.08E-02
mmu-miR-93-3p	1.49	2.77E-03
mmu-miR-15a-3p	1.48	1.89E-02
mmu-miR-674-5p	1.31	4.43E-02
mmu-miR-126a-3p	1.27	4.29E-02
mmu-miR-5100	1.24	1.67E-02
Down-regulated miRNAs in NSCs *vs.* Diff-NSCs		
miRNA	**log2 (fold change)**	**adj. P-value**
mmu-miR-211-5p	-2.90	9.01E-05
mmu-miR-92b-5p	-2.66	1.37E-05
mmu-miR-145a-5p	-2.62	4.73E-04
mmu-miR-129-1-3p	-2.61	8.65E-05
mmu-miR-2137	-2.46	4.73E-04
mmu-miR-187-5p	-2.42	2.03E-03
mmu-miR-92b-3p	-2.42	4.73E-04
mmu-let-7c-5p	-2.34	3.66E-04
mmu-miR-433-5p	-2.34	1.98E-02
mmu-miR-6516-5p	-2.14	2.77E-03
mmu-miR-7064-3p	-2.07	2.71E-02
mmu-miR-221-5p	-2.04	4.85E-02
mmu-let-7b-5p	-2.02	8.86E-04
mmu-miR-6546-3p	-2.02	4.83E-02

mmu-miR-491-5p	-2.00	3.88E-03
mmu-miR-6988-5p	-1.93	2.36E-02
mmu-miR-7004-5p	-1.92	1.98E-02
mmu-miR-874-3p	-1.89	1.46E-02
mmu-miR-22-5p	-1.88	8.86E-04
mmu-miR-185-5p	-1.86	1.98E-02
mmu-miR-187-3p	-1.77	3.95E-02
mmu-miR-22-3p	-1.74	6.10E-03
mmu-miR-878-5p	-1.73	2.25E-02
mmu-miR-99a-5p	-1.73	2.00E-02
mmu-miR-185-3p	-1.72	1.97E-03
mmu-miR-3084-3p	-1.72	3.83E-02
mmu-miR-23b-3p	-1.64	2.77E-03
mmu-miR-494-3p	-1.63	3.96E-02
mmu-miR-30a-3p	-1.61	5.84E-03
mmu-miR-1249-3p	-1.60	1.14E-02
mmu-miR-153-5p	-1.59	3.83E-02
mmu-miR-470-5p	-1.56	4.94E-02
mmu-let-7k	-1.53	1.98E-02
mmu-miR-1843b-5p	-1.51	4.14E-02
mmu-miR-3083-5p	-1.46	2.17E-02
mmu-miR-146b-5p	-1.45	1.67E-02
mmu-let-7b-3p	-1.39	4.14E-02
mmu-miR-1843b-3p	-1.35	3.96E-02
mmu-miR-30e-3p	-1.31	1.67E-02

mmu-miR-6944-5p	-1.11	4.89E-02

Supplementary Table 3. The 80 miRNAs displaying differential expression in NSCs vs. Diff-NSCs.

Supplementary Table 4. miRTarbase: Validated murine gene targets of the Foxm1-regulated miRNAs.

Target Gene	Target Gene (Entrez Gene ID)	miRTarBase ID	miRNA	Experiments	Support Type	References (PMID)
Acbd5	74159	MIRT590765	mmu-miR-130b-3p	HITS-CLIP	Functional MTI (Weak)	25083871
Arrdc3	105171	MIRT590623	mmu-miR-130b-3p	HITS-CLIP	Functional MTI (Weak)	25083871
Fgfr1op2	67529	MIRT595360	mmu-miR-130b-3p	HITS-CLIP	Functional MTI (Weak)	23142080
Homez	239099	MIRT600788	mmu-miR-130b-3p	HITS-CLIP	Functional MTI (Weak)	21258322
Inpp5e	64436	MIRT606373	mmu-miR-130b-3p	HITS-CLIP	Functional MTI (Weak)	21258322
Kdm2a	225876	MIRT582794	mmu-miR-130b-3p	HITS-CLIP	Functional MTI (Weak)	25083871

Map3k12	26404	MIRT604876	mmu-miR-130b-3p	HITS-CLIP	Functional MTI (Weak)	21258322
Meox2	17286	MIRT006124	mmu-miR-130b-3p	Luciferase reporter assay//qRT-PCR//Western blot	Functional MTI	21941297
Mup13	100039089	MIRT592586	mmu-miR-130b-3p	HITS-CLIP	Functional MTI (Weak)	23597149
Mup7	100041658	MIRT592545	mmu-miR-130b-3p	HITS-CLIP	Functional MTI (Weak)	23597149
Nfia	18027	MIRT594100	mmu-miR-130b-3p	HITS-CLIP	Functional MTI (Weak)	23142080
Snx27	76742	MIRT580804	mmu-miR-130b-3p	HITS-CLIP	Functional MTI (Weak)	25083871
Tgfb1	21803	MIRT438308	mmu-miR-130b-3p	Luciferase reporter assay//qRT-PCR	Functional MTI	25204661
Timp2	21858	MIRT595108	mmu-miR-130b-3p	HITS-CLIP	Functional MTI (Weak)	23142080
Tmem25	71687	MIRT580366	mmu-miR-130b-3p	HITS-CLIP	Functional MTI (Weak)	25083871

Ubap2l	74383	MIRT580136	mmu-miR-130b-3p	HITS-CLIP	Functional MTI (Weak)	25083871
4930444A02Rik	74653	MIRT592367	mmu-miR-15b-5p	HITS-CLIP	Functional MTI (Weak)	23597149
Angel1	68737	MIRT592353	mmu-miR-15b-5p	HITS-CLIP	Functional MTI (Weak)	23597149
Arl2	56327	MIRT003376	mmu-miR-15b-5p	Luciferase reporter assay//qRT-PCR//Western blot	Functional MTI	20007690
Armcx6	278097	MIRT592342	mmu-miR-15b-5p	HITS-CLIP	Functional MTI (Weak)	21258322
Bcl11b	58208	MIRT601136	mmu-miR-15b-5p	HITS-CLIP	Functional MTI (Weak)	21258322
Bcl2l2	12050	MIRT438297	mmu-miR-15b-5p	Western blot	Functional MTI	24070634
Bicd1	12121	MIRT592811	mmu-miR-15b-5p	HITS-CLIP	Functional MTI (Weak)	19536157
Bri3bp	76809	MIRT601123	mmu-miR-15b-5p	HITS-CLIP	Functional MTI (Weak)	21258322
Creb5	231991	MIRT584147	mmu-miR-15b-5p	HITS-CLIP	Functional MTI (Weak)	25083871
Ddx19b	234733	MIRT591938	mmu-miR-15b-5p	HITS-CLIP	Functional MTI (Weak)	23597149

Dedd	21945	MIRT054236	mmu-miR-15b-5p	ELISA//Flow cytometry//Luciferase reporter assay//Microarray//QRTPCR//Western blot	Functional MTI	23517578
Dhdh	71755	MIRT578978	mmu-miR-15b-5p	HITS-CLIP	Functional MTI (Weak)	21258322
Erlin2	244373	MIRT583723	mmu-miR-15b-5p	HITS-CLIP	Functional MTI (Weak)	25083871
Fbxo21	231670	MIRT592718	mmu-miR-15b-5p	HITS-CLIP	Functional MTI (Weak)	21258322
Fgd4	224014	MIRT599014	mmu-miR-15b-5p	HITS-CLIP	Functional MTI (Weak)	21258322
Idua	15932	MIRT598640	mmu-miR-15b-5p	HITS-CLIP	Functional MTI (Weak)	21258322
Irgq	210146	MIRT578443	mmu-miR-15b-5p	HITS-CLIP	Functional MTI (Weak)	19536157
Itgav	16410	MIRT592669	mmu-miR-15b-5p	HITS-CLIP	Functional MTI (Weak)	23597149
Klc1	16593	MIRT591288	mmu-miR-15b-5p	HITS-CLIP	Functional MTI (Weak)	21258322
Lpcat2b	70902	MIRT603789	mmu-miR-15b-5p	HITS-CLIP	Functional MTI (Weak)	21258322
Mapkap1	227743	MIRT592205	mmu-miR-15b-5p	HITS-CLIP	Functional MTI (Weak)	21258322

Ncl	17975	MIRT598105	mmu-miR-15b-5p	HITS-CLIP	Functional MTI (Weak)	21258322
Pacsin2	23970	MIRT597925	mmu-miR-15b-5p	HITS-CLIP	Functional MTI (Weak)	21258322
Rnf168	70238	MIRT577817	mmu-miR-15b-5p	HITS-CLIP	Functional MTI (Weak)	25083871
Sorcs2	81840	MIRT592078	mmu-miR-15b-5p	HITS-CLIP	Functional MTI (Weak)	23597149
Spsb4	211949	MIRT592430	mmu-miR-15b-5p	HITS-CLIP	Functional MTI (Weak)	23597149
Tacc1	320165	MIRT592410	mmu-miR-15b-5p	HITS-CLIP	Functional MTI (Weak)	21258322
Tifab	212937	MIRT600293	mmu-miR-15b-5p	HITS-CLIP	Functional MTI (Weak)	21258322
Trim2	80890	MIRT600256	mmu-miR-15b-5p	HITS-CLIP	Functional MTI (Weak)	21258322
Btg2	12227	MIRT596475	mmu-miR-92a-3p	HITS-CLIP	Functional MTI (Weak)	23142080
Cd69	12515	MIRT595903	mmu-miR-92a-3p	HITS-CLIP	Functional MTI (Weak)	23142080
Chm	12662	MIRT595805	mmu-miR-92a-3p	HITS-CLIP	Functional MTI (Weak)	23142080

Cpeb1	12877	MIRT584193	mmu-miR-92a-3p	HITS-CLIP	Functional MTI (Weak)	25083871
Fam136a	66488	MIRT583677	mmu-miR-92a-3p	HITS-CLIP	Functional MTI (Weak)	25083871
Gm14420	628308	MIRT598840	mmu-miR-92a-3p	HITS-CLIP	Functional MTI (Weak)	21258322
Gm5148	381438	MIRT587067	mmu-miR-92a-3p	HITS-CLIP	Functional MTI (Weak)	23142080
Hipk3	15259	MIRT002971	mmu-miR-92a-3p	Luciferase reporter assay//Reporter assay	Functional MTI	17575136
Il5ra	16192	MIRT598598	mmu-miR-92a-3p	HITS-CLIP	Functional MTI (Weak)	21258322
Map2k4	26398	MIRT007244	mmu-miR-92a-3p	Luciferase reporter assay	Functional MTI	23355465
Mylip	218203	MIRT002978	mmu-miR-92a-3p	Luciferase reporter assay//Western blot	Functional MTI	17575136
Ncam2	17968	MIRT578185	mmu-miR-92a-3p	HITS-CLIP	Functional MTI (Weak)	25083871
Rhbdl3	246104	MIRT589036	mmu-miR-92a-3p	HITS-CLIP	Functional MTI (Weak)	25083871
Shox2	20429	MIRT054792	mmu-miR-92a-3p	Luciferase reporter assay//immunofluorescence	Functional MTI	24927531
Stk10	20868	MIRT580680	mmu-miR-92a-3p	HITS-CLIP	Functional MTI (Weak)	19536157

Tagap	72536	MIRT596301	mmu-miR-92a-3p	HITS-CLIP	Functional MTI (Weak)	23142080
Tagap1	380608	MIRT596292	mmu-miR-92a-3p	HITS-CLIP	Functional MTI (Weak)	23142080
Tbx3	21386	MIRT054699	mmu-miR-92a-3p	ChIP-seq//Immunofluorescence//In situ hybridization//Luciferase reporter assay//qRT-PCR	Functional MTI	24068957
Trp63	22061	MIRT004280	mmu-miR-92a-3p	Luciferase reporter assay//qRT-PCR//Western blot	Functional MTI	19608627
Uba1y	22202	MIRT601409	mmu-miR-92a-3p	HITS-CLIP	Functional MTI (Weak)	21258322
Zfp300	245368	MIRT606063	mmu-miR-92a-3p	HITS-CLIP	Functional MTI (Weak)	21258322
Zfpm2	22762	MIRT053813	mmu-miR-92a-3p	Luciferase reporter assay//qRT-PCR//Western blot	Functional MTI	22267003
Zpbp	53604	MIRT595174	mmu-miR-92a-3p	HITS-CLIP	Functional MTI (Weak)	23142080

Abbreviations: HITS-CLIP, Crosslinking immunoprecipitation coupled with high throughput sequencing; ELISA, enzyme-linked immunosorbent assay; Functional MTI, Functional miRNA–target interaction;

Supplementary Table 4. miRTarbase: Validated murine gene targets of the Foxm1-regulated miRNAs.

Supplementary Table 5. Transcripts differentially expressed in NSCs and Diff-NSCs identified by all three methods							
	log2 (fold change NSC vs. Diff-NSC)				**log2 (fold change NSC vs. Diff-NSC)**		
Gene	**DESeq**	**CuffLinks whole-read prot.**	**CuffLinks trimmed-read prot.**	**Gene**	**DESeq**	**CuffLinks whole-read prot.**	**CuffLinks trimmed-read prot.**
1700003e16Rik	-3.11	-3.60	-3.02	*Kirrel2*	3.57	3.58	3.65
1700084c01Rik	-6.79	-7.06	-7.09	*Klf10*	1.45	1.41	1.33
1810058i24Rik	-1.69	-1.63	-1.66	*Klf11*	-1.98	-1.91	-1.91
2310022b05Rik	-2.45	-2.44	-2.36	*Klf12*	1.34	3.17	1.46
2510003e04Rik	-1.48	-1.41	-1.40	*Klk14*	7.79	6.19	7.99
2610318n02Rik	5.2	4.06	4.74	*Kntc1*	5.35	5.57	5.55
2700094k13Rik	2.8	2.45	2.90	*Kpna2*	2.65	2.39	2.56
2810459m11k	-2.15	-2.51	-2.07	*Lama4*	Inf	6.05	5.95
2900026a02Rik	-2.24	-3.07	-2.30	*Lamb1*	2.28	2.13	2.17
4930427a07Rik	3.06	2.90	3.22	*Lamb2*	-1.93	-1.90	-1.81

4930451c15Rik	-4.92	-3.62	-4.86	*Lamb3*	4.67	4.94	3.89
4932438h23Rik	-3.76	-3.60	-3.95	*Lamp2*	-1.59	-1.79	-1.70
4933407l21Rik	-3.05	-3.13	-3.14	*Laptm4a*	-2.13	-2.04	-2.12
5033411d12Rik	-4.52	-4.57	-4.76	*Lbp*	-9.15	-8.43	-9.30
5430435g22Rik	-4.73	-5.35	-4.75	*Lbr*	2.97	3.08	2.98
6330403a02Rik	-5.18	-5.08	-4.79	*Lcat*	-3.66	-3.78	-3.56
9530053a07Rik	-3.03	-3.06	-3.11	*Lcn2*	-10.18	-6.91	-8.67
A2m	-4.56	-4.63	-4.63	*Ldlr*	2.38	2.29	2.32
Aatk	2.13	2.17	2.20	*Lect1*	-5.37	-5.16	-4.93
Abat	-1.96	-1.94	-1.82	*Lgals3*	-5.5	-3.72	-5.89
Abca1	-4.28	-4.34	-4.38	*Lgals8*	-1.67	-1.84	-1.70
Abhd4	-2.31	-2.40	-2.27	*Lgi4*	-10.39	-9.43	-9.64
Ablim2	-4.86	-5.29	-4.85	*Lgmn*	-2.18	-2.16	-2.16
Acaa2	-1.47	-1.51	-1.48	*Lhx2*	2.75	2.90	2.81
Acad11	-1.97	-1.90	-1.89	*Lig1*	3.96	3.95	3.96
Acadm	-1.6	-1.65	-1.56	*Lix1*	-4.92	-5.47	-4.95
Acap3	2.18	2.05	2.13	*Lmcd1*	2.82	2.81	2.86
Acat2	1.62	1.58	1.61	*Lmnb1*	3.27	4.15	4.17
Acbd5	-1.37	-5.81	-1.43	*Lmo1*	2.64	2.76	2.76
Acox1	-2.16	-2.07	-2.17	*Lmo3*	2.19	2.59	2.16

Acox3	-1.66	-1.74	-1.70	*Lor*	5.49	4.70	5.60
Acsf2	-3.65	-3.86	-3.59	*Lpar1*	-4.95	-4.75	-5.04
Acsl6	-2.75	-2.03	-2.73	*Lphn2*	2.45	2.55	2.41
Adam12	5	5.08	4.90	*Lpin3*	-3.42	-3.23	-3.20
Adam19	3.26	3.42	3.40	*Lrp10*	-1.34	-1.36	-1.27
Adamts14	2.65	2.52	2.66	*Lrrc16a*	-1.37	-2.33	-1.46
Adamts19	6.9	6.50	6.52	*Lrrc2*	-4.15	-4.41	-4.21
Adamts7	2.17	2.18	2.16	*Lrrc32*	3.96	4.73	4.00
Adc	-4.12	-4.13	-3.96	*Lrrfip1*	1.69	2.14	1.77
Adcy1	1.67	1.64	1.66	*Lrrn4*	5.42	5.02	5.56
Add3	-1.37	-2.17	-1.33	*Lsm4*	1.68	1.56	1.82
Adora1	-2.16	-2.36	-2.11	*Lss*	1.75	1.84	1.85
Adra2a	-3.96	-3.25	-3.85	*Lxn*	-3.02	-2.96	-2.93
Agpat3	-1.92	-2.12	-1.89	*Ly6h*	-6.29	-5.77	-5.99
Agt	-3.14	-2.98	-3.08	*Ly75*	3.78	3.98	4.18
Aldh9a1	-1.8	-2.08	-1.83	*Lyn*	2.77	2.61	2.81
Alpl	3.12	3.20	3.16	*Lynx1*	-2.77	-2.76	-2.67
Amotl2	-1.77	-1.72	-1.72	*Lyz2*	-4.45	-4.17	-4.70
Angptl4	-8.25	-7.78	-7.56	*Mad2l1*	3.86	3.69	3.82
Ank	-2.47	-2.44	-2.42	*Man1c1*	-3.71	-3.77	-3.71
Ankle1	6.68	7.30	6.83	*Man2b 2*	-1.98	-1.91	-1.86
Ankrd35	-4.62	-4.08	-4.18	*Maoa*	-1.8	-1.69	-1.82
Anln	4.12	3.81	4.50	*Map1lc 3b*	-1.45	-1.83	-1.81
Anp32b	1.44	1.93	1.86	*Mapk7*	1.45	2.40	1.47

Anp32e	1.8	1.73	1.66	*March2*	-2.02	-2.07	-1.92
Antxr1	-2.14	-1.94	-2.03	*Masp1*	2.52	2.74	2.32
Anxa5	-2.98	-2.93	-2.91	*Mastl*	3.83	3.32	3.76
Ap3m2	-1.98	-1.97	-2.03	*Mb*	-6.35	-7.28	-5.99
Apitd1	3.06	3.32	3.11	*Mcm10*	5.55	6.30	5.52
Aplp2	2.35	2.57	1.59	*Mcm2*	4.03	4.00	4.09
Apoc1	-5.03	-5.00	-4.81	*Mcm3*	3.45	3.56	3.56
Appl2	-1.54	-2.31	-1.53	*Mcm4*	2.35	2.47	2.36
Aqp4	-5.91	-6.39	-5.92	*Mcm5*	5.04	5.19	5.10
Arc	3.42	3.55	3.58	*Mcm7*	2.63	2.69	2.67
Arhgap11a	3.43	3.45	3.45	*Mdc1*	2.16	2.24	2.08
Arhgap18	2.43	2.49	2.39	*Mdga1*	-1.51	-1.95	-1.77
Arhgap19	3.39	3.76	3.53	*Melk*	5.74	6.19	6.10
Arhgap23	-1.91	-2.33	-1.97	*Mest*	2.22	2.35	2.22
Arhgap33	1.96	3.70	2.03	*Met*	-6.52	-6.58	-6.56
Arhgap5	-1.53	-1.40	-1.61	*Mfsd7b*	-3.56	-3.34	-3.58
Arhgef10	-1.82	-1.89	-1.81	*Mgll*	-2.69	-2.48	-2.60
Arhgef12	-1.39	-1.46	-1.37	*Mgst1*	-3.17	-3.07	-3.18
Arhgef4	-2.62	-2.67	-2.60	*Mical2*	3.49	3.83	3.73
Arid5a	-2.26	-2.30	-2.21	*Mki67*	7.11	7.22	7.22
Armc2	-3.7	-4.03	-4.07	*Mkrn1*	-1.39	-1.84	-1.84
Arsb	-1.79	-1.71	-1.77	*Mlc1*	-1.99	-1.63	-1.93
Asap3	-4.07	-4.11	-3.99	*Mmp11*	-3.99	-3.87	-3.90
Asf1b	4.18	4.10	4.11	*Mmp15*	2.73	2.88	2.89
Aspm	6.82	7.10	6.92	*Mms22l*	3.3	3.78	3.25

Asrgl1	-1.64	-1.69	-1.65	*Moxd1*	5.29	5.56	5.81
Ass1	-5.39	-4.73	-4.73	*Mpp3*	2.86	2.81	2.76
Atad2	3.19	3.46	3.18	*Mpp5*	-1.59	-1.48	-1.63
Atad5	2.02	2.12	2.27	*Mpp6*	-2.16	-2.14	-1.62
Atf3	-4.85	-4.96	-4.92	*Mpv17l*	-2.57	-2.30	-2.23
Atoh8	-4.39	-4.47	-4.32	*Msi1*	-1.83	-2.02	-1.76
Atp1a1	-3.38	-3.29	-3.31	*Mt1*	-2.8	-2.53	-2.45
Atp1a3	2.84	2.78	2.92	*Mt2*	-3.65	-3.79	-3.64
Atp1b1	-3.09	-3.14	-3.10	*Mt3*	-3.26	-3.22	-3.19
Atp1b2	-3.25	-3.44	-3.25	*Mthfd1l*	2.82	2.88	2.85
Atp6v0a2	-2.48	-2.23	-2.32	*Mthfd2*	4.02	4.18	4.03
Atrn	-1.74	-2.10	-2.19	*Mtmr10*	-2.44	-2.13	-2.23
Atxn1	-2.6	-2.29	-2.48	*Mutyh*	2.92	3.01	3.14
Aurka	5.12	4.82	5.10	*Mvp*	-2.79	-2.95	-2.77
Aurkb	7.38	7.30	7.38	*Mybl2*	5.13	5.10	5.17
Axl	-2.71	-2.74	-2.75	*Myh15*	-3.22	-4.03	-3.21
Bace2	-4.64	-4.51	-4.64	*Mylk*	3.93	3.23	2.23
Bahcc1	2.3	1.77	2.33	*Naaa*	-7.13	-7.15	-7.50
Banf1	1.56	1.56	1.62	*Naaladl 1*	4.52	4.51	4.35
Bard1	5.25	5.35	5.08	*Nacc2*	-1.58	-1.72	-1.59
Barx2	6.11	7.30	7.46	*Nasp*	2.12	2.02	2.06
Bbs1	-1.74	-1.72	-1.76	*Nbl1*	-3.65	-3.72	-3.57
Bc030867	3.84	3.80	3.88	*Ncapd2*	3	2.90	3.02
Bcar1	-1.7	-1.94	-1.60	*Ncapd3*	1.68	1.86	1.63
Bcar3	-3.92	-4.18	-3.55	*Ncapg2*	3.18	3.64	3.44

Bcas3	-1.84	-1.97	-1.84	*Ncaph*	4.34	4.34	4.34
Bcat1	3.02	2.94	3.05	*Ncor2*	1.31	1.73	1.38
Bdh2	-4.71	-5.12	-4.67	*Ndc80*	Inf	6.05	5.99
Bex2	2.2	2.31	2.19	*Ndst1*	-1.44	-1.83	-1.47
Birc5	6.02	6.28	6.36	*Neat1*	-2.09	-2.01	-2.09
Bmf	-4.37	-4.56	-4.49	*Nebl*	-2.45	-2.83	-2.74
Bmp1	-1.4	-1.77	-1.39	*Neil3*	8.67	8.21	8.32
Bmp2k	-3.03	-2.90	-2.70	*Nek11*	-6.3	-5.97	-6.24
Bmp7	4.86	5.20	5.03	*Nek2*	6.6	6.67	6.33
Bok	3.48	3.46	3.66	*Nek6*	-1.72	-1.67	-1.65
Brca1	4.09	4.57	4.33	*Neto1*	2.64	2.73	2.65
Brip1	4.19	4.27	3.70	*Neurl1a*	3.69	2.97	3.72
Bub1	6.42	7.79	6.72	*Neurl1b*	4.77	4.89	4.94
Bub1b	5.49	5.42	5.51	*Nfasc*	-1.61	-2.24	-2.12
C1ql1	-4.47	-4.64	-4.40	*Ngef*	-3.51	-3.63	-3.47
C1rl	-4.71	-4.77	-4.78	*Nipal3*	-3.3	-3.33	-3.28
C1s	-4.96	-4.78	-5.13	*Nkain1*	1.51	1.79	1.61
C3	-10.21	-11.03	-9.87	*Nkain4*	-1.98	-1.94	-1.94
C330027c 09rik	3.71	3.87	3.61	*Nmb*	-3.7	-4.22	-3.62
C4b	-6.9	-6.54	-6.92	*Nme5*	-4.28	-5.11	-4.34
Cachd1	-2.39	-2.38	-2.31	*Nomo1*	1.51	1.49	1.52
Cacnb4	-2.67	-3.56	-2.95	*Nos1*	-5.59	-6.16	-5.86
Cad	1.62	1.45	1.54	*Npdc1*	-1.43	-1.54	-1.31
Cadm4	-1.63	-1.72	-1.53	*Nptx1*	4.76	4.83	4.80
Calcoco1	-1.6	-1.76	-1.55	*Nrbp2*	-2.48	-2.39	-2.42

Calm2	2.24	2.56	2.10	*Nrgn*	6.02	6.43	6.48
Calml3	-5.61	-5.75	-5.75	*Nrm*	3.43	3.52	3.54
Camk1g	6.24	6.08	6.00	*Nsl1*	4.08	4.23	3.54
Camk2b	2.21	3.11	2.24	*Ntn1*	1.65	1.86	1.71
Camkk2	1.92	1.80	1.83	*Ntn4*	1.58	2.20	1.70
Capg	-4.17	-4.00	-4.36	*Ntrk2*	-2.52	-1.52	-2.47
Capn1	-5	-4.31	-4.89	*Nuak1*	-3.03	-3.19	-3.28
Capn2	-1.61	-1.60	-1.60	*Nudt4*	-1.61	-1.55	-1.59
Capns1	-2.21	-2.49	-2.06	*Nuf2*	5.6	2.36	3.41
Car3	4.38	4.14	3.93	*Nup107*	1.87	1.95	1.86
Car5b	-4.88	-4.45	-4.79	*Nup188*	1.36	1.42	1.41
Car6	5.4	5.79	5.46	*Nup205*	1.72	1.92	1.78
Carns1	-3.36	-2.86	-3.34	*Nup210*	4.31	4.46	4.26
Casc5	6.47	7.11	6.00	*Nup85*	1.73	1.77	1.75
Casq2	-5.69	-6.32	-5.80	*Nusap1*	3.7	3.67	3.61
Cat	-1.79	-1.74	-1.77	*Nxn*	-2.27	-2.55	-2.49
Ccdc103	-3.77	-3.58	-3.82	*Nxph3*	-3.69	-4.00	-3.53
Ccdc13	-5.34	-6.09	-5.80	*Oat*	-2.71	-1.93	-2.73
Ccdc135	-9.85	-10.09	-10.51	*Olfm2*	2.42	2.60	2.57
Ccdc148	-5.1	-4.28	-4.93	*Olig1*	2.31	2.24	2.41
Ccdc153	-6.34	-8.26	-6.26	*Olig2*	2.72	2.63	2.82
Ccdc74a	-3.31	-3.33	-2.89	*Ophn1*	-1.9	-2.12	-1.92
Ccdc96	-2.67	-2.62	-2.71	*Orc1*	3.59	4.31	3.63
Ccna2	4.91	6.75	5.66	*Ormdl3*	-1.37	-1.70	-1.36
Ccnb1	7.39	6.92	7.28	*Osbpl5*	-1.86	-2.07	-2.04

Ccnb2	6.6	6.61	6.70	*Osgin2*	-2.04	-1.95	-2.06
Ccnd1	4.94	5.09	4.87	*Osmr*	-5.58	-5.01	-5.46
Ccnd2	3.93	4.25	4.12	*Otoa*	4.06	4.56	4.17
Ccne1	3.2	3.29	3.20	*P2rx6*	-3.46	-4.57	-3.34
Ccnf	4.72	4.72	4.73	*P4ha3*	-4.62	-4.49	-4.80
Cd109	-2.7	-2.65	-2.87	*Pacrg*	-2.87	-3.56	-2.86
Cd248	3.44	3.74	3.89	*Pacs2*	-1.55	-1.62	-1.60
Cd276	1.78	1.86	1.82	*Padi2*	-6.04	-6.09	-6.09
Cd38	-4.95	-4.77	-4.30	*Palld*	-1.94	-2.82	-2.05
Cd44	-1.6	-1.51	-1.74	*Palm*	-1.83	-3.21	-1.72
Cd93	5.61	5.63	5.37	*Paqr4*	-2.45	-2.23	-2.39
Cdc20	6.12	6.08	6.14	*Paqr8*	-1.67	-1.70	-1.73
Cdc25b	2.7	2.95	2.76	*Pard3b*	-2.03	-2.12	-2.10
Cdc25c	6.89	6.36	6.23	*Pard6b*	-3.44	-3.31	-3.33
Cdc42ep4	-3.37	-3.40	-3.27	*Parp3*	-3.77	-3.66	-3.56
Cdc45	4.31	3.29	4.26	*Parp4*	-1.96	-1.85	-1.96
Cdc6	4.94	4.91	4.98	*Pask*	2.74	2.92	2.74
Cdc7	3.54	3.83	3.65	*Pbk*	6.92	6.92	6.64
Cdca2	6.43	7.16	6.51	*Pcna*	2.28	2.13	2.13
Cdca3	6.22	6.18	6.17	*Pcp4l1*	-2.89	-2.81	-2.94
Cdca5	4.58	4.66	4.66	*Pcx*	-2.09	-2.18	-2.03
Cdca7	3.99	3.83	4.01	*Pdia4*	-1.37	-1.32	-1.39
Cdca8	5.78	5.72	5.85	*Pdia5*	2.57	2.90	2.89
Cdh13	2.7	2.73	2.72	*Pdk2*	-2.07	-2.08	-2.03
Cdh4	1.74	1.84	1.84	*Peg10*	1.75	1.88	1.72

Cdhr1	5.44	5.12	5.19	*Peg12*	3.18	3.15	3.25
Cdk1	5.23	6.64	5.32	*Peli2*	-2.1	-2.26	-2.31
Cdkn3	5.47	6.06	5.66	*Per1*	1.7	3.41	1.69
Cdon	2.86	2.96	2.83	*Pfkfb3*	-2.98	3.03	-2.78
Cdr2l	2.18	2.31	2.39	*Pgap1*	2.32	2.69	2.31
Cdt1	4.31	4.28	4.43	*Phkg1*	-5.14	-5.36	-5.07
Celsr2	-2.01	-1.87	-1.70	*Phyhd1*	-3.73	-3.53	-3.78
Cenpa	5.89	5.79	5.67	*Pi15*	-6.88	-6.75	-6.76
Cenpe	5.76	6.12	5.95	*Pif1*	7.55	7.53	7.55
Cenpf	7.67	7.75	6.61	*Pik3ip1*	-2.26	-2.19	-2.15
Cenph	4.26	4.45	4.37	*Pink1*	-2.7	-2.68	-2.57
Cenpi	3.68	4.49	3.69	*Pkd1*	1.78	1.94	1.94
Cenpm	6.03	5.70	5.83	*Pkp4*	-1.84	-2.06	-1.86
Cenpn	4.36	4.50	4.40	*Pla2g16*	-1.87	-1.99	-2.01
Cenpq	3.15	3.16	2.99	*Pla2g3*	2.8	3.72	3.74
Cenpw	3.43	3.57	3.52	*Plat*	-1.51	-1.58	-1.58
Cep55	5.88	4.30	5.41	*Plbd2*	-1.38	-1.38	-1.34
Cetn4	-4.18	-4.21	-4.05	*Plce1*	-4.19	-3.87	-4.24
Cftr	5.44	5.45	5.35	*Pld1*	1.68	2.47	1.69
Chaf1a	2.58	2.55	2.61	*Plec*	-3.78	-4.08	-3.87
Chaf1b	3.98	3.88	3.89	*Plekha6*	-5.53	-5.52	-5.23
Chek1	3.98	3.31	3.98	*Plekhb1*	-2.72	-2.67	-2.67
Chgb	-2.87	-2.86	-2.88	*Plk1*	6.93	6.75	6.99

Chi3l1	-5.14	-5.62	-5.26	*Plk2*	2.09	2.11	2.09
Chn2	2.18	2.18	1.75	*Plk4*	4.48	5.51	4.06
Chrm3	3.85	4.64	3.86	*Plp1*	-3.06	-3.45	-3.09
Chst7	4.06	2.94	4.18	*Plscr2*	-8.18	-7.69	-8.42
Chst8	-5.06	-5.21	-4.79	*Pltp*	-4.54	-4.82	-4.43
Chtf18	3.77	3.76	3.89	*Plvap*	3.64	3.45	3.78
Ckap2	2.06	2.26	1.94	*Plxdc1*	-7.18	-7.13	-7.32
Ckap2l	5.45	4.33	5.41	*Plxnb1*	-1.97	-1.94	-1.94
Cks1b	3.14	3.02	3.15	*Pmf1*	3.02	2.95	3.12
Cks2	4.04	5.23	4.21	*Pnpla7*	-1.95	-1.99	-2.01
Cldn9	-5.68	-5.55	-6.66	*Pola1*	1.94	2.06	1.88
Clip4	-2.79	-3.00	-2.82	*Pold1*	3.46	3.41	3.58
Clspn	4.63	4.92	4.98	*Pole*	4.01	4.12	4.08
Clu	-5.62	-6.69	-5.62	*Polq*	4.19	4.62	4.04
Cml1	-2.17	-2.62	-2.60	*Pom121*	1.38	1.46	1.46
Cmtm5	-2.61	-2.55	-2.49	*Porcn*	-2.36	-3.26	-2.26
Cmya5	-2.72	-2.73	-2.95	*Pou3f1*	4.95	4.86	5.13
Cnn3	-1.5	-1.43	-1.47	*Ppp1r3c*	-2.28	-2.30	-2.37
Cnp	-2.13	-2.13	-2.06	*Ppp2r2b*	-2.53	-2.59	-2.52
Cobll1	-1.88	-2.52	-1.86	*Ppp2r5a*	-1.81	-1.87	-1.65
Col22a1	-3.79	-4.01	-3.57	*Prc1*	5.41	5.40	5.42
Col23a1	-4.19	-9.47	-3.95	*Prdx6*	-3.77	-3.20	-3.79

Col4a5	-4.28	-4.30	-4.31	*Prelp*	-4.39	-4.31	-4.43
Col6a1	-2.58	-2.63	-2.57	*Prim1*	2.87	2.91	2.81
Col8a2	-4.23	-3.81	-4.20	*Prkca*	-2.07	-1.92	-2.05
Cotl1	-2.28	-2.26	-2.14	*Prkcb*	3.76	4.18	3.96
Cpeb2	-2.02	-2.11	-2.08	*Prmt1*	1.57	1.59	1.57
Cpne7	Inf	6.18	6.88	*Pros1*	-1.59	-1.51	-1.63
Creb5	3.44	3.48	3.49	*Prr11*	4.58	4.84	4.33
Crip2	-1.53	-1.52	-1.40	*Prr18*	2.56	2.41	2.60
Crtap	2.02	2.04	2.07	*Prune2*	-4.66	-5.12	-4.92
Cryab	-3.44	-2.43	-3.40	*Psen2*	-2.25	-2.19	-2.27
Crygs	-5.12	-4.43	-4.58	*Pstpip2*	4.35	4.70	4.51
Csf1	-2.98	-2.87	-2.91	*Pth1r*	-4.24	-5.55	-3.98
Cspg4	2.41	2.49	2.58	*Ptn*	1.73	1.74	1.78
Cspg5	2.57	1.40	1.50	*Ptplb*	-2.96	-3.36	-2.93
Cst3	-1.98	-1.75	-1.77	*Ptprf*	-1.41	-1.46	-1.34
Ctnnal1	-2.6	-2.56	-2.61	*Ptprj*	2.62	2.49	2.40
Ctps	1.88	1.81	1.63	*Pvalb*	-7.56	-8.58	-7.91
Ctsf	-2.2	-2.19	-2.14	*Pygb*	-3.48	-3.52	-3.44
Ctsl	-2.23	-2.14	-2.24	*Rab26*	6.88	6.25	6.97
Cxcr4	-5.72	-5.36	-5.76	*Racgap 1*	4.64	4.38	4.68
Cyp4v3	-3.56	-3.84	-3.71	*Rad51*	3.34	3.42	3.29
D10jhu81e	-1.6	-1.56	-1.57	*Rad51a p1*	5.11	4.54	5.06
Daam2	-6.52	-6.50	-6.56	*Rad51c*	3.28	3.39	3.10
Dapk1	-2.5	-2.43	-2.33	*Ran*	1.41	1.66	1.43

Dazap1	1.58	1.74	1.74	*Rap1gap*	3.05	3.13	3.02
Dbf4	3.58	3.87	3.55	*Rasa3*	1.82	1.98	1.88
Dbndd2	-2.98	-2.19	-2.79	*Rasal1*	6.16	6.71	5.84
Dcdc2a	-5.27	-4.57	-5.06	*Rassf3*	3.08	3.14	3.10
Ddo	-6.65	-6.75	-6.87	*Rb1*	-1.93	-1.95	-2.10
Ddr1	-1.61	-3.51	-1.57	*Rbl1*	3.29	3.64	3.33
Ddx11	3.34	3.29	3.28	*Rcc1*	2.05	2.98	2.13
Depdc1a	6.72	7.69	7.05	*Rcor2*	2.22	2.15	2.35
Depdc1b	5.97	6.15	6.00	*Rdh5*	-4.82	-3.64	-4.71
Dgkk	4.52	4.99	4.11	*Reep1*	-1.79	-1.81	-1.81
Dgkz	1.7	1.60	1.81	*Retsat*	-2.87	-2.64	-3.06
Dhcr24	1.63	1.53	1.58	*Rev3l*	1.81	1.52	1.33
Dhfr	2.49	2.57	2.41	*Rfc3*	2.17	2.28	2.23
Dhrs1	-3.73	-3.72	-3.64	*Rfx2*	-2.77	-2.81	-2.83
Dhx32	-2.22	-2.31	-2.22	*Rgma*	-1.41	-1.78	-1.58
Diap3	4.59	4.44	3.35	*Rgs4*	-5.87	-5.54	-6.04
Dirc2	-1.77	-1.77	-1.74	*Rgs5*	-6.28	-6.65	-7.52
Dixdc1	-2.46	-3.16	-2.36	*Rhbdf1*	1.88	2.03	2.01
Dlgap3	2.05	1.96	2.20	*Rhou*	-2.65	-2.60	-2.60
Dlgap5	5.6	7.17	5.33	*Rhpn2*	-3.66	-3.75	-3.71
Dmp1	3.49	4.07	3.41	*Rims4*	2.82	4.48	3.11
Dna2	3.34	3.35	3.34	*Rin2*	-1.58	-1.64	-1.62
Dnajb2	-2.04	-2.30	-2.07	*Ripply1*	-8.44	-8.20	-8.28
Dnajb4	-1.61	-1.87	-1.60	*Rnase1*	-8.99	-8.61	-9.03
Dnajb9	-2.6	-2.50	-2.58	*Rnf13*	-1.97	-1.89	-2.04

Dock10	2.15	2.55	2.37	*Rnf182*	-3.9	-3.82	-4.01
Drp2	-4.18	-5.22	-3.49	*Rnf19b*	-2.37	-2.64	-2.41
Dscc1	6.94	5.62	5.31	*Rorc*	-3.14	-3.46	-3.17
Dtl	4.76	4.08	4.77	*Rpa2*	1.84	1.85	1.84
Dusp18	-2.31	-2.07	-2.26	*Rpe65*	-7.99	-7.75	-7.52
Dusp6	6.29	6.23	6.22	*Rpl13a*	1.34	1.80	1.53
Dut	2.87	4.09	2.93	*Rplp1*	1.38	1.53	1.32
Dync2li1	-2.18	-2.06	-2.13	*Rps20*	1.54	1.52	1.56
E2f1	3.92	4.76	3.96	*Rps5*	1.38	1.57	1.58
E2f2	5.1	4.88	4.97	*Rrm1*	1.67	1.82	1.67
E2f7	5.46	6.20	5.15	*Rrm2*	4.66	4.78	4.67
E2f8	4.66	4.18	4.70	*Rsph9*	-3.27	-3.14	-3.18
Ech1	-2.13	-2.20	-2.10	*Rtkn2*	3.99	6.69	4.10
Ecm2	-3.07	-3.50	-3.81	*S100a3*	-5.87	-5.65	-6.29
Ect2	5.12	5.93	4.90	*S100a4*	-6.64	-7.17	-6.69
Ednra	-2	-1.91	-2.02	*S1pr1*	-3.23	-3.28	-3.22
Ednrb	-1.85	-2.05	-1.89	*Sall3*	2.45	2.30	2.51
Eef1b2	1.4	1.50	1.35	*Samd9l*	-3.36	-3.45	-3.31
Efhd1	-3.22	-3.31	-3.20	*Sbno2*	-1.79	-4.02	-2.41
Efhd2	-2.66	-2.66	-2.59	*Scara5*	-4.15	-3.80	-4.02
Efs	1.44	1.47	1.61	*Scarb1*	2.49	2.31	2.33
Egr1	3.06	3.00	3.06	*Scg3*	-2.52	-2.70	-2.58
Elfn2	3.45	3.15	3.50	*Scml2*	3.09	3.26	3.13
Eln	4.51	3.23	3.35	*Scp2*	-1.37	-1.53	-1.44
Elovl6	1.98	4.98	2.05	*Sdc2*	-1.75	-1.70	-1.85

Enho	-2.28	-2.45	-2.13	*Sdc3*	1.59	1.63	1.71
Enkur	-6.39	-6.27	-6.38	*Sdc4*	-2.71	-2.70	-2.70
Enpp3	5.34	6.55	5.52	*Sema5b*	2.62	2.70	2.80
Entpd2	-5.66	-5.69	-5.69	*Sema6a*	1.51	2.34	1.63
Ephb1	-1.57	-1.60	-1.64	*Sema6d*	-1.4	-3.06	-1.44
Ephx4	-3.2	-3.19	-3.22	*Sepp1*	-1.89	-1.85	-1.96
Epn2	1.99	2.21	2.02	*Sept6*	3.08	6.29	2.96
Eps15	-1.42	-1.68	-1.58	*Sept9*	2.32	3.02	2.35
Erbb2ip	-1.45	-1.36	-1.49	*Serpina3n*	-6.34	-6.35	-6.38
Ercc6l	4.08	4.26	4.05	*Serpinb1a*	-3.87	-4.11	-3.96
Esco2	5.6	5.84	5.71	*Serpinb1b*	-5.44	-5.47	-5.57
Espl1	5.48	6.58	6.09	*Serpinb9*	-3.37	-3.18	-3.36
Esrrb	3.78	4.23	3.87	*Serping1*	-5.23	-5.34	-5.52
Etv4	3.65	3.37	3.67	*Sez6l*	1.88	2.33	1.90
Etv5	4.36	4.36	4.27	*Sfxn5*	-2.21	-2.20	-2.24
Exo1	3.93	4.82	4.74	*Sgol1*	6	5.95	5.93
Ezh2	2.3	2.60	2.32	*Sgol2*	4.23	5.15	4.35
Ezr	-3.49	-3.54	-3.54	*Shc3*	2.65	3.42	2.73
F3	-2.98	-2.99	-2.98	*Shcbp1*	5.72	5.86	5.61
Fads2	-1.82	-1.63	-1.74	*Shmt1*	3.11	1.90	3.22

Fam102a	-1.89	-1.76	-1.83	*Sidt2*	-1.57	-1.54	-1.56
Fam111a	3.96	3.84	3.74	*Sirt2*	-1.76	-1.78	-1.73
Fam129b	-3.12	-3.21	-3.02	*Ska1*	6.84	7.97	6.89
Fam134b	-5.33	-5.09	-5.31	*Skp2*	2.87	2.96	2.77
Fam171a1	1.44	3.34	1.48	*Slc14a 1*	-9.09	-7.87	-9.24
Fam179a	-3.71	-4.40	-4.15	*Slc16a 1*	-3.05	-2.86	-3.07
Fam189a2	-3.5	-3.53	-3.46	*Slc1a5*	2.55	2.50	2.60
Fam20a	-2.65	-2.96	-2.84	*Slc1a6*	3.41	3.47	3.52
Fam53b	-2.12	-1.81	-2.10	*Slc22a 23*	-1.57	-1.64	-1.53
Fam63b	-1.45	-1.56	-1.59	*Slc22a 5*	-2.53	-2.51	-2.52
Fam64a	7.53	7.31	7.57	*Slc25a 10*	-1.6	-2.07	-1.52
Fam84b	-3.25	-3.37	-3.29	*Slc25a 25*	2.65	3.45	2.66
Fancb	3.6	4.58	4.40	*Slc25a 33*	-2.72	-2.67	-2.63
Fancd2	4.63	5.57	5.32	*Slc38a 1*	-3.16	-2.85	-3.21
Fas	-4.65	-4.51	-4.56	*Slc39a 1*	-1.44	-1.53	-1.54
Fbln1	2.87	2.87	3.00	*Slc39a 12*	-4.4	-4.32	-4.40
Fbln2	9.26	9.60	9.62	*Slc39a 14*	-2.09	-2.23	-2.11

Fbn2	3.91	3.50	3.56	*Slc39a 4*	-4.5	-4.43	-4.09
Fbxo32	-2.67	-2.63	-2.71	*Slc41a 1*	-1.86	-1.89	-1.86
Fbxo5	3.79	3.64	3.72	*Slc41a 3*	-2.34	-2.31	-2.35
Fcgr2b	-7.09	-7.54	-6.28	*Slc43a 2*	-1.71	-2.11	-1.80
Fcgrt	-2.88	-2.90	-2.86	*Slc44a 3*	-6.2	-6.27	-6.44
Fdps	1.96	1.86	2.01	*Slc4a2*	-1.99	-1.77	-1.70
Fen1	2.22	2.20	2.30	*Slc4a4*	-2.03	-2.65	-2.16
Fez2	-1.57	-1.67	-1.53	*Slc4a8*	-2.83	-1.53	-1.50
Fgd3	-2.67	-2.63	-2.68	*Slc6a8*	-2.37	-2.00	-2.32
Fgl2	-4.96	-5.11	-4.81	*Slc7a1*	2.67	2.90	2.80
Fignl1	4.07	4.31	4.03	*Slc7a1 1*	-2.87	-2.54	-3.12
Fkbp5	2.5	2.47	2.50	*Slc9a3r 1*	-1.76	-2.23	-2.15
Fmn1	-3.09	-3.18	-3.15	*Slfn9*	3.98	5.19	3.93
Fmn2	-3.08	-2.97	-3.15	*Slit1*	4.7	4.64	4.80
Fmod	-8.28	-7.73	-8.35	*Smad6*	-4.54	-4.03	-4.41
Fndc1	4.76	4.22	4.44	*Smad9*	-3.68	-3.37	-3.73
Folr1	-7.38	-7.60	-7.50	*Smc2*	2.6	2.44	2.81
Fos	-1.59	-1.75	-1.60	*Smc4*	2.21	2.10	1.93
Foxj1	-3.86	-3.99	-3.76	*Smpd1*	-1.66	-1.69	-1.59
Foxm1	4.81	4.81	4.83	*Smtn*	3.28	3.17	3.36

Fras1	2.12	2.06	1.94	*Snta1*	-3.52	-3.18	-3.18
Fxyd1	-9.97	-9.67	-9.73	*Soat1*	-2.22	-1.44	-2.12
Fxyd7	-7.48	-5.44	-7.71	*Socs3*	-2.72	-3.09	-2.81
Fyn	1.45	3.12	1.42	*Sorbs1*	-2.84	-3.40	-2.98
Fzd3	-1.54	-1.43	-1.64	*Sorbs2*	-3.25	-3.38	-3.45
Gabarapl1	-1.75	-1.72	-1.72	*Sorl1*	-4.02	-3.94	-3.96
Gadd45a	-2.48	-2.44	-2.64	*Sox11*	2.1	1.99	1.88
Gadd45b	-3.24	-3.33	-3.10	*Sox9*	-2.39	-2.39	-2.38
Gadd45g	-2.53	-2.74	-2.39	*Spag5*	2.53	2.56	2.53
Garnl3	-3.36	-4.92	-3.35	*Spag6*	-10.21	-7.54	-8.52
Gas1	1.97	1.96	2.10	*Sparc*	-2.29	-2.20	-2.39
Gas2l3	5.04	6.05	4.85	*Spata17*	-5.52	-4.39	-4.29
Gbp2	-6.65	-6.56	-6.54	*Spc24*	6.57	6.26	6.06
Gdf11	-2.46	-2.16	-2.02	*Spc25*	4.14	4.31	4.21
Gdpd2	-2.12	-4.13	-2.06	*Spop*	-1.48	-1.38	-1.54
Gen1	4.02	4.97	3.93	*Spp1*	3.96	3.99	3.97
Gins1	3.56	3.78	3.58	*Spred1*	3.88	1.69	1.38
Gja1	-4.95	-4.79	-4.94	*Spry1*	4.19	2.82	4.26
Glcci1	2.22	2.22	2.10	*Spry2*	1.8	2.04	2.13
Glipr2	-3.24	-3.12	-3.21	*Spry4*	5.68	5.79	5.76
Glis3	-4.17	-3.51	-4.18	*Spsb1*	-2.48	-2.51	-2.41
Glt25d1	1.43	1.45	1.48	*Spsb4*	3.03	2.75	2.88
Glud1	-1.73	-1.72	-1.75	*Sqstm1*	-1.69	-1.67	-1.66
Gm11992	-4.35	-4.18	-4.23	*Srcin1*	-4.99	-4.29	-5.04
Gm973	-3.5	-3.69	-3.60	*Srgap3*	-1.46	-1.35	-1.39

Gmnn	4.45	4.42	4.54	*Srm*	1.88	1.86	2.02
Gnb2l1	1.53	1.66	1.56	*St8sia1*	1.96	2.05	1.90
Gpam	-3.51	-2.99	-3.39	*St8sia2*	-4.05	-3.89	-4.03
Gpd2	-1.82	-1.99	-1.95	*Stard13*	-2	-1.99	-1.98
Gpr123	-2.39	-2.32	-2.31	*Stard8*	-4.4	-3.53	-4.21
Gpr137b-ps	-1.81	-1.67	-1.86	*Stil*	4.53	6.11	4.55
Gpr137b	-2.6	-2.35	-2.54	*Stim1*	-2.11	-2.03	-2.14
Gpr17	-4.9	-5.01	-4.86	*Stim2*	2.26	2.53	2.16
Gpr179	-4.13	-6.05	-4.52	*Stom*	-3.18	-3.20	-3.18
Gpr37l1	-3.78	-3.69	-3.64	*Sulf1*	-4.63	-3.70	-3.54
Gpr55	-3.19	-3.09	-3.32	*Synpo2*	-5.5	-5.85	-6.25
Gprc5b	-2.27	-2.34	-2.30	*Tab2*	-1.92	-1.89	-1.94
Gpx1	-2.76	-2.83	-2.64	*Tacc3*	3.84	3.31	3.64
Gpx4	-1.72	-2.38	-2.48	*Tapbp*	-1.71	-1.81	-1.92
Gpx8	-2.26	-2.16	-2.27	*Tbc1d2*	-2.8	-2.81	-2.96
Gria1	-5.08	-4.96	-4.90	*Tbc1d2b*	-2.41	-2.33	-2.37
Grm5	3.61	3.41	3.34	*Tbcel*	-2.82	-3.52	-2.83
Gsg2	4.97	7.51	4.92	*Tcp11l2*	-3.61	-3.45	-3.51
Gstm6	4.16	3.88	4.03	*Tecta*	-4.72	-4.46	-4.50
Gstm7	2.76	2.88	2.74	*Tex264*	-2.1	-2.93	-2.00
Gtse1	1.92	2.44	1.96	*Tfdp1*	1.33	3.28	1.39
H2afx	2.84	2.70	2.93	*Tgfb2*	-2.95	-3.06	-3.06
H2afz	2.55	2.12	2.43	*Tifa*	-3.69	-3.95	-3.72

Hacl1	-1.99	-2.04	-2.00	*Timeless*	6.94	4.11	3.81
Hc	-5.78	-5.72	-5.81	*Timp2*	-2.72	-2.61	-2.68
Hcfc1r1	-2.59	-2.57	-2.65	*Tipin*	2.08	2.08	2.00
Hectd2	2.06	2.04	2.18	*Tjp2*	-1.69	-1.86	-1.74
Heg1	-2.12	-1.96	-2.09	*Tk1*	7.8	7.68	8.14
Hells	4.64	4.63	4.15	*Tle2*	3.46	3.31	3.17
Hey1	-2.1	-2.01	-2.04	*Tle6*	4.72	4.96	4.63
Hhatl	-6.79	-6.29	-6.49	*Tlr3*	-2.36	-2.63	-2.43
Hip1	3.5	3.37	3.48	*Tm4sf1*	-4.47	-4.27	-4.50
Hirip3	2.24	2.03	2.18	*Tmem108*	-3.19	-9.98	-3.02
Hivep2	-1.76	-1.74	-1.63	*Tmem132b*	-2.84	-2.71	-2.87
Hmcn1	2.06	2.30	2.06	*Tmem158*	3.2	3.23	3.44
Hmga2	5.1	5.67	4.76	*Tmem173*	2.6	3.42	2.56
Hmgb2	5.09	4.28	4.38	*Tmem43*	-1.57	-1.60	-1.59
Hmgcr	1.48	1.61	1.53	*Tmem47*	-4.39	-4.39	-4.65
Hmgn5	2.74	2.67	2.38	*Tmpo*	1.53	2.84	2.39
Hmmr	6.62	7.59	5.28	*Tnc*	6	7.95	5.92
Hnrnpab	1.59	1.59	1.62	*Tnfaip6*	2.66	2.68	2.68
Hopx	-5.45	-5.42	-5.33	*Tom1l1*	-1.92	-2.28	-2.32
Hprt	2.36	3.67	2.23	*Tom1l2*	-1.59	-1.49	-1.43

Hr	-4.73	-4.17	-4.69	*Tonsl*	3.22	2.48	3.34
Hrsp12	-3.02	-2.80	-3.00	*Top2a*	6.24	5.77	6.17
Hs3st2	Inf	6.61	6.71	*Topbp1*	1.77	1.98	1.87
Hs6st2	3.61	4.40	3.53	*Tprgl*	-1.42	-1.39	-1.30
Hsd17b11	-1.68	-1.72	-1.72	*Tpx2*	5.38	5.36	5.29
Hsdl2	-2.92	-2.81	-2.89	*Traf4*	1.61	1.68	1.69
Hspa1a	-2.93	-3.02	-2.87	*Traip*	3.39	3.03	2.96
Hspa2	-2.36	-2.41	-2.35	*Trappc 10*	-2.83	-2.80	-2.75
Hspb6	-3.42	-3.54	-3.43	*Trib2*	2.9	2.90	2.88
Hspb8	-7.69	-7.81	-7.51	*Trim59*	2.72	4.40	2.48
Htr5b	3.73	3.95	3.79	*Trip13*	3.71	5.21	3.76
Hydin	4.36	5.82	4.51	*Troap*	6.96	6.96	6.99
Iars	1.42	1.60	1.46	*Trp53i11*	4.22	4.14	4.26
Id1	-3.54	-3.70	-3.46	*Tsc22d4*	-1.89	-2.90	-1.78
Id2	-2.44	-2.49	-2.57	*Tspan15*	-2.34	-2.31	-2.31
Id4	-5.81	-6.07	-5.83	*Tspan17*	-3.65	-3.56	-3.54
Idi1	1.73	1.54	1.41	*Tspan5*	2.17	2.27	2.24
Ifit3	-5.3	-5.53	-5.22	*Tspan9*	-2.15	-2.39	-2.17
Igfbp2	5.47	5.31	5.63	*Tst*	-2.6	-2.81	-2.57
Igfbp3	4.92	5.15	5.09	*Ttc12*	-4.29	-3.74	-4.12
Igfbp5	-3.72	-3.44	-3.46	*Ttc25*	-2.82	-2.91	-2.90
Igfbpl1	-5.48	-5.32	-5.27	*Ttc28*	-1.42	-1.45	-1.40

Igsf11	-5.1	-5.00	-5.10	*Ttc30b*	-2.62	-2.51	-2.61
Il1r1	-4.25	-4.21	-4.35	*Ttk*	5.77	5.97	5.80
Il6ra	-2.97	-2.89	-2.96	*Ttyh1*	-2.13	-2.08	-1.92
Il6st	-4.12	-3.99	-4.12	*Ttyh2*	-2.35	-2.17	-2.14
Impdh1	2.09	2.97	2.16	*Ttyh3*	1.71	2.19	1.80
Incenp	4.01	3.78	4.04	*Tub*	2.5	3.25	2.39
Inf2	-3.61	-2.84	-2.65	*Tubb5*	1.89	2.02	1.93
Insig1	1.75	1.66	1.61	*Txlnb*	-2.8	-2.64	-2.95
Insm1	2.98	2.95	3.13	*Txn1*	2.54	2.64	2.68
Ipo5	1.59	1.70	1.56	*Ubash3b*	2.37	2.56	2.36
Iqcg	-4.33	-2.20	-2.15	*Ube2c*	7.07	6.90	6.46
Iqgap3	6.64	5.66	5.54	*Ube2t*	4.55	4.11	4.08
Iqub	-5.17	-5.03	-4.96	*Ucma*	-7.45	-6.66	-7.26
Irgm2	-4.3	-3.99	-4.06	*Ugp2*	-1.91	-2.31	-1.99
Itfg3	-2.58	-2.87	-2.51	*Ugt1a6a*	-4.04	-3.91	-3.98
Itga3	-3.34	-3.41	-3.27	*Uhrf1*	5.5	6.92	5.56
Itga4	5.38	5.56	5.15	*Ulk2*	-1.6	-1.54	-1.64
Itga5	2.03	2.00	2.08	*Ung*	3.07	3.91	3.09
Itga8	6.1	3.54	3.51	*Usp35*	-3.26	-3.18	-3.20
Itm2b	-2.34	-1.51	-2.44	*Usp53*	-5.08	-4.89	-4.69
Itm2c	-2.72	-2.72	-2.66	*Vars*	1.89	1.85	1.96
Itpkb	-2.53	-2.83	-2.44	*Vash1*	2.16	2.26	2.31
Jak1	-1.81	-1.56	-1.68	*Vav3*	2.28	2.22	2.26
Jakmip1	-7.22	-7.02	-8.11	*Vdr*	-7.14	-7.34	-6.78

Kat2b	-2.01	-2.11	-1.87	*Vpreb3*	-7.49	-7.98	-6.68
Kbtbd11	1.36	1.64	1.36	*Vrk1*	2.92	3.43	2.75
Kcna6	-2.56	-2.60	-2.46	*Vtn*	-6.16	-5.97	-5.85
Kcnab2	1.73	2.43	1.77	*Vwa3a*	-5.45	-5.13	-5.12
Kcnc1	1.96	1.95	2.04	*Vwa5a*	-2.95	-2.92	-3.14
Kcnc4	3.31	3.34	3.38	*Vwc2*	2.95	3.28	3.05
Kcnj9	-4.21	-4.20	-4.11	*Wdhd1*	3.3	2.83	3.25
Kcnn2	-3	-2.92	-3.06	*Wdr52*	-6.96	-4.56	-6.02
Khdrbs3	1.71	1.91	1.64	*Wdr62*	1.97	3.13	2.03
Kif11	4.94	4.98	4.83	*Wee1*	2.25	2.37	2.35
Kif14	7.14	7.67	6.41	*Wipi1*	-2.4	-2.14	-2.31
Kif15	5.52	5.81	5.26	*Wnt11*	-5.94	-5.58	-5.78
Kif18a	2.98	2.97	2.77	*Wnt9a*	-3.63	-3.64	-3.60
Kif18b	4.24	4.40	4.46	*Wwc1*	-1.73	-1.55	-1.47
Kif1c	-1.35	-1.45	-1.29	*Xdh*	-4.74	-4.85	-4.66
Kif20b	5.04	5.98	4.41	*Xylt1*	2.28	2.45	2.30
Kif21a	-1.78	-2.26	-1.82	*Zbtb20*	-2.37	-5.18	-2.58
Kif22	4.54	4.79	4.70	*Zbtb7c*	2.1	2.11	2.18
Kif23	7.27	6.83	6.71	*Zdhhc23*	-4.3	-4.18	-4.26
Kif2c	6.74	6.99	6.65	*Zeb1*	1.64	1.55	1.58
Kif4	5.04	5.27	5.12	*Zfp651*	-2.09	-2.05	-1.91
Kif6	-5.56	-5.72	-5.36	*Zfp703*	-1.88	-1.96	-1.84
Kif9	-4.39	-4.24	-4.41	*Zhx1*	-1.75	-1.78	-1.81
Kifc1	3.79	3.57	3.75	*Zhx2*	-1.76	-1.85	-1.74
Kifc5b	3.82	3.51	3.77	*Zwilch*	3.05	3.27	3.07

Supplementary Table 5. Transcripts differentially expressed in NSCs and Diff-NSCs identified by all three methods.

Bibliography

Ahn, S., and Joyner, A.L. In vivo analysis of quiescent adult neural stem cells responding to Sonic hedgehog. Nature 437, 894-897 (2005).

Ambros, V., The functions of animal microRNAs. Nature 431, 350–355 (2004).

Balordi, F., and Fishell, G. Hedgehog signaling in the subventricular zone is required for both the maintenance of stem cells and the migration of newborn neurons. The Journal of neuroscience 27, 5936-5947 (2007).

Bartel, D.P. MicroRNAs: target recognition and regulatory functions. Cell 136, 215–233 (2009).

Bian, S. et al. MicroRNA cluster miR-17-92 regulates neural stem cell expansion and transition to intermediate progenitors in the developing mouse neocortex. Cell reports 3, 1398-1406 (2013).

Blakaj A, Lin H. Piecing together the mosaic of early mammalian development through microRNAs. J Biol Chem 283: 9505–9508 (2008).

Campos, L. S. et al. Notch, epidermal growth factor receptor, and β1- integrin pathways are coordinated in neural stem cells. J. Biol. Chem. 281, 5300–5309 (2006).

Chou, C.-H. et al. miRTarBase 2016: updates to the experimentally validated miRNA-target interactions database. Nucleic acids research 44, D239-D247 (2015).

Consortium, I.H.G.S. Finishing the euchromatic sequence of the human genome. Nature 431, 931-945 (2004).

Davis, A. A. & Temple, S. A self-renewing multipotential stem cell in embryonic rat cerebral cortex. Nature 372, 263-266 (1994).

De Smaele, E. et al. An integrated approach identifies Nhlh1 and Insm1 as Sonic Hedgehog-regulated genes in developing cerebellum and medulloblastoma. Neoplasia 10, 89IN35-98IN36 (2008).

Doetsch, F. et al. Subventricular zone astrocytes are neural stem cells in the adult mammalian brain. Cell 97, 703–716 (1999).

Ferretti, E. et al. Alternative splicing of the ErbB-4 cytoplasmic domain and its regulation by hedgehog signaling identify distinct medulloblastoma subsets. Oncogene 25, 7267-7273, doi:10.1038/sj.onc.1209716 (2006).

Ferretti, E. et al. Concerted microRNA control of Hedgehog signalling in cerebellar neuronal progenitor and tumour cells. The EMBO journal 27, 2616-2627, doi:10.1038/emboj.2008.172 (2008).

Ferretti, E. *et al.* MicroRNA profiling in human medulloblastoma. *International Journal of Cancer* **124**, 568-577, doi:10.1002/ijc.23948 (2009).

Gage, F.H. Mammalian neural stem cells. Science 287, 1433-1438 (2000).

Gao, Y. et al. Inhibition of miR-15a Promotes BDNF Expression and Rescues Dendritic Maturation Deficits in MeCP2-Deficient Neurons. Stem Cells 33, 1618-1629 (2015).

Garg, N. et al. microRNA-17-92 cluster is a direct Nanog target and controls neural stem cell through Trp53inp1. EMBO J 32, 2819-2832, doi:10.1038/emboj.2013.214 (2013).

Gemenetzidis, E. et al. Induction of human epithelial stem/progenitor expansion by FOXM1. Cancer research 70, 9515-9526 (2010).

Gong, X. et al. MicroRNA-130b targets Fmr1 and regulates embryonic neural progenitor cell proliferation and differentiation. Biochemical and biophysical research communications 439, 493-500 (2013).

Han, Y.-G. et al. Hedgehog signaling and primary cilia are required for the formation of adult neural stem cells. Nature neuroscience 11, 277-284 (2008).

Harris, L., et al. Insights into the Biology and Therapeutic Applications of Neural Stem Cells. Stem Cells International, 9745315 (2016).

Hong, H. et al. Suppression of induced pluripotent stem cell generation by the p53–p21 pathway. Nature 460, 1132-1135 (2009).

Imayoshi, I. et al. Essential roles of Notch signaling in maintenance of neural stem cells in developing and adult brains. The Journal of Neuroscience 30, 3489-3498 (2010).

Katoh, Y. & Katoh, M. Hedgehog signaling pathway and gastrointestinal stem cell signaling network (review). International journal of molecular medicine 18, 1019-1024 (2006).

Kawamura, T. et al. Linking the p53 tumour suppressor pathway to somatic cell reprogramming. Nature 460, 1140-1144 (2009).

Kim, J. B. et al. Oct4-Induced Pluripotency in Adult Neural Stem Cells. Cell. Volume 136, Issue 3, Pages 411-419, ISSN 0092-8674 (2009).

Koboldt, D.C. et al. The next-generation sequencing revolution and its impact on genomics. Cell 155, 27-38 (2013).

Lai, K. et al. Sonic hedgehog regulates adult neural progenitor proliferation in vitro and in vivo. Nature neuroscience 6, 21-27 (2003).

Lander, E.S. et al. Initial sequencing and analysis of the human genome. Nature 409, 860-921 (2001).

Lee, A., Kessler, J.D., Read, T.-A., Kaiser, C., Corbeil, D., Huttner, W.B., Johnson, J.E., and Wechsler-Reya, R.J. Isolation of neural stem cells from the postnatal cerebellum. Nature neuroscience 8, 723-729 (2005).

Lie, D.C. et al. The adult substantia nigra contains progenitor cells with neurogenic potential. The Journal of neuroscience 22, 6639-6649 (2002).

Lin, T. et al. p53 induces differentiation of mouse embryonic stem cells by suppressing Nanog expression. Nature cell biology 7, 165-171 (2005).

Ma, S. et al. miR-130b promotes CD133+ liver tumor-initiating cell growth and self-renewal via tumor protein 53-induced nuclear protein 1. Cell stem cell 7, 694-707 (2010).

Martin, J. A. and Wang, Z. Next-generation transcriptome assembly. Nature Reviews Genetics 12, 671–682 (2011).

Martino G., Pluchino S. The therapeutic potential of neural stem cells. Nature Reviews Neuroscience 7, 395–406 (2006).

Metzker, M.L. Sequencing technologies—the next generation. Nature reviews genetics 11, 31-46 (2010).

Montalbán-Loro, R., Domingo-Muelas, A., Bizy, A. & Ferrón, S. Epigenetic regulation of stemness maintenance in the neurogenic niches. World journal of stem cells 7, 700 (2015).

Morozova, O. et al. Application of new sequencing technologies analysis. Annu.Rev. Genomics Hum. Genet. 10:135-51 (2009).

NCBI. National Center for Biotechnology Information, <https://www.ncbi.nlm.nih.gov/gene/22061>

Ng, J.M., and Curran, T. The Hedgehog's tale: developing strategies for targeting cancer. Nature Reviews Cancer 11, 493-501 (2011).

Ozsolak, F., & Milos, P. M. RNA sequencing: advances, challenges and opportunities. Nature Reviews. Genetics, 12(2), 87–98 (2011).

Palm, T. et al. A systemic transcriptome analysis reveals the regulation of neural stem cell maintenance by an E2F1–miRNA feedback loop. Nucleic acids research 41, 3699-3712 (2013).

Palm, V. et al. Sonic hedgehog controls stem cell behavior in the postnatal and adult brain. Development 132, 335-344 (2005).

Palma, V. and i Altaba, A.R. Hedgehog-GLI signaling regulates the behavior of cells with stem cell properties in the developing neocortex. Development 131, 337-345 (2004).

Pierfelice, T. et al. Notch in the vertebrate nervous system: an old dog with new tricks. Neuron 69, 840-855 (2011).

Po, A. et al. Hedgehog controls neural stem cells through p53-independent regulation of Nanog. EMBO J 29, 2646-2658, doi:10.1038/emboj.2010.131 (2010).

Rivron, N. C. et al. Sonic Hedgehog-activated engineered blood vessels enhance bone tissue formation. Proceedings of the National Academy of Sciences 109, 4413-4418 (2012).

Schüller, U. et al. Forkhead transcription factor FoxM1 regulates mitotic entry and prevents spindle defects in cerebellar granule neuron precursors. Molecular and cellular biology 27, 8259-8270 (2007).

Shi, C. et al. Aberrantly activated Gli2-KIF20A axis is crucial for growth of hepatocellular carcinoma and predicts poor prognosis. Oncotarget 7, 26206 (2016).

Solozobova, V. & Blattner, C. p53 in stem cells. World journal of biological chemistry 2, 202 (2011).

Tay, Y. et al. MicroRNAs to Nanog, Oct4 and Sox2 coding regions modulate embryonic stem cell differentiation. Nature 455, 1124–1128 (2008).

Teh, M.T. et al. FOXM1 is a downstream target of Gli1 in basal cell carcinomas. Cancer research 62, 4773-4780 (2002).

van Dijk, E.L. et al. Ten years of next-generation sequencing technology. Trends in genetics 30, 418-426 (2014).

Voelkerding, K.V. et al. Next-generation sequencing: from basic research to diagnostics. Clinical chemistry 55, 641-658 (2009).

Wakabayashi, T. et al. MicroRNAs and epigenetics in adult neurogenesis. Adv Genet 86, 27-44 (2014).

Wang, D. et al. Aberrant activation of hedgehog signaling promotes cell proliferation via the transcriptional activation of forkhead Box M1 in colorectal cancer cells. Journal of Experimental & Clinical Cancer Research 36, 23 (2017).

Wang, Z. et al. FoxM1 in tumorigenicity of the neuroblastoma cells and renewal of the neural progenitors. Cancer research 71, 4292-4302 (2011).

Wang, Z. et al. RNA-Seq: a revolutionary tool for transcriptomics. Nature reviews genetics 10, 57-63 (2009).

Wierstra, I. The transcription factor FOXM1 (Forkhead box M1): proliferation-specific expression, transcription factor function, target genes, mouse models, and normal biological roles. Advances in cancer research 118, 97-398 (2013).

Xie, Z. et al. Foxm1 transcription factor is required for maintenance of pluripotency of P19 embryonal carcinoma cells. Nucleic acids research 38, 8027-8038 (2010).

Yao J., Mu Y. e Gage F.H. Neuronal stem cells: mechanisms and modelling. Protein cell, 3(4): 251-261 (2012).

Ye, J. et al. Primer-BLAST: a tool to design target-specific primers for polymerase chain reaction. BMC bioinformatics 13, 134 (2012).

Zhang S, Cui W. Sox2, a key factor in the regulation of pluripotency and neural differentiation. World Journal of Stem Cells, 6(3):305-311 (2014).